TECHNISCHE UNIVERSITÄT MÜNCHEN

Fakultät für Medizin

Institut für Zellbiologie des Nervensystems

IN VIVO IMAGING OF THE MITOCHONDRIAL LIFE-CYCLE IN ZEBRAFISH

Gabriela Barbara Plucińska

Vollständiger Abdruck der von der Fakultät für Medizin der Technischen Universität München zur Erlangung des akademischen Grades eines

Doctor of Philosophy (Ph.D.)

genehmigten Dissertation.

Vorsitzender: Univ.- Prof. Dr. Claus Zimmer

Betreuer: Univ.-Prof. Dr. Thomas Misgeld

Prüfer der Dissertation:

1.Univ.- Prof. Dr. Dr. h.c. Christian Haass, Ludwig-Maximilians-Universität München

2. Univ.-Prof. Dr. Stefan Lichtenthaler

Die Dissertation wurde am 10.12.2013 bei der Fakultät für Medizin der Technischen Universität München eingereicht und durch die Fakultät für Medizin am 30.01.2014 angenommen.

ACKNOWLEDGEMENTS

I would like to thank:

My supervisors: Prof Thomas Misgeld and Dr Leanne Godinho.

Members of my thesis advisory committee: Prof Christian Haass and Prof Juliane Winkelmann.

Collaborators from Prof Haass' laboratory: Dr Bettina Schmid, Dr Dominik Paquet and Alexander Hruscha.

Members of the Misgeld and Kerschensteiner lab: Barbara, Cathy, Michael, Monika, Laura, Phil, Petar, Peter, Tatjana and Yvonne. As well as technical staff in the Misgeld lab: Kristina, Monika, Sarah, Vlad and Yvonne.

My family and friends.

Thank you for all your guidance and support throughout!

ABSTRACT

Mitochondria produce the vast majority of cellular ATP, but their role is not restricted to providing energy; they also maintain calcium homeostasis and are key players in apoptotic cell death. Thus, proper functioning and distribution of mitochondria are critical for neuronal cells due to their large size and complex geometry. In order to maintain neurons throughout their life, mitochondria undergo various dynamic changes, which allow these organelles to maintain their functionality and provide energy – while at the same time avoiding harm to their host cells. Thus, disturbances in the dynamics of mitochondria often lead to neuronal malfunctioning or even degeneration. So far, various models have been developed to study mitochondrial dynamics in living cells. While these models have all greatly contributed to our knowledge of mitochondrial dynamics, most of them are *in vitro* models, hence our understanding of mitochondrial behavior *in vivo* remains limited. To address this shortcoming, in my Ph.D. thesis I developed tools to study mitochondrial dynamics *in vivo* in zebrafish, a genetically and optically accessible vertebrate. These tools involve visualizing individual mitochondria in singly labeled sensory neurons, which enabled me to characterize axonal transport of this organelle. Further, in collaboration with the group of Prof. Christian Haass at LMU in Munich, we developed a transgenic *MitoFish* to ease screening for genetic and pharmacological modulators of axonal transport. Additionally, I started developing tools to study fusion of mitochondria using photo-convertible and photo-activateable proteins. Finally, I attempted to identify the location of mitophagic sites and therefore explored use of specific markers of autophagy and mitophagy. Overall my Ph.D. work has established zebrafish as a versatile model for studying mitochondrial dynamics *in vivo*.

ZUSAMMENFASSUNG

Mitochondrien sind Zellorganellen, die den Großteil des zellulären ATPs bereitstellt. Ihre Funktion beschränkt sich allerdings nicht nur auf die Energieproduktion - sie sind auch verantwortlich für die Aufrechterhaltung der Kalziumhomöostase und spielen eine wichtige Rolle bei der Apoptose. Aufgrund der Größe und komplexen Geometrie von Nervenzellen ist eine korrekte Verteilung und Funktion der Mitochondrien in diesen Zellen von entscheidender Bedeutung. Um Nervenzellen über ihre gesamte Lebensdauer hinweg mit Energie zu versorgen und somit die zelluläre Funktionalität aufrecht zu erhalten, sind diese Zellorganellen einer Vielzahl von dynamischen Veränderungen unterworfen. Eine Störung dieser Dynamik führt häufig zu Fehlfunktionen der Nervenzellen oder gar zu deren Degeneration. In der Vergangenheit wurden bereits mehrere Modellsysteme entwickelt mit denen es möglich ist, die Dynamik der Mitochondrien in lebenden Zellen zu beobachten. Diese Techniken haben einen großen Beitrag geleistet, die Mitochondriendynamik besser zu verstehen, allerdings basieren die meisten Ansätze auf *in vitro* Modellen, was dazu führt, dass über das Verhalten der Mitochondrien im lebenden Organismus noch wenig bekannt ist.

Um dieser Frage nachzugehen wurde in der folgenden Doktorarbeit eine Methode entwickelt, die es erlaubt die Dynamik von Mitochondrien im lebenden Zebrafisch zu untersuchen - ein Modellorganismus, der hierfür perfekt geeignet ist, da er genetisch manipulierbar und optisch leicht zugänglich ist. Auf diese Weise können einzelne Mitochondrien fluoreszenz-markiert werden und deren axonaler Transport in den Nervenzellen charakterisiert werden. In Kollaboration mit der Arbeitsgruppe von Professor Christian Haas an der Ludwig-Maximilians Universität in München haben wir einen transgenen „*MitoFish*“ entwickelt, mit dessen Hilfe ein Screening nach genetischen und pharmakologischen Modulatoren von axonalem Transports durchgeführt werden kann. Darüber hinaus wurde damit begonnen photo-konvertierbare und photo-aktivierbare Proteine zu entwickeln, die es erlauben die Fusion einzelner Mitochondrien zu visualisieren. Außerdem sollen spezifische Marker für Autophagie und Mitophagie helfen, aufzuklären, wo in den Nervenzellen Mitochondrien abgebaut werden.

Insgesamt hat diese Doktorarbeit durch die Entwicklung eines neuen Zebrafischmodells einen entscheidenden Beitrag geleistet, die Dynamik von Mitochondrien in lebenden Organismen visualisieren und besser verstehen zu können.

1. Introduction

Mitochondria are vital for all aerobic cells. This is because cell's production of ATP critically depends on mitochondrial oxidative phosphorylation. Neurons depend on this more than other cells, for example to maintain ion gradients, which costs a substantial part of a neuron's overall energy budget (up to 50%; Attwel and Lauglin, 2001). But this is not all that mitochondria do in neurons. Besides additional metabolic roles, e.g. for fatty acid turn-over, mitochondria can also buffer calcium and hence influence genuinely "neuronal" properties, such as neurotransmission or neuroplasticity (Verstreken et al., 2005; Cheng et al., 2010). Moreover, neurons are very susceptible to local proapoptotic and reactive oxygen species (ROS) signaling processes in which mitochondria are critically involved. Therefore, the proper function and distribution of mitochondria is undoubtedly of great importance to neurons. Many of the open issues surrounding mitochondrial dynamism amount to the question of how the mitochondrial "life-cycle" can be mapped on the extended, branched and compartmentalized geometry of a mature neuron.

The aim of this PhD thesis was to establish zebrafish as a new vertebrate model organism for studying mitochondrial dynamics with a special focus on the topology of the mitochondrial "life-cycle". Therefore I will first review the current state of knowledge about mitochondrial dynamics and the available techniques and models for such studies. I will then outline the basic characteristics of zebrafish that make it particularly suitable for studying mitochondrial dynamics.

I would like to stress that sections 1.1 – 1.3 in the Introduction and Discussion are modified from a review article I am currently writing (Plucińska et al. "*Studying the 'life-cycle' of neuronal mitochondria in vivo"*, in preparation). The Results section 3.1, 3.2.1, and 3.3 are derived from my first-author publication, Plucińska et al. 2012 "*In vivo imaging of disease-related mitochondrial dynamics in a vertebrate model system"* J Neurosci.; 32(46):16203-12.

1.1. Mitochondrial life-cycle

In neurons, as in other cells, mitochondria pursue their own semi-autonomous "life-cycle" (O'Toole et al., 2008; Westermann, 2010), which consists of several steps: (1) biogenesis, (2) fission/ fusion and (3) mitophagy (**Fig. 1.1**). For all of these processes a wealth of mechanistic information is available from work in cell lines or primary neurons *in vitro*, but often this contrasts with a lack of knowledge about how all these mechanisms play out in neurons *in vivo*. Below, I will first provide three brief summaries of these life-cycle processes individually and what is known about their roles specifically in neurons. I will try to integrate these individual steps into a full circle, stressing what is currently known about where within a neuron these processes are compartmentalized. Given this compartmentalization, transport obviously plays a central role in tying the different steps of the mitochondrial life-cycle together.

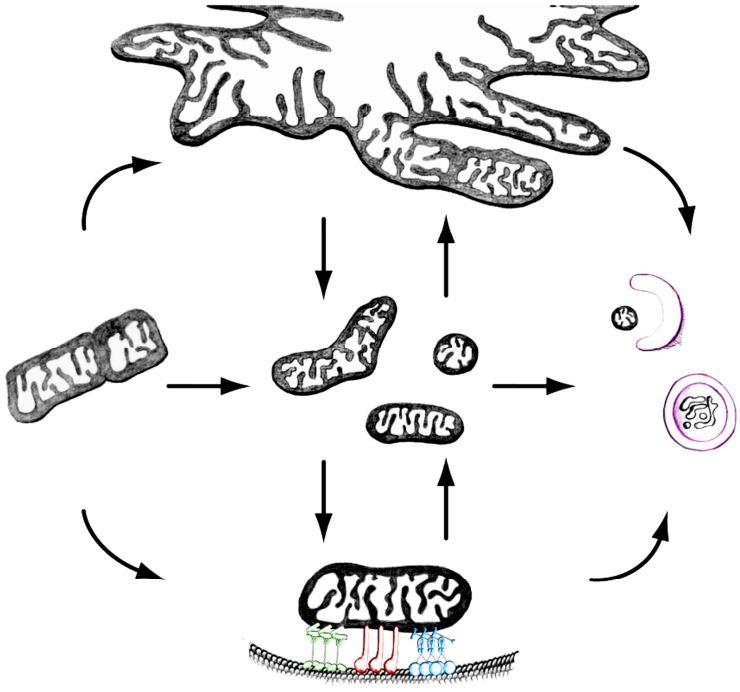

Figure 1.1. Scheme of mitochondrial dynamics in neuronal cells.

The figure represents biogenesis of mitochondria, network and single mitochondria formation through fusion and fission, transport of single organelles and mitophagy. Arrows indicate possible relations between individual steps.

1.1.1. Biogenesis

The life-cycle of a mitochondrion begins with its biogenesis. Unfortunately, the moment when a new mitochondrion is “born”, is hard to pinpoint. This is due to the fact that mitochondrial biogenesis is a drawn-out process with many steps, which in principle can occur independently and be balanced in different ways depending on the cell's metabolic needs. The term "biogenesis" stands for an increase in mitochondrial mass and hence requires expression of mitochondrial proteins encoded in the nucleus and in the mitochondrial genome, commensurate replication of mitochondrial (mt) DNA, and finally budding off – fission – of a new discrete organelle. Mechanisms of each of these steps are well characterized and have been previously extensively reviewed (Clayton, 2003; Chacinska et al., 2009). A number of factors have been described which synchronize all of these processes and hence regulate mitochondrial mass. Peroxisome proliferator-activated receptor γ co-activator 1-α (PGC-1α) is a central master regulator – this has been most clearly demonstrated in non-neuronal tissues (Wu et al., 1999), but also appears to apply to neurons (Wareski et al., 2009). PGC-1α regulates expression of mitochondrial genes from the nuclear genome by binding to nuclear respiratory factors (NRF) 1 and 2, two major transcription factors that regulate mitochondrial genes. Among the genes activated by PGC-1α and NRF-1/2 is mitochondrial transcription factor A (TFAM), a regulator of mtDNA replication and transcription (Virbasius and Scarpulla, 1994). Further, NRF-1 binds to the promoter of the subunit of the translocase of the outer membrane (TOM20), the main protein import channel of the outer mitochondrial membrane (Blesa et al., 2007), suggesting that the described molecular regulators control and coordinate mitochondrial DNA synthesis, protein translation and import.

So where in the neuron does biogenesis happen? Surprisingly, this has not been entirely resolved. Generally it is assumed that most mitochondria are produced in the cell body – for example, peptides corresponding to the mitochondrial targeting sequence that aid in the import of mitochondrial proteins encoded in the nucleus are mostly found near the soma (Davis and Clayton, 1996). However, there is also evidence that mitochondrial DNA replication and division happen in the axon (Gioio et al., 2001; Amiri and Hollenbeck, 2008), suggesting that biogenesis is not confined to the soma. One reason, why pinpointing the site of biogenesis is difficult is the fact that mtDNA and protein synthesis only increase mitochondrial mass, while in most practical definitions of mitochondrial biogenesis, generating a "discrete" mitochondrion (and hence increasing the number of mitochondria) is

also part of the biogenic cascade. Thus, the mechanisms of fission (and the converse process of fusion) have to be considered in the context of biogenesis.

1.1.2. Fission

Scission from the mitochondrial network is of obvious importance in neurons, where the "network" of interconnected mitochondria is mostly restricted to the soma. In this process a "single" mitochondrion is generated, which can then be exported to a neuron's periphery by axonal (or dendritic) transport. Depending on the context of such a fission event, it either contributes to biogenesis (i.e. matching the number of single mitochondria to an increasing mitochondrial mass, ensuring constancy of mass per mitochondrion) or fragmentation (where an increased number of smaller mitochondria are generated). Proteins engaged in this process are well characterized (Westermann, 2010) and are partly shared with the division machinery of peroxisomes (Yan et al., 2005). One key protein, called Dynamin-related protein 1 (Drp1; Dnm1 in yeast) accumulates at the site of scission and in interplay with the endoplasmatic reticulum forms a tightening ring that cuts a single mitochondrion in two (Ingerman et al., 2005; Friedman et al., 2011). Still, not all processes where mitochondrial material is released are Drp1- dependent. Alternative mechanisms appear to exist that result in so-called ‘mitochondrial derived vesicles’ (MDV) that are targeted for degradation (Neuspiel et al., 2008; Rival et al., 2011).

1.1.3. Fusion

The opposing process to fission is fusion, where the membranes of two mitochondria are joined together to form one mitochondrion. The main players in this process are mitofusins 1 and 2 and optic atrophy factor 1 (OPA-1). Mitofusins are responsible for fusion of the outer mitochondrial membrane, whereas OPA-1 merges the inner membranes (Westermann , 2010). To merge two mitochondria, fusion of both membranes is necessary. A recent study has shown however that sometimes mitochondria fuse only partly in a process called ‘kiss and run’ (Liu et al., 2009). A number of mutations in fusion- and fission-related proteins have been described in humans, and interestingly, the phenotypes are invariably neurological (Westermann, 2010; Ranieri et al., 2013). While for fission this would be expected – as blocking fission amounts to abolishing anterograde mitochondrial transport in axons – the number of such cases is rare, suggesting that an earlier lethality might be at fault (Ishihara et al., 2009). In contrast, mitofusin and OPA-1 mutations are well recognized and manifest as neuropathies, either of the peripheral (Charcot-Marie-Tooth disease type 2a; Züchner et al.,

2004) or of the central nervous system (optic nerve atrophy; Shimizu et al., 2003). The specific dependence of neurons on fusion is not obvious from first principles, but might relate to the longevity of post-mitotic neurons. Fusion is seen as particularly important for mitochondrial quality control (Shutt and McBride, 2012), and might play protective roles during starvation (Gomes et al., 2011; Rambold et al., 2011) or stress conditions (Tondera et al., 2009). Indeed, fusion appears to be a mechanism employed as a first resort to rescue impaired mitochondria, by intermixing damaged proteins and genomes with a larger pool of less damaged mitochondrial building blocks. Still, given the limited self-repair of mitochondrial DNA (Boesch et al., 2011), complete removal of damaged mitochondria might be the most desirable outcome. Here, once again, fission might contribute by allowing the "budding off" of mitochondrial sub-compartments in which damaged components are concentrated and which can be targeted for degradation. Which form the degraded "junk material" takes – i.e. whether this would be *bona fide* mitochondria (Narendra et al., 2008) or specialized "micro-vesicles" (Soubannier et al., 2012) is currently open and might depend on the localization and dynamics of the mitochondria involved. Obviously, mitochondria in their entirety could also be targeted for degradation should their overall bioenergetic performance fall below a certain level. In such a case, a specific form of autophagy – "mitophagy" – comes into play.

1.1.4. Mitophagy

Mitochondria that are severely impaired and hence might harm the cell (by production of ROS or release of pro-apoptotic factors) need to be targeted towards mitophagy. The proteins involved have received much attention due to their likely role in Parkinson's disease: PINK1 (PTEN induced putative kinase 1) forms a mitochondria-associated "performance sensor" that accumulates parkin, a cytoplasmic E3 ubiguitin ligase, to "stressed" (i.e. depolarized) mitochondria (Matsuda et al., 2010; Vives-Bauza et al., 2010). Parkin in turn ubiquitinylates mitochondrial proteins (e.g. α-synuclein, mitofusins, synphilin-1, and itself (Cookson, 2003; Ziviani et al., 2009)), which results in engulfment by autophagic "isolation membranes", fusion to lysosomes and subsequent degradation. Compelling as this scenario is, most of the evidence was gathered *in vitro* and often using rather drastic insults to mitochondria, such as chemical uncoupling (Narendra et al., 2008). Adaptation of this molecular model to the *in vivo* situation and natural mitochondrial aging is an ongoing quest in many labs. As a result, some uncertainty about the natural site of mitophagy in neurons exists. Recent work has shown that even after chemical induction, mitophagy appears to mostly take place close to the

soma. This localization seems to depend on the ability of mitochondria to translocate towards the soma, as blocking such transport resulted in mitophagic activity at distal sites in neurites (Cai et al., 2012). Indeed, in parallel, it was shown that autophagosome formation can initiate in neurite tips, but that maturation into autophago-lysosmes happens during retrograde translocation (Maday et al., 2012). However, another string of experiments has suggested that activation of the PINK1-parkin pathway might abolish mitochondrial translocation, rather suggesting an “on-site” degradation model (Wang et al., 2011). Again, whether this possible scenario applies to neurons *in vivo* and most spontaneous mitophagy remains to be seen – in either case, the central role of transport in tying the mitochondrial life-cycle together in neurons is apparent.

1.2. Transport of mitochondria

The discovery of the key steps in the mitochondrial life-cycle and deciphering their molecular mechanisms has been a monumental achievement. Now, however, as often happens after an initial phase of accelerated progress, complexity is emerging. For example, within a cell, and certainly *in vivo*, many of the processes described are interrelated – and individual molecules appear to multi-task at several places. Molecules that regulate fission, for example, are part of the biogenic machinery, but also feature in the sequestration of impaired mitochondrial components (Wang et al., 2013). Similarly, parkin can ubiquitinylate mitofusins and hence prevent fusion (Ziviani et al., 2009; Tanaka et al., 2010). Mitofusins in turn have been implicated in Ca^{2+}-buffering by mediating interactions between mitochondria and the endoplasmic reticulum (de Brito and Scorrano, 2008). And, as a final example, PINK1 and parkin might also interact with molecular motors to immobilize severely damaged mitochondria for "on the spot" degradation (Wang et al., 2011).

In neurons, this web of mechanistic interactions is stretched upon the extended geometry of these cells, adding another layer of complexity: Regulation might not only be molecular, but equally spatial, meaning that a mitochondrion might need to be moved from one site to another to advance in its life-cycle. This is achieved by actively transporting mitochondria – in axons this amounts to a variant of fast axonal transport, but similar processes take place in dendrites (Hirokawa et al., 2010). As a result, inter-compartmental transport of mitochondria depends on the same general players as other forms of axonal transport – motor proteins and cytoskeletal tracks. What gives the transport of neuronal mitochondria extra levels of regulation – and probably answers many questions related to life-cycle homeostasis – is the

involvement of a series of adaptor and anchoring proteins that determine whether a mitochondrion moves or stays put.

1.2.1. Motor proteins

Efficient axonal transport of mitochondria is achieved through the action of molecular motors, which are proteins that use ATP to translocate along the cytoskeleton. Three large super-families of molecular motors have been identified: kinesins, dynein and myosins (**Fig. 1.2**; Hirokawa et al., 2010). Kinesins and dynein play crucial roles in long-range mitochondrial transport. Kinesins transport a wide variety of cargoes towards the plus-end of microtubules (Vale et al., 1985; Hirokawa et al., 2010). Many different kinesins have been characterized, which specialize in the transport of a limited number of cargos – mitochondrial transport mostly relies upon KIF1Bα and KIF5. Given the polarized orientation of microtubules in axons (“plus-end” towards the synapse), kinesin-mediated transport in axons is mostly anterograde. In contrast, the dynein complex is involved in transport towards the minus-end of microtubules – and hence retrograde axonal transport. In contrast to kinesins, only one dynein heavy chain (Dync1h1) seems to generate force for retrograde transport of a plethora of cargos, while a wide variety of auxiliary chains might add flexibility, regulation and cargo-specificity (Hirokawa et al., 2010). Hence, the strategies of anterograde and retrograde transport differ down to the level of the single-molecular behaviour of the motors involved. A single cargo – e.g. a mitochondrion – carries multiple kinesin and dynein motors at the same time (Hendricks et al., 2010), implying that the activity of opposing motors is coordinated. This notion is supported by a number of studies showing that depleting one of the motors has an effect on overall transport rather than selectively affecting anterograde or retrograde transport in isolation (Pilling et al., 2006). The nature of the coordination remains elusive, but probably is more complex than a simple "tug-of-war" – and could involve several levels from motor-to-motor regulation to changes in cargo flux or fate (i.e. if not enough cargos are delivered anterogradely, retrograde transport will eventually diminish). Another area of current uncertainty are the rules that govern transport in settings where tracks are not polarized, e.g. in mammalian dendrites with their mixed microtubule orientation. Indeed, differences between mitochondrial transport in axons and dendrites have been shown, e.g. in the frequency and lengths of stops interspersed in the translocation of a moving mitochondrion (Overly et al., 1996), suggesting that cargos might interact with tracks of opposing directionality.

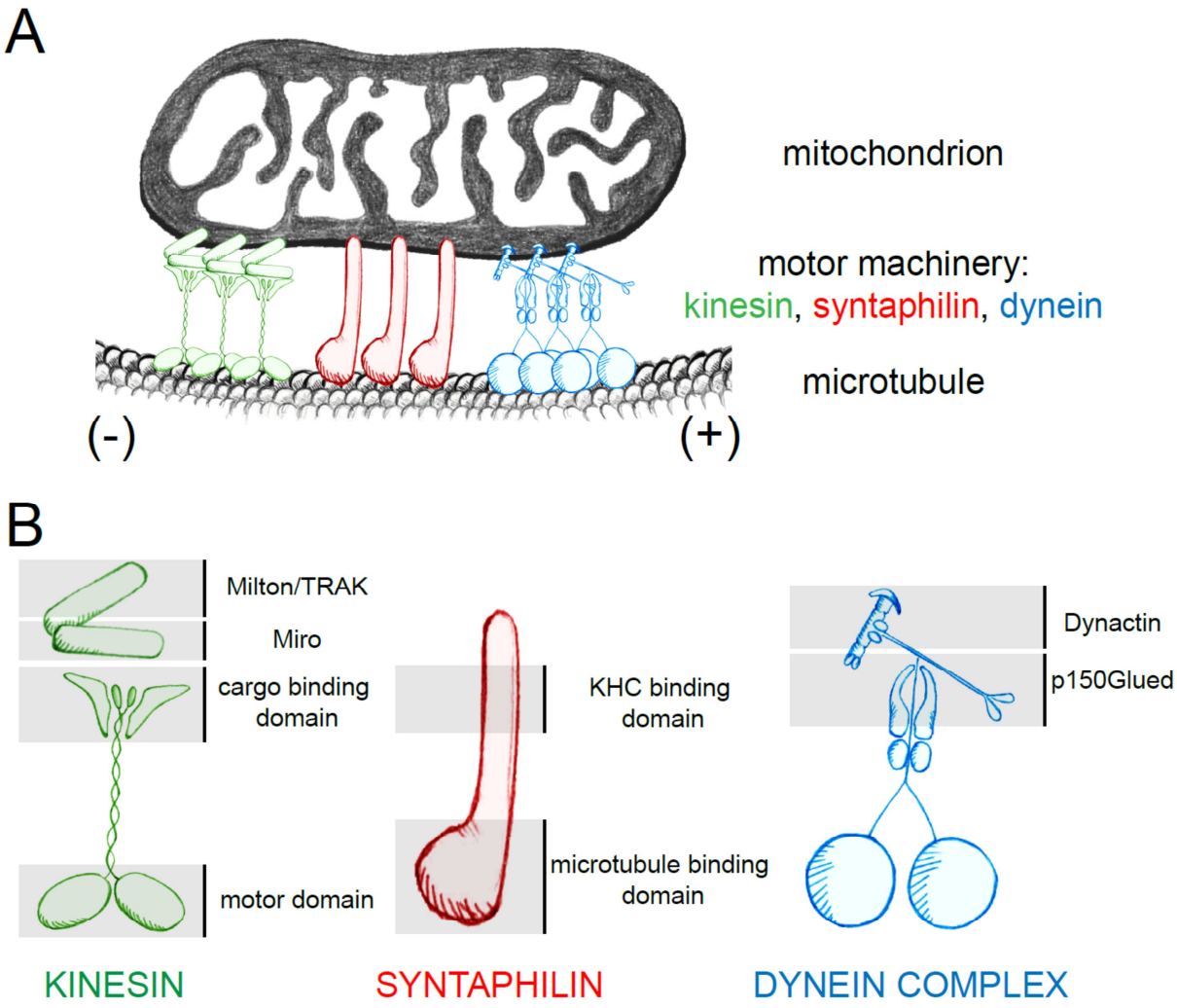

Figure 1.2. Schematic representation of mitochondrial motor machinery.

(A) Overview of molecular motors driving mitochondrial movement and docking. (B) Schematic of single components of motor machinery including kinesin and adaptor proteins for anterograde movement, syntaphilin for docking and dynein for retrograde movement.

1.2.2. Adaptor and docking proteins

Cargos which move anterogradely connect to the kinesins via a number of adaptor proteins. These proteins are considered important regulators of mitochondrial movement and pausing. The prototypic mitochondrial adaptor proteins are Miro and Milton, which were identified in Drosophila screens (Stowers et al., 2002; Guo et al., 2005). Two mammalian Milton orthologues, TRAK1 and TRAK2, have been identified (also named OIP106 and GRIF1). Unlike Milton in Drosophila, which exclusively binds to mitochondria, TRAK1 and TRAK2 are also involved in the transport of endosomes and other cargoes (Webber et al., 2008). Moreover, recent work suggests that the two homologues might specialize in targeting mitochondria into axons or dendrites (van Spronsen et al., 2013). In parallel to the Miro/Milton complex, further proteins have been shown to associate with kinesins and mitochondria: syntabulin (Cai et al., 2005), FEZ1 (Fujita et al., 2007) and RANBP2 (Cho et al., 2007). While mitochondria bind to KIFs via adaptors, for dynein it is not entirely clear which, if any, adaptors are involved. The prevailing view is that the dynein complex binds directly to mitochondria (Hirokawa et al., 2010). This interaction could be directly mediated by different combinations of dynein light or intermediate chains. Alternatively, dynein-associated proteins (such as dynamitin and $p150^{Glued}$) could mediate motor protein interaction and specificity (Waterman-Storer et al., 1997). In addition to coupling motors to mitochondria, adaptor proteins also appear to be the site where molecular signals converge that regulate whether a mitochondrion rests or moves. After all, it is a striking peculiarity of neuronal mitochondria that extremely stable mitochondria coexist with highly dynamic ones. The exact mechanism of the transition between immobility and transport remains unknown. However, some hints have emerged recently that allow formulating a plausible model. Miro has been shown to be sensitive to calcium due to the presence of EF hand motifs (Saotome et al., 2008). This means that at sites of high intracellular calcium the Miro/Milton complex would change its conformation and detach cargos from microtubules – whether this releases the cargo from the motor or rather the motor from the track is an area of active investigation (MacAskill and Kittler, 2010). This mechanism endows mitochondrial transport in neurons with activity-dependence and could explain, why mitochondria accumulate in specific neuronal compartments, where ion fluxes imposes high metabolic demands such as the synapse (Macaskill et al., 2009), or around nodes of Ranvier (Ohno et al., 2011).

Growing evidence supports this hypothesis: For example, a recent cell culture study from the Okabe lab has shown that mitochondria at synaptic sites are less probable to initiate

movement than mitochondria in non-synaptic axon segments. Further experiments showed that this probability can be altered by blocking neuronal activity (Obashi and Okabe, 2013). Another line of work, using imaging of mitochondria and synaptic vesicle (SV) release, provided evidence that repetitive SV release requires the presence of a mitochondrion at the synaptic bouton (Sun et al., 2013). Both of the above studies implicate activity-induced energy demand as the main mechanism of mitochondrial trapping at synaptic sites. However, a definite answer to the question of how much mitochondrial distribution in neurons mirrors local energy demands or rather other roles of this organelle, is still lacking. Indeed, a number of mechanisms that regulate mitochondrial movement or accumulation have been proposed and their activity-dependence is not established for all of them. Such mechanisms include: specific proteins that can anchor mitochondria to microtubules (e.g. syntaphilin, Kang et al., 2008), phosphorylation of motors (Morfini et al., 2002) or adaptors (Wang et al., 2011), modification of tracks, e.g. by microtubule associated proteins, such as Tau (Mandelkow et al., 2003). Of those mechanisms syntaphilin gained a lot of attention recently as a regulator of mitochondrial docking. Work of the Sheng lab points to syntaphilin as a competitor of the Miro/Milton complex in binding kinesin. In this view, high Ca^{2+} levels induces a conformational change in Miro, detaches this protein from kinesin to which syntaphilin could then bind and block kinesin's motor activity (Chen and Sheng, 2013).

1.3. Tools to study mitochondrial dynamics in neurons

As discussed above the molecular basis of the life-cycle of mitochondria is by now well understood and characterized. In this section I will briefly discuss currently available systems for studying mitochondria and point out their advantages and disadvantages.

1.3.1. In vitro systems

For *in vitro* studies, various neuronal populations have been used, including cortical and hippocampal neurons. Such cell cultures allow straight-forward labelling with dyes or genetic constructs (Bakota and Brandt, 2009; Chazotte, 2011), visualization by wide-field microscopy (which can be automatized for high-content screens), as well as the potential to ‘scale-up’ for biochemical analysis. Such systems are also accessible to pharmacological and genetic manipulation. Although primary neuronal cultures have proven a powerful model to investigate many aspects of neuronal cell biology, they still lack certain properties of neurons *in vivo*, such as three-dimensionality, myelination, contact with other cells (glia or specific post-synaptic partners) or extracellular cues, which together result in the absence of a well-

defined cellular geometry. Moreover, most neuronal cultures are derived from early stages of mouse development, which means that their final degree of maturation is hard to define. The notable exception here is adult-derived dorsal root ganglionic neurons; still, as these cells are axotomized during isolation, spurious effects of this disruptive origin might persist. A number of options exist to more closely approximate the natural environment in the culture dish, for example co-culture with glial cells or seeding into microfluidic devices that impose shape. Moreover, organotypic preparations, where brain slices are isolated and cultured, e.g. of midbrain or cerebellum, can be used to study mitochondrial distribution and transport (Ohno et al., 2011; Pham et al., 2012). Still, also here developing tissue is mostly required, tissue remodels after excision and imaging tends to get more difficult due to glial proliferation. So, while some shortcomings can be remedied, *in vitro* studies often require *in vivo* corroboration. Moreover, some questions can simply not be addressed in isolated and immature cells, because they directly relate to aspects of neuronal geometry or ageing. Among available animal models for *in vivo* mitochondrial studies Drosophila and mouse are the two most commonly used.

1.3.2. Drosophila melanogaster

The fruit fly has proven to be an excellent model to study mitochondria. It is highly suitable to perform large genetic screens (short life-cycle, of approximately 15 days from the laying of the egg to eclosion of the adult from the pupa). Additionally gene expression can be easily altered by overexpression or knockout of genes. These properties have made Drosophila a powerful model to study mitochondria. Thanks to easiness of conducting genetic studies a number of proteins important for mitochondrial dynamics have been identified (Stowers et al., 2002; Guo et al., 2005) or characterized (Park et al., 2006) in this model. Finally larvae preparation at the third instar stage allows imaging of mitochondrial behavior in different neuronal populations (sensory and motor neurons; Pilling et al., 2006; Tao and Rolls, 2011). Mitochondria can be easily labeled by introducing transgenes encoding fluorescent proteins tagged to mitochondria. Such imaging studies helped to characterize kinesin and dynein mutants and their effect on mitochondrial transport (Pilling et al., 2006). It is important though to remember that as an invertebrate, Drosophila differs in certain characteristics from mammalian systems, for example with regards to myelination or regeneration. Therefore, the relevance of findings in fly for vertebrate physiology and disease often needs to be independently established. Thus the use of vertebrate systems is often warranted, albeit at the cost of losing genetic and optical accessibility.

1.3.3. Mouse

The mouse remains the most commonly used model for studying mitochondrial dynamics. It is used as a source of neuronal cells (see above) or for studying cells in their natural habitat either in the form of an explant or directly in the living organism. Mitochondrial labels can be introduced into mice through various means such as *in utero* electroporation, viral transfection, or delivery of genes to fertilized oocytes to create transgenic lines. The latter have numerous advantages for research and a number of transgenic lines were generated in recent years (Misgeld et al., 2007; Abe et al., 2011; Pham et al., 2012). The main advantage of transgenic lines is that they offer stable and well characterized labelling of mitochondria. Moreover, the use of specific promoter elements can restrict mitochondrial labelling to neurons or even neuron sub-types, if this is desired. However, there are a few drawbacks that should be considered. For example, the generation of mouse transgenic lines remains both costly and time consuming. Additionally, many mouse lines with labelled (neuronal) mitochondria that have been created to date are not ideal for studying mitochondrial dynamics in early developmental stages as the promoter elements used to drive expression often only starts during the first few postnatal weeks. Moreover, access to the tissue can be achieved only through surgery or explant preparation. Examples of acute explants that can be used for studying mitochondrial dynamics are the triangularis sterni muscle explant (Marinkovic et al., 2012) or acute brain slices (Xiong et al., 2002). The main advantage of the *ex vivo* approach is that the observed cells remain in their immediate natural surroundings while at the same time affording convenient access for observation and intervention. Still, while acute pharmacological manipulations are relatively easy (drugs can be directly applied to the explant), genetic interventions require either viral transfection *in vivo* (for gene overexpression) or creating a genetically modified organism. Notably, disadvantages are the limited life-time of most acutely isolated neuronal tissues, as well as the damage associated with excision, loss of blood flow and the physiological milieu. To overcome some of these issues, neurons can be observed directly in the living organism. While this approach resembles the physiological situation more than an explant it has certain disadvantages that mostly relate to surgery and anaesthesia, which may have an impact on mitochondrial dynamics (Bai et al., 2013). One of the strengths of the mouse system is the availability of well-characterized disease models, in which the role of mitochondria can be studied using imaging (Sorbara et al., 2012). At the same time, the ability to manipulate mechanisms of mitochondrial dynamics and function often requires substantial efforts in mice. Pharmacological manipulation of the living organism is not trivial and needs to be carefully

controlled for. Such controls would include examining for unspecific effects, as well as careful control of drug delivery to its target - for example using appropriate biosensors. This is especially important for studies in the CNS, when drugs need to cross the blood-brain barrier. Imaging of mitochondria can also be combined with selective gene knock-out, but this requires availability or generation of the appropriate knock-out models, which is time-consuming and expensive, and still entails complex breeding schemes. In addition, non-specific effects emerging from other cells (such as glia in the case of studies centered on neuronal mitochondria) or due to developmental compensation can confound results. This can be overcome by using a conditional transgenic line (Rajewsky et al., 1996; Hayashi and McMahon, 2002), when genes can be deleted or introduced with spatial and temporal control - again generally increasing the time, effort and resources needed to conduct a given experiment.

So, while all these are powerful approaches to characterize mitochondrial behaviour they do not satisfy all experimental needs. Hence, what would a "perfect" model to study mitochondrial dynamics in neurons look like? First, it would be characterized by ease of labelling neuronal mitochondria; second, it would be accessible for both pharmacological and genetic manipulations; third, it would allow visualizing cells in their entirety without invasive access; fourth, it would afford the ability to perform longitudinal studies across developmental stages; and finally, it would allow studying all these aspects of neuronal mitochondria in the “natural habitat” of an intact organism *in vivo*. Unfortunately, no currently available system matches this ideally; and probably none ever will. Thus, several models will always co-exist - still, the zebrafish fulfil many of the above-mentioned criteria. Hence, as outlined in the next sections, I set out to introduce zebrafish as a new model for studying mitochondrial dynamics in neurons.

1.4. Zebrafish model

Zebrafish, *Danio rerio*, are small (2.5 - 4 cm in length) fresh-water teleosts. During the 1980s the work of George Streisinger established the groundwork for utilizing zebrafish as an experimental system. His research established zebrafish as a model organism for genetic screens by developing techniques of mutagenesis and genetic mapping as well as clonal analysis (Streisinger et al., 1981; Streisinger et al., 1989; Grunwald and Streisinger, 1992). Nowadays zebrafish are not only used as genetic tools, but are also commonly used in behavioral, developmental, biochemical and many other studies.

Maintenance of adult fish is relatively easy as they can be kept at a high density (e.g. 10 fish per 3.5 liter tank) in slightly brackish water, neutral pH and the temperature at approximately 28ºC. Zebrafish reach sexual maturity generally around 3 months of age and females can produce 100 - 200 embryos per week. Fertilization occurs externally and at initial developmental stages embryos are transparent. Approximately at 24 hours post fertilization (hpf) the pigmentation of the embryos begins. However, by adding chemical compounds (e.g. 1-phenyl-2-thiourea, PTU) melanin synthesis can be blocked (Westerfield, 2000). Developmental stages of the embryo and larvae have been characterized in detail (Kimmel et al., 1995). Between 48 and 72 hpf zebrafish embryos hatch and become free swimming larva. At this early stage of development fish already display certain behaviors: they swim, show an escape response and are touch sensitive (Quigley and Parichy, 2002). These characteristics make zebrafish a very good model for genetic screens (for which they were primarily used), but also for all sort of developmental studies (thanks to *ex utero* development and transparency). In the following sections I will review the most common applications for zebrafish stressing their advantages over other animal models and at the same time pointing out some of the limitations of this model organism.

1.4.1. Forward genetics

Zebrafish first became a popular animal model because of the relative ease with which forward genetic screens could be performed in a vertebrate species. In this approach fish are treated with a chemical, which induces random changes in the genome. The most commonly used chemical to induce mutations is ethylnitrosourea (ENU) due to its high efficiency (Mullins MC et al., 1994). Selected fish can then be analyzed to identify the disrupted gene. Such genetic screens have proven to be of great value when in the ’90s the groups of Christiane Nüsslein-Wolhard and Wolfgang Driever published a set of articles describing

approximately 1800 mutants (Haffter et al., 1996; Kane et al., 1996; Odenthal et al., 1996). Since then a number of other genetic screens has been conducted, including targeted screens (focusing not only on developmental stages but also on fish behavior, reactions to stressors, or reproductive function (Brockerhoff et al., 1998; Bauer and Goetz, 2001; Wienholds et al., 2002)) and retroviral-insertion screens in which mutations are introduced *via* the insertion of viral DNA (Gaiano et al., 1996). While the latter approach is easier to analyze as disrupted genes can be identified with PCR, the technical aspects of the screen are more challenging (production and handling of viruses).

1.4.2. Reverse genetics

While forward genetics starts with a phenotype and aims to identify the responsible gene, reverse genetics begins with a gene and attempts to discover its function by manipulating its expression and examining the resulting phenotype. Various approaches are used in fish to manipulate gene expression. These include: gain-of-function approaches such as overexpression (via transient DNA or RNA injections, or the generation of stable transgenic fish), and loss-of-function approaches, including gene knock-down (morpholino injections), or deletion (e.g. locus-specific mutagenesis). Each of these techniques has its strengths and weaknesses.

1.4.2.1. Gain-of-function approaches

The simplest way to manipulate gene expression in fish is through injecting DNA constructs into one-cell stage embryos and examining the ensuing effects at appropriate times during development. The injected construct, can include the full coding sequence of a gene, a dominant negative version, or mutant and truncated forms of genes. A number of systems for gene delivery have been developed, the most common being direct expression of a gene under the control of specific promoter elements (Pittman et al., 2008). An alternative, the Gal4-UAS bi-partite gene expression system, utilizes two or more plasmids one of which (driver) contains the promoter driving expression of the yeast transcriptional activator, Gal4 (Köster and Fraser, 2001). To increase expression levels, the Gal4 gene has been modified by adding the herpes simplex virus transcriptional activation domain VP16 (Sadowski et al., 1988). Once expressed, Gal4 binds to the upstream activating sequence (UAS) on another plasmid construct, which drives the expression of the gene of interest. Depending on the promoter elements in use, the Gal4-UAS system can be used to drive the expression of genes in specific cell populations and/or during specific developmental stages. The advantage of this system is

its flexibility in combining driver and reporter constructs, which allows co-expression of genes in specific cell populations. On one hand injecting constructs into the one cell stage embryo results in mosaic expression patterns, which in extreme cases leads to only a single labeled cell that can be studied in isolation in the living animal (Niell et al., 2004; O'Brien et al., 2009). On the other hand, stable transgenic lines can be generated with small modifications to the DNA injection procedures used to generate so-called 'transient transgenic' fish. For this, the transgene expression cassette is flanked with non-autonomous transposon elements (Tol2), which are recognizable by a specific transposase (Clark et al., 2011). When such a DNA fragment is co-injected with transposase mRNA, the transgene is efficiently integrated into the genome. Insertions occur with sufficient efficiency so that only a small number of animals need to be screened to identify stable transgenic lines. While the Gal4-UAS system is very effective and can be used for numerous applications, the high overexpression of genes that results from its amplification step can interfere with physiological cellular processes. Injections of *in vitro* transcribed capped RNA offer an alternative to DNA injections for gene expression (as illustrated above for transposase expression, Ro et al., 2004). Here too, injections are done at the one-cell stage. This generally results in ubiquitous expression of the relevant gene. Alternative way to achieve mosaic expression is injecting can be performed into individual blastomeres at later stages (16-128 cell stage, England and Adams, 2011). However, as RNA degrades over time, expression is usually limited to the first two days of development.

1.4.2.2. Loss-of-function approaches

The most commonly used method of knocking-down gene expression in zebrafish is the use of synthetic oligonucleotides, called morpholinos, to block the translation of mRNA or inhibit pre-mRNA splicing (Nasevicius and Ekker, 2000). Morpholino injections are rapid, relatively inexpensive and high-throughput. Once injected into one-cell staged embryos, morpholinos are believed to distribute equally among the increasing number of cells at progressive stages of development. However, a diluting effect over time results in their effectiveness being generally limited to the first two to three days post-fertilization. Furthermore the extent to which morpholinos knock-down gene expression is variable between experiments and laboratories. Observed phenotypes could be due to off-target effects, which include widespread cell death, defects in epiboly and neural degeneration (Eisen and Smith, 2008). Some of these off-target effects can be reduced by carefully titrating

the morpholino into an effective but non-toxic dose. Nevertheless there is a need for developing techniques which would be more effective.

1.4.2.3. Locus specific mutagenesis

Generating specific knock-outs of genes have been a big challenge for researchers using zebrafish as a model organism. On one hand morpholinos are not depleting gene product completely and their effects are restricted in time. On the other hand mutagenesis is not target specific. The first promising results of targeted gene knock outs were obtained using zinc fingers nucleases (ZFNs, Doyon et al., 2008). This technique combines sequence specific DNA binding domains fused with a specific DNA cleavage module (Fok1 restriction nuclease). When two ZFNs heterodimerize with genomic DNA in close proximity, Fok1 creates double strand breaks in the target gene. Double strand breaks can be repaired through non-homologous end joining, which is error prone and can result in permanent disruption of the targeted locus. Despite the initial optimism, zinc fingers probes are still not routinely used. This is due to the fact that their design is challenging and requires a lot of expertise, but also the high cost of generating a ZFN mutant. Discovery of transcription activator-like effector nucleases (TALENs), which can recognize specific DNA sequences, led to developing an alternative approach of gene knock out in zebrafish (Bedell et al., 2012). TALEs contain 33-35 amino acid repeat domains that each recognizes a single baspair via two hypervariable residues. TALENs also provide the possibility of knocking-in genes. This happens through homology-directed repair. In this process, the supplied homology-containing donor fragment is inserted at the site of the cleavage. Finally the most recent technique of gene knock-out named after "clustered regulatory interspaces short palindromic repeats" (CRISPR) employs "programmable" RNA-guided DNA endonucleases (Cas, Hwang et al., 2013). Briefly, specially engineered RNA containing the “seed” sequence (crRNA) transcribes to transactivating crRNA, which then binds to the target DNA sequence and results in cleavage by Cas proteins. Since they were first published, all of the described techniques have been modified in order to simplify the process of designing probes, as well as to improve their specificity. One remaining uncertainty is the extent of off-target effects (which after all ended the "glory days" of the morpholinos), where a final consensus on the "gold standard" controls that are required is still outstanding. Moreover, despite the tremendous progress, gene-editing tools are still not commonly used as only a few laboratories have fully mastered their use in the fish model (Schmid et al., 2013). Still, it can be expected that over the next few years "clean" genome-editing will become a routine technique in all zebrafish labs - and zebrafish

will join the ranks of fully genetically accessible organisms, where the extent to which genome-edits are routinely done is less limited by technical feasibility, but by more biological constraints, such as generation time or genome structure. Unfortunately, in this respect, the zebrafish does not compare too well with invertebrates or even the mouse. Still, the fact that many questions require combining *in vivo* imaging in vertebrates with genetic tools will mean that zebrafish will in all likelihood defend and expand its role in experimental biology. One example for this trend is the fast growing field of disease modeling in zebrafish.

1.4.3. Fish as a model for neurodegenerative diseases

The techniques of manipulation of gene expression that I described above are not only used to study gene functions, but also for creating disease models including models of neurodegenerative diseases. The hope that human neurodegeneration could be modeled in fish is motivated by the fact that the organization of the fish CNS in many respects its mammalian counterpart (Mueller and Wullimann, 2005) - certainly to a much larger degree than is true for invertebrates. Many structures of the fish CNS correspond to mammalian brain regions and contain the same cell types ((Sager et al., 2010); see for example the fish retina *vs*. its mammalian and insect counterparts), with similar neuron classes that often use the same neurotransmitters (for example cholinergic motor neurons in fish (Clemente et al., 2004; Mueller et al., 2004) as opposed to glutamatergic neuromuscular transmission in flies) and a similar complement of glial cells (including oligodendrocytes (Tomizawa et al., 2000; Brösamle and Halpern, 2002), and microglia, (Peri and Nüsslein-Volhard, 2008; Sieger and Peri, 2013), which lack strict counterparts in invertebrates). Finally, many of the proteins involved in the pathogenesis of neurodegenerative disease are highly conserved between humans and fish (Howe et al., 2013). It is these specific proteins that are usually targeted in order to create an animal model of a disease. Most commonly fish models are based on gene knock-downs or overexpression. Gene knock-down is achieved through morpholinos (see above). So far a number of genes relevant for Parkinson’s disease have been knocked-down this way causing disease-relevant phenotypes such as a decrease in dopaminergic neuron numbers and impairments in the mitochondrial respiratory chain (Flinn et al., 2009). The same approach was used to generate models of tauopathies (Tomasiewicz et al., 2002) or Huntington disease (Karlovich et al., 1998). An alternative approach is to overexpress mutated forms of genes implicated in disease pathogenesis. An example of such models is an overexpression of mutated version of Tau (P301L, Paquet et al., 2009) or huntingtin (Miller et al., 2005). While such models reconstitute some of the disease pathology, they are usually

transient phenotypes and the effects of off-target toxicity are hard to separate from true disease-related pathology. The recent development of gene-editing techniques now opens new possibilities for stable gene deletion or knock-in of mutant genes. Especially ZFN have been successfully used for deleting genes related to motor neuron disease, remarkably resulting in a complex phenotype with vascular pathology as well as muscle and motor neuron aberrations (Schmid et al., 2013).

Despite these methodological advances, fish models are still flawed by the fact that the observed phenotypes are mostly restricted to developmental stages of the fish and only some of the mutant models have been studied in the adulthood (Chapman et al., 2013). The reason for this being, first, that many of the genuine advantages of the fish model (e.g. its transparency) are lost in adulthood and many routine techniques to characterize disease (such as behavioral tests or routine pathology) are not yet well-developed; second, fish have similar life-spans to mice, hence the "speed" advantage that developmental work with fish enjoys is lost when adult fish are being used. The fact that mostly developmental phenotypes have been characterized raises the question of the relevance of current models to age-associated human pathology. Additionally, despite many similarities, some fundamental differences exist between a fish's and higher vertebrate’s brain. These differences include lack of a layered neocortex and the constant growth of the fish brain (Mueller and Wullimann, 2005; Kizil et al., 2012). Therefore the validity of neurodegeneration or aging studies in fish still needs to be firmly established.

1.4.4. In vivo imaging

In vivo imaging of a higher vertebrate’s nervous system requires invasive surgery - which can be an important confounding factor. Externally developing embryos and transparency of fish larvae allow performing imaging studies without the need of any invasive procedures. Additionally, fish imaging is not restricted to widely-spaced single frames or short time-lapses as used in many *in vivo* imaging studies of mice. In fact, imaging in fish can be done over long periods of time, often covering days (Godinho et al., 2007; Dong et al., 2012; Mateus et al., 2012). Within this time frame, a significant number of developmental processes can be observed from beginning to completion (e.g. formation of the layered structure of the retina with all its neuronal cell types; Godinho et al., 2007). This rapid development of fish embryos is another advantage of fish over other vertebrate animal models. The small size and transparency of fish larvae makes it possible to image a significant part of the nervous systems with confocal imaging - and in some instances even with wide-field microscopy.

Some of the deeper brain structures however do require two-photon microscopy (Niell et al., 2004). Labeling of cells and subcellular structures can be done by using a variety of dyes (Cooper et al., 2005; Ko et al., 2011) as well as fluorescent proteins introduced either as transgenes or through DNA/RNA injections, including the Gal4-UAS system. A variety of UAS responder constructs allows combining whole-cell labeling with labeling of organelles, such as mitochondria or endoplasmatic reticulum. Variety of available constructs for monitoring calcium and ATP levels or ROS production (Li et al., 2005; Berg et al. 2009; Breckwoldt et al. 2013) allows also looking at the functional state of cells and organelles. Expression of these fluorescent markers can be restricted to specific subsets of cells by using specific promoters driving Gal4 expression. For example, a group of Islet promoters label sensory neurons (Korzh et al., 1993), vsx-1 promoter elements label bipolar cells (Vitorino et al., 2009), while brn3c marks retinal ganglion cells (Xiao and Baier, 2007). One neuronal cell type that has lent itself particularly to study axon dynamics and homeostasis due to its geometry, are so called Rohon-Beard sensory neurons (RBNs) that innervate the fish's skin and that can be easily visualized (see below).

1.4.5. Imaging Rohon-Beard neurons

Sensory neurons are commonly chosen for studying axon degeneration and regeneration using *in vivo* imaging (Sagasti et al., 2005; Martin et al., 2010; Rieger and Sagasti, 2011). Sensory neurons can be divided into trigeminal neurons that innervate the head, RBNs that innervate the body at early larval stages and dorsal root ganglia (DRG) that innervate the body at later stages (Metcalfe et al., 1990). From these three types RBNs are particularly interesting due to their optical accessibility for *in vivo* imaging. Most of these cells are born and begin to differentiate by the 2 somite stage. The somata of RBNs are located in the dorsal spinal cord and is easily identifiable in differential interference contrast (DIC)/Nomarski microscopy, which allows electrophysiological recordings without additional labelling (Ribera and Nüsslein-Volhard, 1998). RB cells have two thin, ipsilateral longitudinal axons: one ascending and one descending. The ascending axon extends through the spinal cord and terminates in the hindbrain. The descending axon extends within the spinal cord and then projects directly to the surface, penetrates the basal cell layer of the skin and branches profusely as “free endings” between the two layers of skin (O'Brien et al., 2009). Peripheral sensory axons begin innervating the skin at early developmental stages, when it consists of just few epithelial layers. At 21 hpf axons start to relay mechanosensory stimuli from the trunk and tail regions to the CNS (Saint-Amant and Drapeau, 1998). Superficiality and

relative flatness of RBNs together with easiness in labelling this specific neuronal population by using specific promoters (islet-1, islet-2b; Ben Fredj et al., 2010) makes them a perfect cell type for performing *in vivo* imaging using simple tools like wide field microscopy without the need of surgery. Also, due to the small size of fish larvae, they can be visualized in their entirety without the need of performing surgery.

Despite many advantages of using RBNs for imaging purposes, it is also important to keep in mind some of the disadvantages. First of all, RBNs are a transient population of sensory neurons and at later developmental stages are replaced by DRGs. According to first studies of this transition, RBNs undergo apoptosis around 3 to 4 dpf (Reyes et al., 2004), in an activity-dependent fashion (Svoboda et al., 2001). However there is increasing evidence that they can survive for much longer and do so under physiological conditions. Secondly, peripheral RB axons are unmyelinated. Instead they can be enveloped by keratinocytes and project through the “tunnels” within basal skin cells (O'Brien et al., 2009). This makes them more similar to mammalian nociceptors than to larger-caliber myelinated fibers, which are commonly targeted for regeneration studies (Kang et al., 2008; Duffy et al., 2012; Fricker et al., 2013). Finally, endings of the peripheral neurites do not form synapses. While this preclude studies of synaptogenesis or synaptic plasticity, for studies of mitochondrial dynamics is not relevant or even may be considered an advantage. Therefore zebrafish RBNs fulfil most of the criteria of the perfect model for investigating mitochondrial life-cycle. These include ease of labelling by combing sensory promoter and Gal4-UAS system and relatively easy pharmacological and genetic manipulations. Moreover neurons can be visualized in their entirety using cheap and easy microscopy techniques. Therefore I set out to perform studies of mitochondrial dynamics in this vertebrate model organism.

2. Aims and Rational

The aim of my study was to answer a number of seminal questions regarding the mechanisms that contribute to the proper positioning and homeostasis of neuronal mitochondria in a popular vertebrate model organism - zebrafish. Specifically, I wanted to accomplish the following aims:

1) To develop tools to label and track neuronal mitochondria over long periods of time in zebrafish embryos. Zebrafish larvae are optically accessible to a degree that permits visualizing neurons in their entirety *in vivo*. Hence, zebrafish allow the parallel study of cellular and sub-cellular dynamics in multiple subcompartments of a neuron (e.g. its soma and neurites).

2) To generate a "base-line" data set on mitochondrial dynamics in both single sensory neurons of the fish, as well as a transgenic fish line (*MitoFish*). This data-set provides a back-drop against measurements upon disturbing different parts of motor machinery through both pharmacological and genetic means. Part of this aim was performed in collaboration with Dominik Paquet, Bettina Schmid and Prof. Christian Haass, (LMU, DZNE).

3) To develop tools to study mitochondrial dynamics in single sensory neurons. In this part of my work I especially focussed on identifying sites of mitophagy, a process responsible for removing damaged mitochondria from the peripheral arbor. This is a topic about which very little is currently known. Further I established methods to study mitochondrial fusion using photo-convertible and photo-activateable fluorescent proteins. This part of my work forms the basis of ongoing and future work in my host laboratory.

3. Materials and Methods

3.1. Animals

I used wild-type zebrafish of AB and TLF strains. The following transgenic fish were also used: Isl2b:Gal4 (Ben Fredj et al., 2010), HuC:Gal4-Tau:UAS:DsRed (*TauFish*; Paquet et al., 2009), HuC:Gal4-UAS:DsRed (*RedFish*; Paquet et al., 2009), Huc:Gal4 (neuronal driver; Paquet et al., 2009). The fish were maintained, mated, and raised as previously described (Mullins MC et al., 1994) by our lab's technicians, Yvonne Hufnagel and Kristina Wullimann. Embryos were maintained in E3 or 0.3x Danieau's solution (for recipes see the section **3.12 Solutions and buffers**) at 28.5°C and staged as described (Kimmel et al., 1995). All experiments were performed in accordance with local animal protection standards and were approved by the government of Upper Bavaria (Regierung von Oberbayern, Munich, Germany).

3.2. Cloning protocols

2.2.1. Standard sticky-end cloning protocol

Restriction digest. Both the vector back-bone and plasmid containing the gene of interest were digested with restriction enzymes that are compatible, allowing the annealing of complementary 'sticky' or cohesive ends and thus directional cloning. The reaction was set up according to following protocol:

Reagent	Quantity for 50 µL reaction
DNA	5 – 10 µg
10 x buffer (appropriate for the enzyme, NEB)	5 µL
10 x bovine serum albumin (BSA, NEB, B9001S)	5 µL
Enzyme	10 Units
dH_2O	up to 50 µL

Gel electrophoresis and fragment purification. Following restriction digest, the DNA fragments were run on a gel (typically 1% agarose, Lonza, 50004L), dissolved in TAE buffer (Rotiporese® 50 × TAE Puffer, Roth CL86.1). After separating the restriction enzyme-

digested DNA fragments on a gel, bands of the appropriate size were cut out and purified using a Gel Extraction Kit (Qiagen, #28704).

Ligation. Purified fragments were ligated overnight at 16ºC using T4 ligase (NEB, M0202L) in ligase buffer (NEB, B0202S). Vector and insert were ligated at a ratio 1:3, taking into account their respective size (in base pairs). Typically the vector was used at a final concentration of 50 ng. The formula used to calculate the final concentration of the insert was:

$$ng\ of\ insert = \frac{3 * \text{ ng of vector} * \text{insert size (number of base pairs)}}{\text{vector size (number of base pairs)}}$$

Transformation. 50 µl of competent *Escherichia coli* cells (*E. coli,* NEB, C2988J) were defrosted on ice. Half of the ligation mix volume was added and incubated together with the cells on ice for 30 min. Following a brief heat-shock (42ºC water bath for 30 sec), the cells were allowed to recover for 2 min on ice. 950 µl of super optimal catabolite-repression (SOC) medium (NEB, B9020S) was added to the ligation-bacterial cell mix and incubated for 1 hour at 37ºC in a rotating shaker at 225 rpm. The reaction was then plated on Luria-Bertani (LB, Roth, X969.2) agar plates containing the appropriate antibiotic (100 µg/mL kanamycin, (Calbiochem, #420411) or 100 µg/mL ampicillin (Merck, #171254)) and incubated at 37ºC overnight. The following day single colonies were picked and inoculated into liquid overnight cultures (3 mL LB medium, Roth, X968.1 with addition of the appropriate antibiotic). Bacterial cultures were spun down and plasmids were isolated using a commercial miniprep kit (Qiagen, #27106). Final concentration of the DNA was measured using NanoPhotometer (Implen).

3.2.2. Blunt-end cloning protocol

A blunt-end cloning protocol was used when the enzymes used to cut the vector and insert generate fragments that are not compatible. Therefore the ends of the fragments need to be blunted in order to allow ligation. In addition to the sticky-end cloning steps outlined above, blunt-end protocol requires vector dephosphorylation and blunting the ends of both the vector and insert to allow for ligation.

Vector dephosphorylation. This step prevents the recircularization of the vector. Calf intestine phosphatase (NEB, M0290L) was added to the restriction enzyme-digested vector at a concentration of 0.5 units per 1 µg of DNA. The reaction was incubated for 1 hour at 37ºC.

Blunting of the ends. Most restriction enzymes create fragments with so-called overhangs, meaning that one of the strands is not paired at its end. The large Klenow fragment of DNA polymerase I can be used to fill these ends. The reaction requires 1 Unit of Klenow fragment (NEB, M0210L) per 1µg of DNA and dNTPs (NEB, N0447L) at a concentration of 33 µM each. The reaction was incubated for 15 minutes at room temperature (25^{o}C) and then stopped by adding EDTA (AppliChem, A1104) at a final concentration of 10 mM and incubating at 75ºC for 20 min.

3.2.3. Gateway/TOPO cloning

The Gateway system, which is commercially available from Invitrogen, is based on the well-characterized bacteriophage lambda-based site-specific recombination system. In overview, Gateway is a 2-step cloning process; in the first step a PCR-amplified DNA sequence of interest is inserted into a TOPO Vector to create a so-called Entry Clone.

Reagent	Quantity for 6 µL reaction
Fresh PCR product	0.5 - 4 µL
Salt Solution (Invitrogen, P/N 46-0205)	1 µL
TOPO Vector	1 µL
dH_2O	To final volume of 6 µL

The reaction was incubated for 30 minutes at room temperature. The Entry Clone was subsequently transformed into competent *E.coli*.

The second step transfers the sequence from an Entry Clone into a one of the variety of attB-containing Expression Vectors that can be propagated and expressed in a range of host cells for a given experiment.

Reagent	Quantity for 8 µL reaction
Entry clone	1 - 7 µL (50 – 150 ng)
Destination vector	1 µL (150 ng/µL)
LR Clonase™ II enzyme (Invitrogen, 11791100)	2 µL
TE buffer, pH 8.0	To final volume of 8 µL

The reaction was incubated for 1 hour at 25ºC. Afterwards the 1 µL of the LR reaction was transformed into competent *E.coli*.

3.3. Constructs

To visualize Rohon-Beard sensory neurons and their mitochondria I used plasmid constructs based on the bipartite Gal4-UAS system. We obtained the following plasmids: sensory Isl1:Gal4-VP16 (sensory neuron driver, gift from Alvaro Sagasti, UCLA; Sagasti et al., 2005), UAS:memYFP (gift from Rachel Wong; University of Washington; Schroeter et al., 2006), UAS:mGFP and UAS:TagRFP-T (gift from Martin Meyer, UCL; Hunter et al., 2013), Tau:UAS:DsRed, UAS:DsRed, UAS:GFP.LC3 (gifts from Bettina Schmid; Paquet et al., 2009). Additionally several constructs were generated. These include: UAS:mitoCFP, memYFP:UAS:mitoCFP, UAS:mitoTagRFP-T, UAS:mitoKaede, UAS:mitoPA-GFP, UAS:SNPH.GFP, UAS:SNPHΔMTB.GFP, UAS:KHC-CBD.GFP, UAS:parkinYFP. These constructs were generated using conventional (sticky- and blunt-end cloning) or recombination based (TOPO/Gateway cloning) methods. All the constructs are listed in the **Table 2.1**.

Table 2.1. List of constructs obtained for this study.

construct	source	reference
Islet1:Gal4	Alvaro Sagasti, UCLA	Sagasti et al., 2005
UAS:memYFP	Rachel Wong, University of Washington	Schroeter et al., 2006
UAS:TagRFP-T	Martin Meyer, UCL	Hunter et al., 2013
UAS:mGFP	Martin Meyer, UCL	Hunter et al., 2013
PA-GFP	George Patterson, NIH	Patterson and Lippincott-Schwartz, 2002
SNPH-GFP	Zu-Hang Sheng, NIH	Kang et al., 2008
SNPHΔMTB-GFP	Zu-Hang Sheng, NIH	Kang et al., 2008
KHC.CBD-GFP	Zu-Hang Sheng, NIH	Cai et al., 2005
Kaede	MBL	Ando et al., 2002
Tau:UAS:DsRed	Bettina Schmid, LMU	Paquet et al., 2009
UAS:DsRed	Bettina Schmid, LMU	Paquet et al., 2009
MARK	E.M. Mendelkow	Drewes et al., 1997
ParkinYFP	Konstanze Winkelhofer, LMU	Fett et al., 2010

3.3.1. Cloning of UAS:mitoCFP

The UAS:mitoCFP responder construct was generated by Leanne Godinho by conventional blunt-end cloning (see above). Briefly, a fragment from pECFP-mito (Clontech), encoding a fusion of the mitochondrial targeting sequence of human cytochrome C oxidase and ECFP (mitoCFP), was digested with NheI (NEB, R3131L) and NotI (NEB, R3189L). The mitoCFP fragment was blunted and cloned into a UAS expression vector (cut with EcoRI (NEB, R3101S) and NotI), downstream of a 14-mer UAS Gal4 binding sequence fused to a fish basal promoter *E1b* (Köster and Fraser, 2001).

3.3.2. Cloning of UAS:mitoTagRFP-T

The UAS:mitoTagRFP-T responder construct was generated by Monika Brill. This construct was generated in two steps; first the mitochondrial tag was added by replacing CFP in the pECFPmito vector (digest with NheI and NotI) with TagRFP-T (gift from Martin Meyer, UCL, Hunter et al., 2013; cut out with NotI and XmaI (NEB, R0180L)) by blunt end cloning. In the second step, mitoTagRFP-T fragment was digested with EcoRI and SmaI (NEB, R0141L) restriction enzymes, blunted and cloned downstream of a 14-mer UAS Gal4 binding sequence fused to a fish basal promoter *E1b* (cut with XhoI (NEB, R0146S).

3.3.3. Cloning of UAS:mitoKaede

The UAS:mitoKaede responder construct was generated by Leanne Godinho. First, pmitoKaede was generated by creating an N-terminal in-frame fusion between the coding sequence of Kaede (AM-V0011, MBL International Corporation) and the mitochondrial targeting sequence from subunit VIII of the human cytochrome c oxidase gene (Clontech). Here pSL1180 Kaede (containing the coding sequence of Kaede) and pECFP-mito (Clontech) were used as insert and vector backbone respectively. Sequential restriction digests with BamHI (NEB, R3136L) and NotI were used for cloning using sticky-end cloning protocol (see above). The mitoKaede fragment from pmitoKaede was digested using NheI, blunted and cloned into a UAS expression vector (cut with EcoRI and NotI), downstream of a 14-mer UAS Gal4 binding sequence fused to a fish basal promoter *E1b*.

3.3.4. Cloning of UAS:mitoPA-GFP

The UAS:mitoPA-GFP was cloned from pPA-GFP (kind gift from George Patterson, NIH; Patterson and Lippincott-Schwartz, 2002) in two steps. In the first step pmitoPA-GFP was generated by replacing CFP with PA-GFP in the pECFPmito plasmid (Clontech) using conventional sticky-end cloning. Briefly, pPA-GFP and pECFPmito were digested with BamHI and NotI and cloned according to the sticky-end cloning protocol. In the second step mitoPA-GFP fragment was cut out with NheI and XbaI (NEB, R0145L) and inserted downstream of a 14-mer UAS sequence in our standard UAS expression vector (cut with EcoRI and NotI) by blunt-end cloning.

3.3.5. Cloning of memYFP:UAS:mitoCFP

The bidirectional memYFP:UAS:mitoCFP construct was generated by Dominik Paquet from the laboratory of Prof. Christian Haass. It was made by replacing DsRed and the Gateway Cassette GW-R1-R2 in the vector pT2d-DEST_pA_DsRed-T4_E1b_UAS_E1b_GW-R1-R2_pA (Paquet et al., 2009) with memYFP and mitoCFP. In a first step E1b_UAS_E1b was subcloned into pCS2+_memYFP by EcoRI. Then, E1b_UAS_E1b_memYFP_pA was transferred to pT2d-DEST_pA_DsRed-T4_E1b_UAS_E1b_GW-R1-R2_pA by a StuI (NEB, R0187L) and PspOMI (NEB, R0653L) digest. MitoCFP was amplified by PCR using the following primers: mitoCFP-F Kozak 5'-GCCACCATGTCCGTCCTGACGCCG-3' and GFP-R BamHI 5'-GGCGGCCGCGGATCCTTACTTGTACAGCTCGTCCATGC-3', TOPO-cloned into pCR8/TOPO/GW (Invitrogen) and sequenced. MitoCFP was then LR recombined into pT2d-DEST_pA_memYFP_E1b_UAS_E1b_GW-R1-R2_pA, using LR Clonase II according to the manufacturer's instructions, which yielded the Expression construct pT2d-EXP_pA_memYFP_E1b_UAS_E1b_mitoCFP_pA.

3.3.6. Cloning of UAS:syntaphilin.GFP and UAS:syntaphilinΔMTB.GFP

Human syntaphilin (SNPH) fused with GFP and a truncated form of syntaphilin lacking the microtubule binding domain (SNPHΔMTB) also fused with GFP were kind gifts from Prof. Zu-Hang Sheng (NIH; Kang et al., 2008). These two genes were cloned by Monika Brill. SNPH-GFP was cut out with NheI and SacII (NEB, R0157S) and SNPHΔMTB-GFP was cut out with SmaI and NheI. Both fragements were then blunt-end cloned into a UAS

expression vector (cut with EcoRI and NotI), downstream of a 14-mer UAS Gal4 binding sequence fused to a fish basal promoter *E1b*.

3.3.7. Cloning of UAS:kinesin heavy chain cargo binding domain

Human kinesin heavy chain – cargo binding domain (KHC-CBD) fused to a GFP was a kind gift from Prof. Zu-Hang Sheng (NIH; Cai et al., 2005). This encodes a truncated form of kinesin which lacks a motor domain and therefore acts as a dominant negative construct. This construct was cloned by Monika Brill. Briefly, KHC-CBD.GFP was cut out with NheI and XbaI and blunt-end cloned into a UAS expression vector (cut with XhoI), downstream of a 14-mer UAS Gal4 binding sequence fused to a fish basal promoter *E1b*.

3.3.8. Cloning of UAS:parkinYFP

The parkinYFP construct was a kind gift from Konstanze Winkelhofer (Fett et al., 2010). ParkinYFP was cloned into UAS vector using Gateway cloning technique. ParkinYFP was amplified by PCR using parkin forward primer (5'-ACCATGATAGTGTTTGTCAGGTTCA-3') and YFP reverse primer (5'-TTACTTGTACAGCTCGTCCATGCCGAGAGT-3').

PCR reaction:

Reagent	Quantity for 50 µL reaction
30 µg/µL DNA template	5 – 10 µg
10 x High Fidelity PCR Buffer (Invitrogen, P/N 52045)	5 µL
10 mM dNTPs mix (NEB, N0447L)	1 µL
50 mM $MgSO_4$ (Invitrogen, P/N 52044)	2 µL
10 pM forward primer	2 µL
10 pM reverse primer	2 µL
5 Units/µL Platinum Taq High Fidelity polymerase (Invitrogen, 11304011)	0.2 µL
dH_2O	35.8 µL

PCR steps		Temperature	Duration
Initial denaturation		94ºC	2 min
30 cycles	Denaturation	94ºC	30 sec
	Annealing	60ºC	30 sec
	Elongation	68ºC	3 min
Final elongation		72ºC	10 min

The PCR product was cloned into an Entry vector (pCR8/GW/TOPO vector, Invitrogen, 12355-079) according to manufacturer's instructions. Next I performed an LR reaction in order to insert parkinYFP into a destination vector (pT2d-DEST_UAS_E1b_GW-R1-R2_pA, gift from Dominik Paquet). The final construct was transformed to *E.coli* using standard transformation protocol.

3.4. Single cell labeling of Rohon-Beard neurons and their mitochondria

For measurements in single cells I used a sensory neuron-specific driver construct (Isl1:Gal4-VP16; Sagasti et al., 2005) together with separate UAS responder constructs. Driver and responder constructs (each at concentrations between 5 – 10 ng/µl diluted in 1x Danieau's) were co-injected into fertilized eggs of AB wild-type zebrafish at the one-cell stage, resulting in mosaic expression of the transgenes. As an alternative I used the Isl2b:Gal4 or HuC:Gal4 driver line and injected only responder constructs. Newly collected eggs were put in agarose molds and oriented so that the cell would be on the top left hand side. DNA construct mix was injected using glass injection capillaries (World Precision Instruments Inc., TW100F-4). Suitable glass capillaries were drawn out on a Sutter puller (Sutter Instruments Co., Flamming/Brown Micropippette Puller P-97). These capillaries were backfilled with the DNA mix, fixed on the injection holder and attached to the injector (Eppendorf). The tip of the needle was then cut in order to allow release of the DNA mix when pressure was applied. Needles were pushed through the chorion and the yolk and targeted to the cell. Once in the cell a single air pressure pulse was applied to inject the DNA into the cell. Injected eggs were maintained in 0.3x Danieau's solution or in E3 medium. At 24 hpf embryos were transferred to and maintained in 1% N-phenylthiourea (PTU) solution (in 0.3x Danieau's solution or in E3 medium) in order to prevent pigmentation.

3.5. Generation of transgenic ‘MitoFish’

Transgenic *MitoFish* with fluorescently labeled mitochondria and cell membranes were generated by Dominik Paquet from the laboratory of Prof. Christian Haass (LMU, Munich). The expression construct (mitoCFP:UAS:memYFP) was introduced into the fish genome as previously described (Paquet et al., 2009). Transgenic *MitoFish* were obtained by crossing the memYFP:UAS:mitoCFP responder line to HuC:Gal4 driver line.

3.6. Nocodazole treatment

Embryos for nocodazole treatment were kept in E3 medium. At 1dpf, embryos were transferred to nocodazole (200 nM, Sigma, M1404) dissolved in E3 medium containing DMSO (1%, Sigma, D2650) and PTU (1%) and maintained in this solution for 24 hours prior to imaging at 2 dpf. Control embryos were maintained in E3 medium containing DMSO (1%) and PTU (1%) without nocodazole. Nocodazole treatment experiments with *MitoFish* were performed by Dominik Paquet.

3.7. MARK mRNA synthesis and injection

To overexpress MARK or mutant MARK in zebrafish embryos, Dominik Paquet and Alex Hruscha from the laboratory of Prof. Christian Haass (LMU, Munich) generated mRNA from pcDNA3.1_HA-MARK-WT or T208A/S212A (a gift from E.M. Mandelkow, DZNE Bonn; Drewes et al., 1997) using the Ambion mMESSAGE mMACHINE kit (Applied Biosystems, AM1340) according to the manufacturer’s instructions. mRNA was injected at 300 ng/µl into one-cell-stage zebrafish embryos.

3.8. In vivo imaging

At different ages (from 2 to 7 dpf), embryos were prepared for *in vivo* imaging as described in (Godinho, 2011). Briefly, following manual dechorionization embryos were anesthetized using tricaine in Danieau’s solution or E3 medium containing PTU (1%). Embryos were then embedded in low melting agarose (0.7 - 0.8 %, Sigma) containing PTU and tricaine and subsequently immersed in medium which also contained both PTU and tricaine. For nocodazole-treated embryos also 1% DMSO was added to both the medium and agarose. For experiments in which cells were to be re-imaged on the following day, embryos were unmounted from the agarose, allowed to recover in PTU-containing medium overnight

and remounted in agarose prior to imaging at 3 dpf. For long-term tracking experiments fish were mounted and imaged at days 3, 5 or 7dpf.

To investigate mitochondrial dynamics in single cells, agarose-embedded embryos were screened for co-expression of fluorescent proteins in isolated Rohon-Beard sensory neurons. Mitochondrial transport was imaged in the stem axon using a wide-field fluorescence microscope (Olympus BX51W1) equipped with a ×100/ N.A. 1.0 water-immersion dipping cone objective, an automated filter wheel (Sutter) and a cooled CCD camera (either Retiga EXi; Qimaging; Photometris CoolsnapHQ2, Visitron Systems or SensiCam, Pco Imaging) and controlled by μManager, an open source microscopy software (http://valelab.ucsf.edu/~MM/MMwiki/index.php/MicroManager%20Project%20Overview;). I acquired twelve ten-minute movies with an imaging frequency of 0.5 Hz and an exposure time between 200 and 500 ms. Neutral density filters were used to attenuate the light when necessary. Embryos were maintained at 27-28^{o}C for the duration of imaging. Following transport measurements, the morphology and mitochondrial distribution of the soma, stem axon and entire peripheral axonal arbor of the Rohon-Beard neuron was reconstructed by confocal microscopy (Olympus FV1000, ×20/ N.A. 0.95 water-immersion dipping cone objective).

For the bulk mitochondrial assays, sensory neurons from the caudal part of the tail region in transgenic MitoFish (HuC:Gal4 driven) were imaged using a Zeiss Axioplan 2 wide-field fluorescence microscope equipped with a ×40/N.A. 0.8 water-immersion dipping cone objective, an automated filter wheel (Zeiss) and a cooled CCD camera (Retiga 2000R; Qimaging) or automated filter wheel (Sutter) and a cooled CCD camera (SensiCam, Pco Imaging) controlled by μManager software. For each specimen, we first took single frames of each fluorescent channel and then acquired ten-minute movies of the mitoCFP channel with an imaging frequency of 1 Hz. An exposure time of 400ms was chosen for all images. Neutral density filters were used to attenuate the light when necessary. Embryos were maintained at 28^{o}C for the duration of imaging.

For long-term imaging I mounted embryos as described above and imaged using Zeiss ×40/ N.A. 1.0 water immersion dipping cone objective with frequency of 0.3 Hz and exposure time of 300ms. The average time of the time-lapse was 1.5 hours depending on the bleaching of the sample. Neutral density filters were used to attenuate the excitation light during imaging.

3.9. Activation of photo-activatable and photo-convertible proteins

Fish injected with mitochondrially-tagged photo-convertible (Kaede) and photo-activatable (PA-GFP) were maintained in the darkness to prevent activation prior to the experiment. Kaede positive fish at 2dpf were mounted as described above and imaged with a confocal microscope (Olympus FV1000) and a ×20/ N.A. 0.95 water immersion dipping cone objective. For activation I used the tornado mode of stimulation and 405 nm laser for duration of 5 to 20 frames and laser power of 5 – 20% depending on the activation efficiency. As scattered light can convert the surrounding of the selected region of interest (ROI), the area to convert was selected smaller than the actual size of the cell body. Images of the peripheral arbor were taken immediately after the activation to ensure no conversion of the distal parts of the arbor, and again one and two hours post- activation.

Fish injected with mitoPA-GFP were mounted at 3dpf and imaged on a wide-field microscope (Olympus BX51W1 with Retiga EXi; Qimaging; Photometris CoolsnapHQ2, Visitron Systems) using a ×60/ N.A. 1.0 water immersion dipping cone objective. Mitochondria were activated with an ultraviolet LED with closed field-stop for 20 – 60 sec depending on the activation efficiency. Following activation, fish were imaged at a frequency of 0.3 Hz, and exposure time of 100 – 500 ms. Neutral density filters were used to attenuate the light during imaging.

3.10. Image analysis and processing

Wide-field images or confocal image stacks were viewed and processed using open-source ImageJ/Fiji software (http://fiji.sc). To represent the spatial location of individual mitochondria over time within the stem axon of RBNs, I generated kymographs using the Reslice tool in Fiji with a slice spacing of 1pixel. To determine the transport flux in single Rohon-Beard neurons, I determined the number of anterogradely and retrogradely moving mitochondria crossing a vertical line drawn across the stem axon.

Mitochondrial volume was calculated under the assumption that a mitochondrion has a cylindrical shape. Half of the mitochondrial width was taken as the radius of the base (r) of the cylinder and the length of the mitochondrium as its height (H). To calculate the volume I used the following equation: $V=H*\pi*r^2$.

To determine the transport characteristics of individual mitochondria, I used the MTrackJ plug-in (ImageJ/Fiji; developed by E. Meijering, Biomedical Imaging Group, Erasmus Medical Center, Rotterdam). I measured the average and moving speed as well as pause

frequency and time spent stopping. A mitochondrion that moved less than 0.25 µm between frames was regarded as having paused, while the periods of movement between pauses were regarded as 'runs'. Average speed was defined as the maximal displacement of a mitochondrion divided by the time over which it was observed, while average moving speed was defined as displacement during uninterrupted 'runs' divided by the duration of the run. I divided the number of pauses during a period by the duration of that period to calculate pause frequency and I defined the average time a mitochondrion spent stopping by calculating the average length of pauses during a period of measurement. In these analyses I only included mitochondria that could be tracked for at least 8 frames.

To determine mitochondrial density in single neurons, the total number of mitochondria in the peripheral axon was counted. The length of the peripheral axon was measured from maximum intensity projections of confocal stacks using the Simple Neurite Tracer plugin in Fiji/ImageJ. The peripheral axon was divided into 3 segments, stem, core and periphery. The axonal segment emanating from the soma but before the first branching point was regarded as the stem. The arbor was divided into a core and periphery, the latter being the very last branches of the arbor that did not branch themselves.

The analysis of transport in the periphery was performed together with Dominik Paquet from the laboratory of Prof. Christian Haass (LMU, Munich). For the bulk mitochondrial assays in transgenic *MitoFish*, wide-field images were cropped to a region of interest, in which most neurites were in focus. Only images with a total neurite length above 2500 pixels (732 µm) after cropping were used for analysis. To determine mitochondrial density, the number of mitochondria and length of the neurites was measured as described above. For the 10-minute movies of the mitoCFP channel, we first enhanced contrast of all pictures to 0.1% saturated pixels in Fiji/Image J using the Enhance Contrast function. Then we reduced background by using the WalkingAverage plugin averaging 3 frames and finally we reduced drifting of the specimen using the StackReg/Rigid Body plugin. Movements of individual mitochondria were then analyzed frame by frame by determining the start and end time-points, the location of the movement and the length of the neurite between these two time-points. From these measurements, we calculated the flux density (density of moving mitochondria) and average mitochondrial speed per fish. For all movement events, we set a minimum threshold of 35 pixels (10 µm) movement distance to exclude paused mitochondria exhibiting Brownian motion.

The long time-lapse movies were analyzed for disappearance of mitochondria manually using Fiji in order to determine the final destination and origin of the moving mitochondria.

Photo-activation efficiency was calculated by measuring the brightness of the somal mitochondria in individual channels and subtracking the background. The same measurement was performed for individual mitochondria at each time point (immediately after, 1 and 2 hours after photo-conversion).

3.11 Statistics

Mean values and standard error of the mean (SEM) were calculated using Microsoft Excel. All of the samples were then tested for normal distribution with D'Agostino-Pearson test using Graphpad Prism 5. To test samples that were normally distributed we used t-tests. Anterograde and retrograde fluxes as well as differences between measurements on day 2 and 3 were compared using paired t-test. To compare mitochondrial speeds, pause frequencies and time spent stopping we used unpaired t-test. When samples did not follow normal distribution we used the Mann-Whitney test calculated by the open source software package R and R commander (http://www.r-project.org/). Data are presented as mean ± SEM. $P < 0.05$ was considered significant.

3.12 Solutions and buffers

All the solutions were made by me, technicians in the lab (Kristina Wullimann, Yvonne Hufnagel and Sarah Bechtold) or other lab members (Peter Engerer).

Danieau's solution

Reagent	Quantity for 1L of 30 x concentrated solution
NaCl (Sigma, S7653)	91.52 g (1.74 M)
KCl (Sigma, P9541)	1.41 g (21 mM)
$MgSO_4$ (Sigma, 230391)	2.66 g (12 mM)
$Ca(NO_3)_2$	3.83 g (18 mM)
HEPES	32.17 g (150 mM)
dH_2O	900 mL
Adjust pH to 7.6	

3-amino benzoic acid ethylester (TRICAINE)

Reagent	Quantity for 50 mL 20x concentrated stock
Tricaine (Sigma, A-5040)	200 mg (15 mM)
dH_2O	48 mL
Tris pH 9	2 mL
Adjust pH to 7	

Aliquot out and store at -20ºC. To prepare 1 x concentrated working solution, 2.5 mL Tricaine aliquot was dissolved in 50 ml of 0.3 x concentrated Danieau's.

1-phenyl-2-thiourea (PTU)

Reagent	Quantity for 100 mL of 50x concentrated solution
PTU (Sigma, P7629)	152 mg (50%)
dH_2O	100 mL

Aliquot out and store at -20ºC. To prepare 1 x concentrated working solution, 1 mL PTU aliquot was dissolved in 50 ml of 0.3 x concentrated Danieau's.

4. Results

4.1. Single cell assay – transport measurements

To visualize single cells and their mitochondria in living fish larvae I used the bipartite Gal4-UAS expression system (Köster and Fraser, 2001). This kind of labeling has been shown to be non-toxic (Kim et al., 2008). Mitochondrially targeted cyan fluorescent protein (UAS:mitoCFP) was co-injected with membrane-targeted responder construct (UAS:memYFP) to visualize mitochondria and the morphology of the cell (**Fig. 4.1**). The expression of the responder constructs was restricted to sensory neuron due to specific Gal4 driver construct (Islet-1:Gal4; Sagasti et al., 2005). Often the pattern of labeling was restricted to single Rohon-Beard neurons (**Fig. 4.1B**). I selected cells the arbors of which could be easily identified. For experiments which required very high expression levels of responder constructs or broader labeling patterns, I used the driver lines HuC:Gal4 (a pan-neuronal line) or Isl2b:Gal4 (sensory neurons line) and co-injected only the responder constructs. This approach shows the versatility of Gal4-UAS system, which permits creating driver and responder lines that can be combined with co-injections of DNA plasmids for achieving versatile and tailored expression patterns.

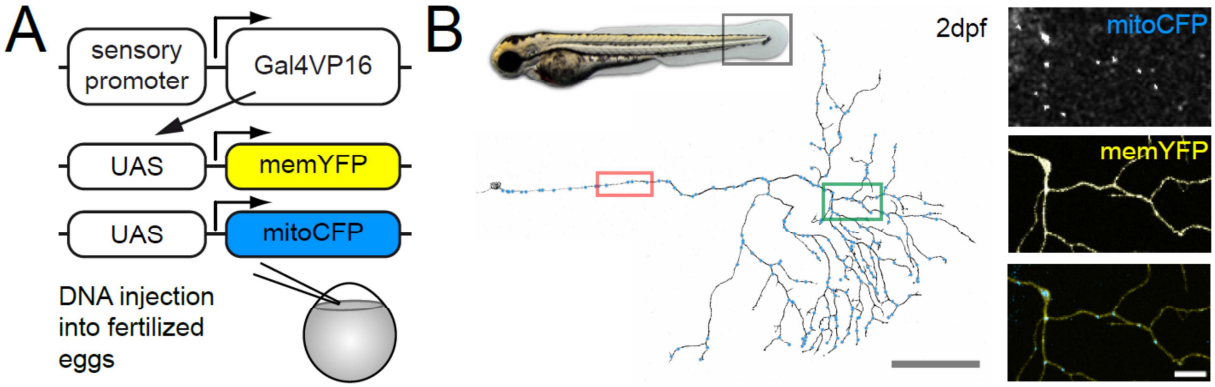

Figure 4.1. Experimental design.

(**A**) Schematic of constructs used to label membrane (memYFP) and mitochondria (mitoCFP) in RB neurons. (**B**) RB neuron at 2dpf (**Grey box**: illustrates imaged area on a small image of a fish larva). **Red box**: Area of "stem axon" imaged in **Fig.4.2**. **Green box**: Area magnified to right, showing mitochondria (top) and membrane (middle); merge at bottom. Scales: **B**, 100µm (magnifications, 20µm).

4.1.1. Measurements in the stem axon

As discussed in the Introduction section, the location of Rohon-Beard neurons and their two-dimensional geometry make them ideal for *in vivo* wide-field microscopy. Therefore at 2 dpf, I selected larvae with singly labeled RBNs and took time-lapse movies of the transport of mitochondria in the stem axon (proximal to the first peripheral branch point; **Fig. 4.1B, 4.2A**). Analysis of these movies revealed that more mitochondria move anterogradely than retrogradely (antero: 0.55 ± 0.04 *vs.* retro: 0.32 ± 0.03 mito/min, n = 26 fish, $p < 0.0001$; **Fig 4.2B**). To test whether this imbalance corresponds to an overall net translocation of mitochondria to the peripheral arbor, I attempted to estimate the volume of motile mitochondria, which traveled in either direction using length and width measurements and a cylindrical approximation. The volumes of mitochondria moving in antero- and retrograde direction, as measured by light microscopy, appears to be the same (antero: 0.21 ± 0.01 *vs.* retro: 0.23 ± 0.01 μm^3; n = 200 mitochondria from 5 fish in each direction, $p > 0.05$; **Fig. 4.2C**).

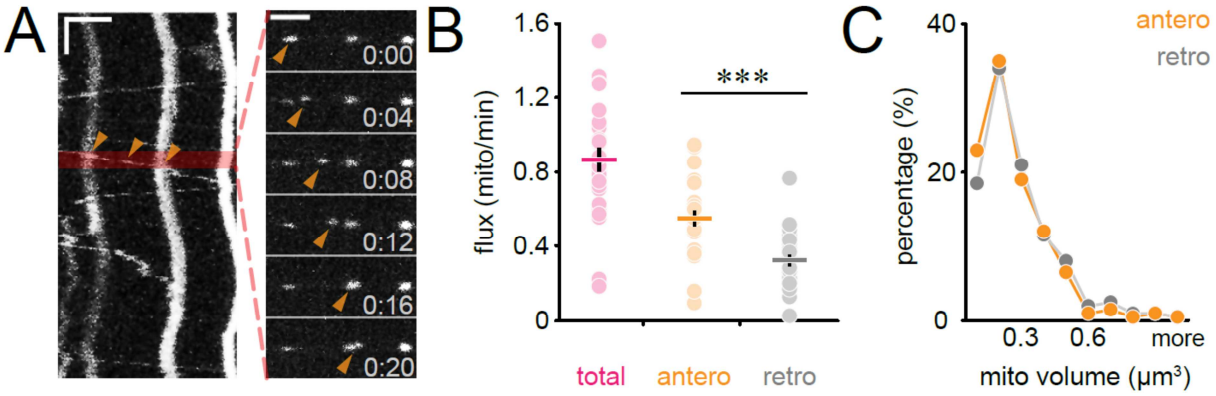

Figure 4.2. Characterization of mitochondrial transport in RB neuron stem axon

(**A**) Kymograph (area in red box in **Fig.1B** imaged for 10 minutes). Arrow-heads: moving mitochondrion (single frames, min:sec). (**B**) Mitochondrial flux (stem, 2 dpf). (**C**) Distribution of the volume of mitochondria moving in antero- and retrograde direction. **A**, vertical (time) 60sec, horizontal (distance) 5µm. Data points: **B**, cells, lines: mean ± SEM.

4.1.2. Mitochondrial movement characteristics

Next, I measured the average speed of moving mitochondria (**Fig. 4.3A**) to be able to compare how transport parameters in the fish compare to measurements from *in vitro* studies, Drosophila and mouse models. The average speed of mitochondria moving in the antero- or retrograde direction did not differ (antero: 0.68 ± 0.02 *vs.* retro: 0.73 ± 0.03 μm/sec, n > 140 mitochondria from 12 fish, p > 0.17; **Fig. 4.3B**). This was a surprise as kinesins and dyneins have been shown to move at different speeds. Therefore I performed a more detailed analysis of mitochondrial movement characteristics, namely, "moving" speed, pause frequency and pause length (for definitions, see *Materials & Methods*; **Fig. 4.3A**). These measurements showed that retrogradely-moving mitochondria displayed significantly faster moving speeds during uninterrupted "runs" than anterogradely-moving ones (antero: 0.77 ± 0.01 *vs.* retro: 0.92 ± 0.02 μm/sec, n > 140 mitochondria from 12 fish, p < 0.0001; **Fig 4.3C**). The discrepancy between average and moving speed is explained when looking at the pause frequency and time spend stopping. It turns out that retrogradely-moving mitochondria paused more frequently (antero: 2.23 ± 0.18 *vs.* retro: 2.83 ± 0.17 pauses/min, n > 140 mitochondria from 12 fish, p < 0.002; **Fig. 4.3C**) and for longer times (antero: 3.6 ± 0.6 *vs.* retro: 4.9 ± 0.5 sec, n > 140 mitochondria from 12 fish, p < 0.001; **Fig. 4.3C**).

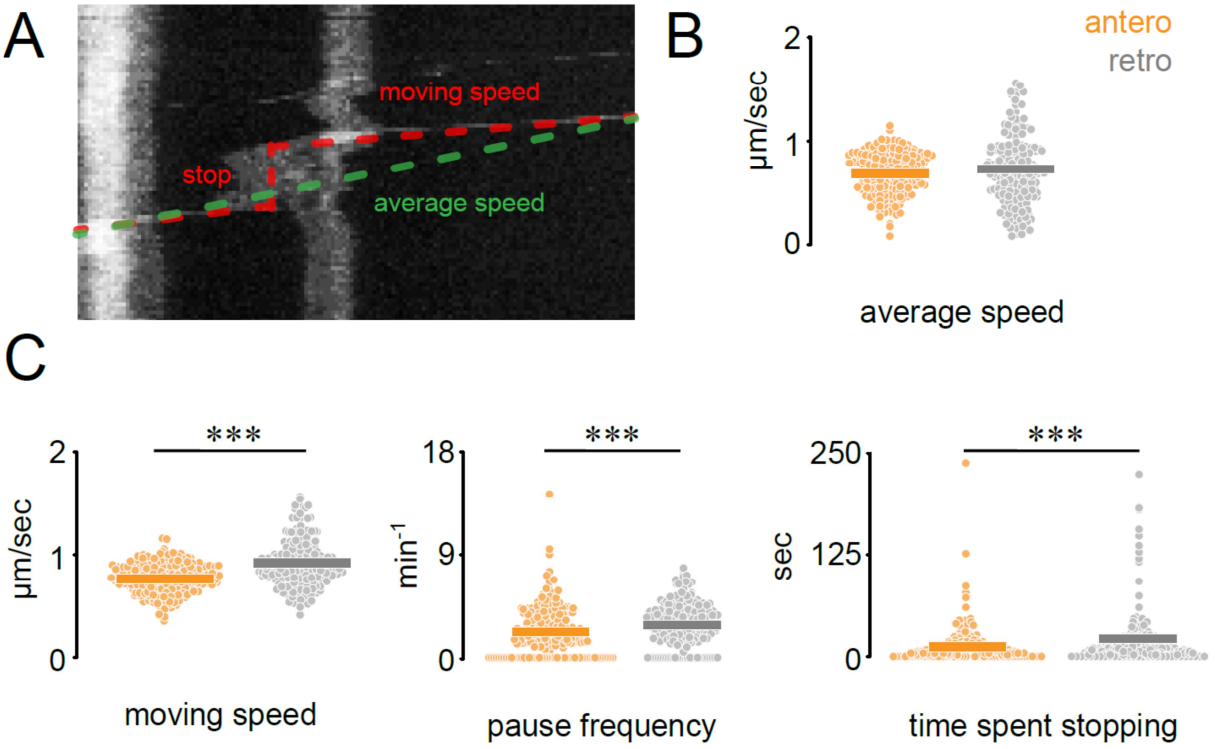

Figure 4.3. Characterization of single mitochondrion movement

(**A**) Schematic representation of measured parameters. (**B**) Average speed of mitochondria. (**C**) Detailed analysis of single mitochondrion movement. **Left**: moving speed, **middle**: pause frequency, **right**: time spend stopping. (**B**, **C**) Data points: mitochondria; lines: mean ± SEM.

4.1.3. Transport changes over time

Following the measurements in the stem axon, I reconstructed the soma and entire peripheral arbor of the neuron using confocal microscope. Afterwards fish were removed from the agarose and allowed to recover. Due to the sparse labeling of the neurons, I was able to re-identify and perform the transport measurement at 3dpf (**Fig. 4.4A**). This kind of experiment allows exploring whether axonal growth and transport are correlated. Surprisingly the analysis of the transport showed that flux rates between day 2 and day 3 post fertilization remain the same (compare values from 2 dpf described above with those at 3 dpf, antero: 0.53 ± 0.04, retro: 0.27 ± 0.03 mito/min, n = 19 cells, p > 0.4; **Fig. 4.4B**), while cells grew by ~30% (3.82 ± 0.32 to 5.02 ± 0.45 mm, n ≥ 19 cells, p < 0.01; **Fig. 4.4C**). Statistical analysis of the growth versus net translocation confirmed that there was no correlation between these parameters. At the same time, the number of mitochondria in the arbors increased from 2 to 3 dpf proportionally to growth (2 dpf: 225 ± 16; 3 dpf: 334 ± 36, n ≥ 14 cells, p < 0.05; **Fig. 4.4C**), leaving density largely constant, even though we detected a small (< 10%), but statistically significant difference (2 dpf: 65 ± 3 *vs.* 3 dpf: 71 ± 4 mito/mm, n ≥ 14 cells, p < 0.05; **Fig. 4.4D**).

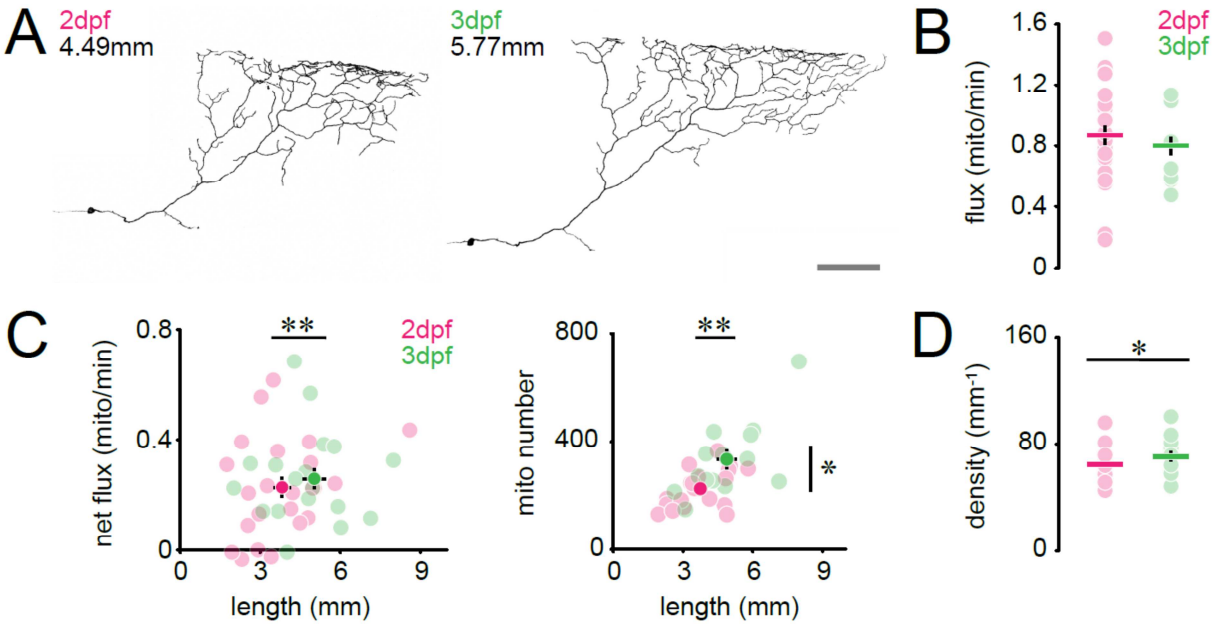

Figure 4.4. Mitochondrial dynamics during cell growth.

(**A**) The same RB neuron at 2 and 3dpf. (**B**) Total mitochondrial flux (anterograde plus retrograde) over time. 2 dpf values in **B** are replotted from **Figure** 4.**2B**. (**C**) Left, net mitochondrial flux (anterograde minus retrograde) and, right, number of mitochondria *vs.* arbor size. (**D**) Density of mitochondria over time. **A**, Scale: 100µm. **B-D**, Data points: cells; lines, mean ± SEM.

4.2. Modulation of transport in single cell assay

In the next step I wanted to evaluate, whether the assay that I developed can be used to analyze changes in transport upon pharmacological and genetic alterations. I chose to test drugs and proteins which are known to be important for mitochondrial transport. For pharmacological manipulation I used nocodazole (a microtubule-destabilizing compound). To disrupt mitochondrial transport through genetic means I used a number of different DNA constructs. These included domains of kinesin (the main motor of anterograde transport; Vale et al., 1985), syntaphilin (a docking protein; Kang et al., 2008) and mutated form of Tau (a microtubule-associated protein; Mandelkow et al., 2003). These proteins are different components of the transport machinery and together they give an overview of possible sites of transport manipulations in the fish model.

4.2.1. Pharmacological transport modulation - nocodazole

Nocodazole is an inhibitor of microtubule assembly (Vasquez et al., 1997), which has been shown to influence the transport of organelles (Morris and Hollenbeck, 1995). To test its effect on mitochondrial distribution, I treated 1-day-old fish with nocodazole (200 - 400 mM in 1% DMSO) and used DMSO as a control. As expected, disruption of microtubular transport tracks caused a reduction in mitochondrial total density (85.8 ± 8.8% of DMSO control; **Fig. 4.5B**), which was even more pronounced in the distal parts of nocodazole-treated axons (73.8 ± 8.8%; **Fig. 4.5B**), while the opposite was seen in the stem axon (127.4 ± 12.2%; **Fig. 4.5B**). These results suggest that mitochondrial trafficking in the nocodazole treated fish is impaired, which results in retention of the cargo in the more central parts of the cell. Changes in transport, however, did not reach statistical significance ($p > 0.4$, $n = 9$ cells). Overall, while I was able to characterize the effect of nocodazole on mitochondrial trafficking, obtaining sufficient numbers of cells to overcome the large base-line variation proved difficult due to the need to identify and measure one cell at a time.

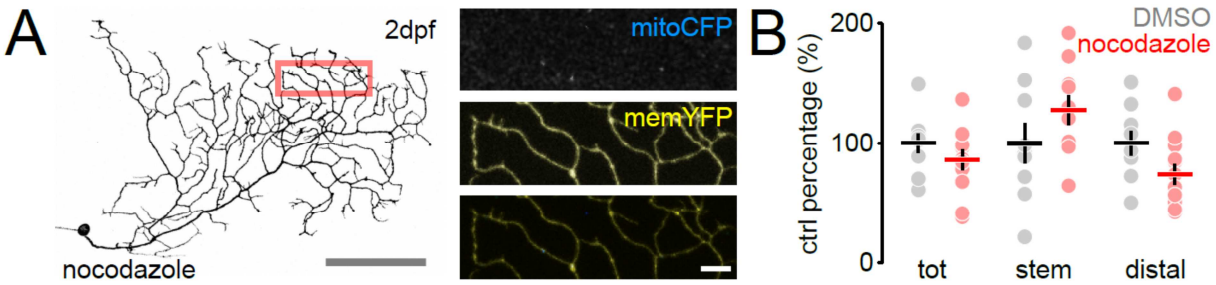

Figure 4.5. Effect of nocodazole treatment on mitochondrial density

(**A**) Nocodazole-treated RB neuron (2dpf). **Red box**: Area magnified to right. Normalized mitochondrial densities (total and in sub-compartments) in vector- (DMSO) and nocodazole-treated RB neurons. **A**, Scales: 100µm (magnifications, 10µm). **B**, Data points: cells; lines, mean ± SEM.

4.2.2. Genetic transport modulation I - kinesin heavy chain

Kinesin is a major motor protein driving anterograde transport of mitochondria (Vale et al., 1985). To modulate mitochondrial transport *in vitro* Prof. Sheng's laboratory at NIH generated a truncated form of kinesin – kinesin heavy chain cargo-binding domain (KHC-CBD), which lacks the motor domain (**Fig. 4.6B)**. This kinesin retains the ability to bind the cargo, but is not able to move along microtubules - and hence, when overexpressed, can act as a dominant-negative inhibitor. This truncated kinesin is fused to GFP to allow identifying positive cells for KHC-CBD. My colleague, Monika Brill cloned this construct under the UAS promoter to allow expression in sensory neurons when combined with Isl1:Gal4 driver (**Fig. 4.6A, C**). Kinesin is expressed throughout the cell; therefore the labeling pattern appeared as cytoplasmic with a gradient towards the tips of the cell (**Fig. 4.6C**). Cells positive for KHC-CBD.GFP had an altered morphology with simplified peripheral arbors. I also measured the transport of mitochondria in the stem axon (**Fig. 4.6D**). As expected, I observed a severe decrease in the mitochondrial flux in both antero- and retrograde direction (GFP: antero: 0.65 ± 0.18, retro: 0.4 ± 0.01 mito/min, n = 3; KHC-CBD.GFP: antero: 0.16 ± 0.05, retro: 0.08 ± 0.05 mito/min; n = 6; p = 0.02; **Fig. 4.6E**).

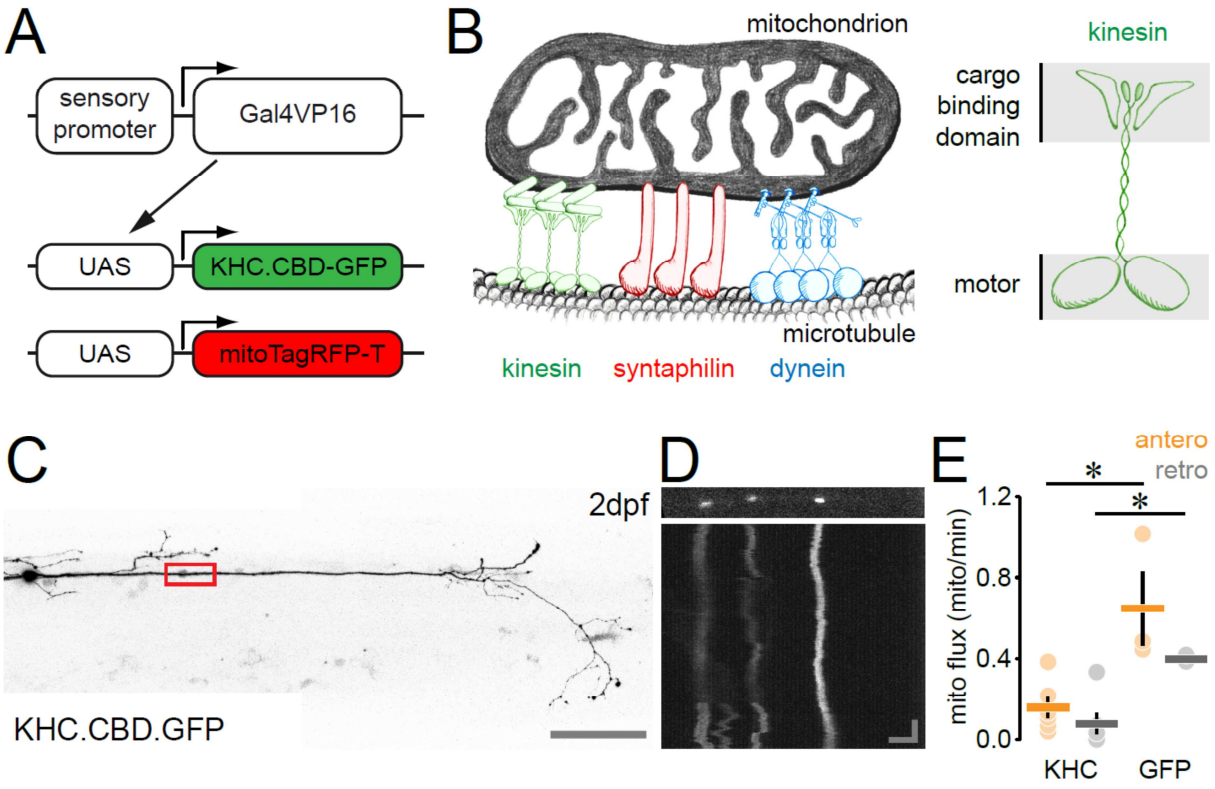

Figure 4.6. Effects of kinesin heavy chain cargo binding domain overexpression on mitochondrial transport

(**A**) Schematic of constructs used to label mitochondria (mitoTagRFP-T) and overexpress kinesin (KHC.CBD-GFP) in RB neurons. (**B**) Schematic of molecular motors and kinesin structure. (**C**) 2dpf RB neuron overexpressing KHC.CBD-GFP **Red box**; Area of "stem axon" imaged in **D**. (**D**) Kymograph (area in red box in **C** imaged for 10 minutes). (**E**) Mitochondrial flux in KHC.CBD-GFP and in GFP only positive cells (stem, 2dpf). Scales: **C** 100µm; **D** horizontal: 5µm, vertical: 60sec; data points: cells; lines mean ± SEM.

4.2.3. Genetic transport modulation II - syntaphilin

The next construct I tested was syntaphilin fused to GFP (SNPH-GFP). Syntaphilin has been identified as a docking protein, present exclusively on stationary mitochondria (Kang et al., 2008; **Fig. 4.7B**). *In vitro* overexpression of syntaphilin results in an increase in the stationary population of mitochondria. Like KHC-CBD.GFP, Monika Brill cloned syntaphilin into a vector, where it is placed under UAS-control. Injection of SNPH-GFP resulted in punctae labeling (**Fig. 4.7A, C**). Most of these punctae co-localized with mitochondria. This is in line with my measurements of the stationary population, which in the peripheral arbor make up app. 99% of all mitochondria (see below). Additionally in the stem axon, overexpression of SNPH-GFP resulted in highly elongated mitochondria, an effect not observed in cell culture. Time-lapse recordings of mitochondria in the stem axon revealed a significant reduction in the number of mitochondria moving in each direction (antero: 0.49 ± 0.09; retro: 0.18 ± 0.09 mito/min; n = 3; **Fig. 4.7D, E**). To control for unspecific effects of syntaphilin overexpression I used a truncated form of syntaphilin lacking the microtubule binding domain (SNPHΔMTB-GFP, **Fig. 7B**). Surprisingly, overexpression of this construct had the same effect on transport of mitochondria (antero: 0.42 ± 0.17; retro: 0.17 ± 0.04 mito/min; n = 3, $p > 0.05$; **Fig. 7D, E**). However, unlike SNPH-GFP truncated form did not had any effect on the length of mitochondria. This argues for some non-specific effects of the expressed constructs and the fact that the observed transport reduction is not due to the expected increase microtubule anchorage of mitochondria.

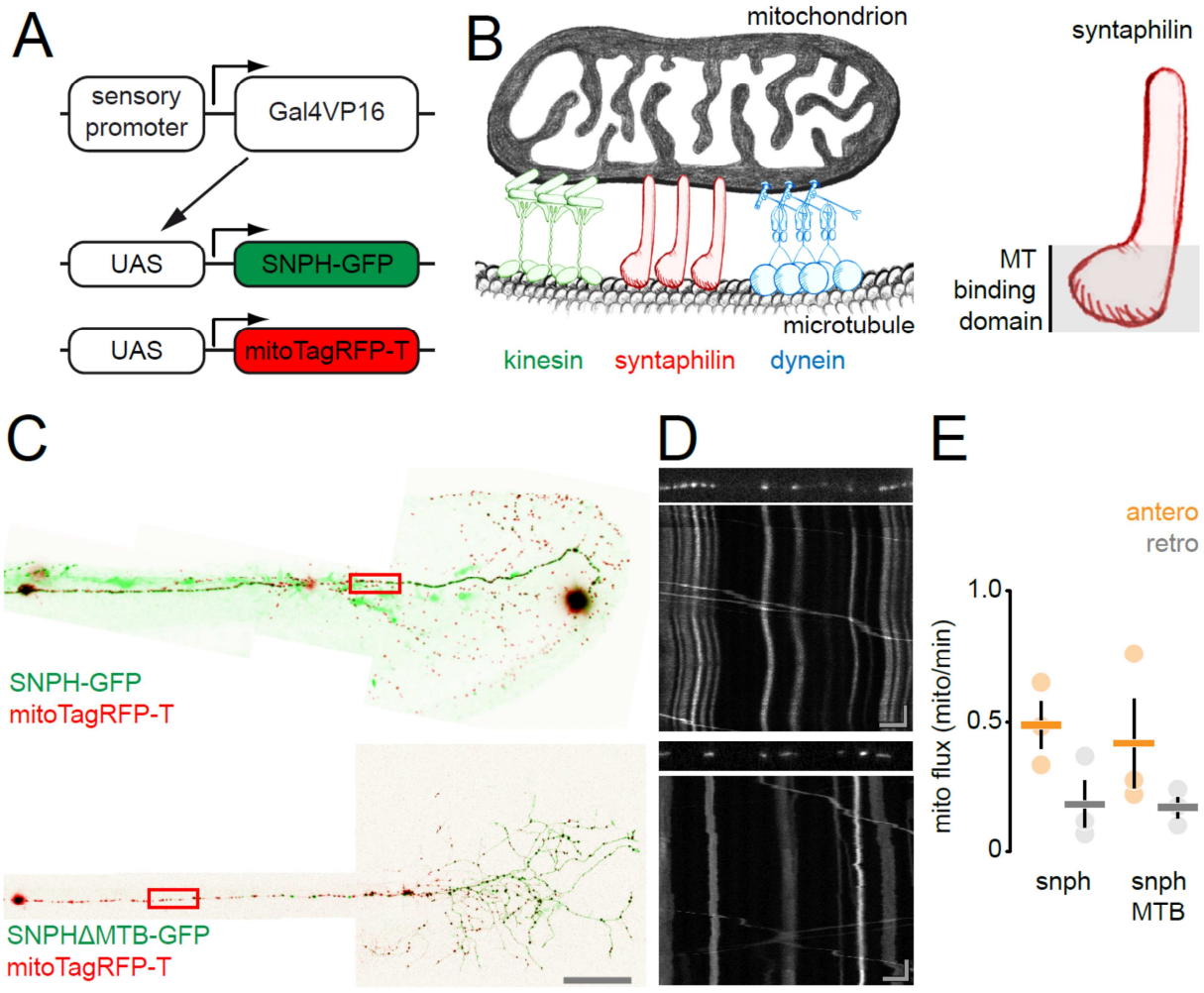

Figure 4.7. Effects of syntaphilin overexpression on mitochondrial transport

(**A**) Schematic of constructs used to label mitochondria (mitoTagRFP-T) and overexpress full length syntaphilin or its truncated form in RB neurons. (**B**) Schematic of molecular motors and syntaphilin structure (**C**) 2dpf RB neuron overexpressing SNPH and SNPHΔMTB **Red boxes**: area of stem axon imaged in **D** (**D**) Kymographs (area in red boxes in **C** imaged for 10 minutes). (**E**) Mitochondrial flux (stem 2dpf). Scales: **C** 100µm; **D** horizontal: 5µm, vertical: 60sec; data points: cells; lines mean ± SEM.

4.2.4. Genetic transport modulation III – Tau P301L

Finally I wanted to explore how disturbing microtubules would affect the transport of mitochondria. To do so, in collaboration with Dominik Paquet from Prof Christian Haass lab, I overexpressed a mutated form of Tau. Tau is a microtubule-associated protein, which upon hyperphosphorylation detaches from microtubules and forms so-called tangles (**Fig. 4.8A**). Mutations in Tau have been associated with frontotemporal lobar degeneration (e.g. Tau P301L; Cowan and Mudher, 2013). To overexpress Tau in RBNs, I used a bidirectional construct generated by Dominik Paquet (**Fig. 4.8A**; Paquet et al., 2009). In this construct, mutated human Tau (P301L) is co-expressed with DsRed to identify TauP301L-bearing neurites. Co-injecting of Tau:UAS:DsRed and memYFP:UAS:mitoCFP constructs with Islet-1:Gal4 driver construct was not sufficient to cause any defects in mitochondrial transport. To increase the expression levels of Tau, I used the HuC:Gal4 transgenic fish and injected responder constructs (**Fig. 4.8A-C**). While some of the triple positive cells showed a significant reduction in mitochondrial flux, on average there was no difference between Tau/DsRed and DsRed only injected larvae (2dpf: DsRed: 0.69 ± 0.14, Tau: 0.59 ± 0.08 mito/min, $n > 5$, $p = 0.7$; 3dpf: DsRed: 0.76 ± 0.14, Tau: 0.55 ± 0.09 mito/min, $n > 5$, $p = 0.2$, **Fig. 4.8D, E**). The same was true for the density of mitochondria (DsRed: 39.8 ± 7.1, Tau: 46.8 ± 3.6; $n \geq 5$, $p > 0.05$; **Fig. 4.8F**). However, closer analysis of mitochondrial density revealed that while overall density remains unchanged the mitochondria are redistributed within the cell and accumulate in the stem axon (DsRed: 64.6 ± 3.2, Tau: 118.4 ± 9.0 mito/mm; $n \geq 5$, $p = 0.01$) and are deficient in the proximal and distal parts (DsRed: proximal: 41.6 ± 9.4, distal: 31.3 ± 5.4, Tau: proximal: 49.7 ± 3.9, distal: 30.1 ± 3.7 mito/min, $n \geq 5$, $p > 0.05$; **Fig. 4.8F**).

The analysis of transport modulation in the single cell assay proved to be a tedious and low-reward approach, where obtaining sufficiently large samples for statistical analysis was difficult. Therefore together with collaborators in Prof. Haass laboratory we set out to develop a bulk assay of mitochondrial transport *in vivo* by generating transgenic fish that stably express mitoCFP and memYFP (*MitoFish*).

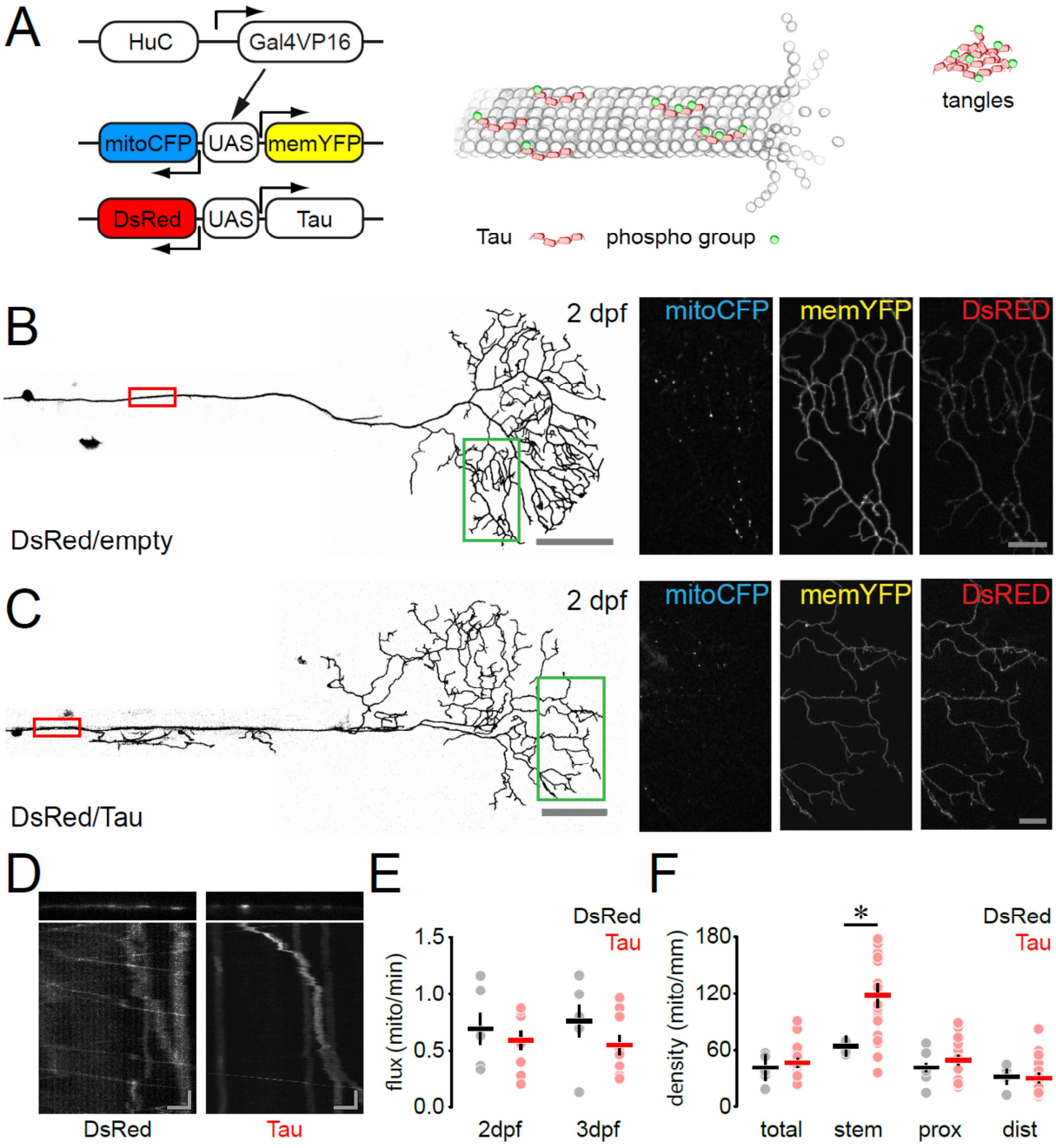

Figure 4.8. Effects of Tau^{P301L} overexpression on mitochondrial transport

(**A**) **Left**: schematic of constructs used to label mitochondria and membranes (mitoCFP:UAS:memYFP) and overexpress Tau (DsRed:UAS:Tau) in RB neurons. **Right**: schematic of pathological Tau accumulations (**C**) 2dpf RB neuron overexpressing DsRed only construct **Red box**; Area of "stem axon" imaged in **D**. **Green box:** Area magnified to right, showing mitochondria (left), membrane (middle) and DsRed (right). (**C**) 2dpf RB neuron overexpressing DsRed:UAS:Tau construct **Red box**; Area of "stem axon" imaged in **D**. **Green box:** Area magnified to right, showing mitochondria (left), membrane (middle)and DsRed (right). (**D**) Kymographs (area in red box in **B** and **C** imaged for 10 minutes). (**E**) Mitochondrial flux (stem 2dpf and 3dpf). (F) Mitochondrial density in Tau and control group total and in different neuronal compartments (stem, proximal and distal) Scales: **B**, **C** 100µm, magnified areas: 20µm; **D** horizontal: 5µm, vertical: 60sec; **E**, **F** data points: cells; lines mean ± SEM.

4.3. Bulk analysis – MitoFish

MitoFish were generated in the laboratory of Prof. Haass. It is a transgenic responder fish that harbors a bidirectional UAS sequence (Paquet et al., 2009) to concomitantly express mitoCFP and memYFP in a Gal4-dependant manner (**Fig. 4.9A, B**). Given the plethora of Gal4-driver lines available, in principle *MitoFish* can be used to examine mitochondrial dynamics in many different cell-types. In contrast to the single cell assay this approach allows imaging many more mitochondria at the same time (**Fig. 4.9C, D**). Firstly, I wanted to confirm that this assay is compatible with the single cell assay. Therefore, I measured the density of mitochondria in the *MitoFish* and compared them with different values from different arbor compartments. The density of resting mitochondria in *MitoFish* matched the density found in the most distal parts of the axonal arbor in the single cell assays (*MitoFish*: 53.1 ± 1.9, n = 10 fish *vs.* single cells: distal 49.2 ± 3.0; proximal 67.0 ± 3.0; stem 97.8 ± 5.9 mitochondria/mm, n = 20 cells; **Fig. 4.9E**). Comparing this values lead me to the conclusion that I mostly assay the distal axon branches. This is in line with the imaging position towards the thin rim of the fin fold, chosen to improve image quality. I also observed the lower percentage of moving mitochondria in the peripheral neurons than in the stem axons in my single cell recordings (periphery: 1.03 ± 0.12 % *vs*. stem axon: 16.6 ± 1.6 %, n = 10 fish for each measurement). This drop in the number of motile mitochondria is expected as density of flux decreases with every branching point by a factor of 2, as cargos are distributed between the branches. Thus, both of our assays allow generating consistent and complementary data sets.

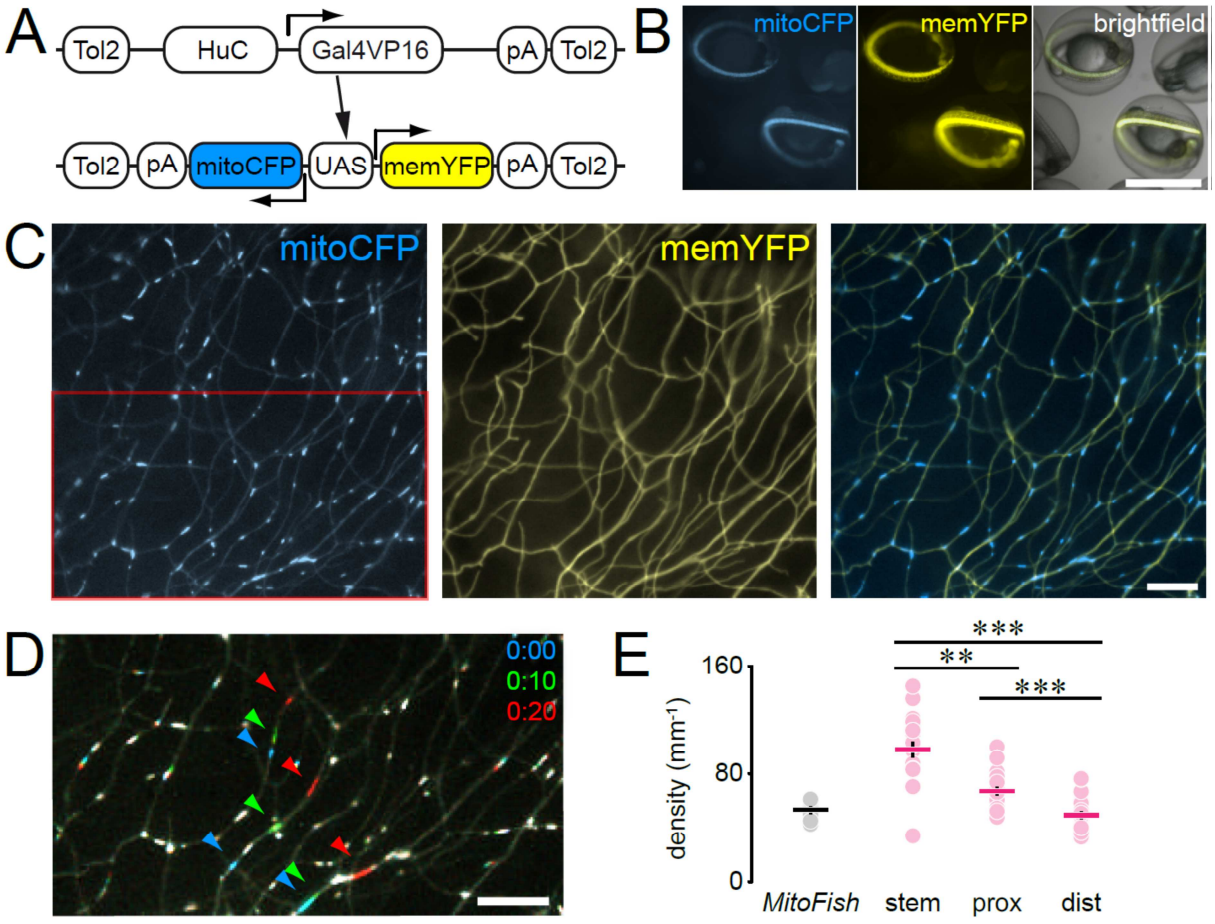

Figure 4.9. Transgenic *MitoFish*.

(**A**) Constructs used to generate *HuC:Gal4* driver fish and reporter *MitoFish*. (**B**) Wide-field image of *MitoFish* at 2dpf. (**C**) Peripheral arbors of *MitoFish* RB neurons. (**D**) Transport of mitochondria in *MitoFish*; superimposition of three pseudo-colored frames of the red box in **C** (color code as indicated, min:sec). (**E**) Mitochondrial density in *MitoFish vs.* single cells. Scales: **B**, 1mm; **C, D** 10µm. Data points: **E**, single fish for *MitoFish*, cells for injections; lines, mean ± SEM.

4.3.1. Pharmacological transport modulation in the bulk assay - nocodazole

To test if *MitoFish* can be used for drug screens, Dominik Paquet treated *MitoFish* with nocodazole. Indeed, treated *MitoFish* showed a dramatic decrease in the total density of mitochondria (total density – nocodazole: 28.8 ± 2.1 *vs.* DMSO: 56.8 ± 3.0 mito/mm, n = 10 fish, $p < 0.001$; **Fig. 4.10**). This is consistent with the observation from the single cell assay, where I observed a most dramatic effect in the distal parts of the arbor. The effect observed in *MitoFish* is more pronounced due to higher overall density of labeling, which allows assaying more neurons at the same time and therefore leads to more consistent results. Nocodazole treated fish not only had reduced overall mitochondrial density, but also reduced flux density (flux density – nocodazole: 1.2 ± 0.3 *vs.* DMSO: 7.3 ± 0.6 mito/mm, n = 10 fish, $p < 0.001$; **Fig. 4.10C**). At the same time, the speed of moving mitochondria was not affected (nocodazole: 0.78 ± 0.05 *vs.* DMSO: 0.83 ± 0.01 µm/sec; $n \geq 7$, $p > 0.05$).

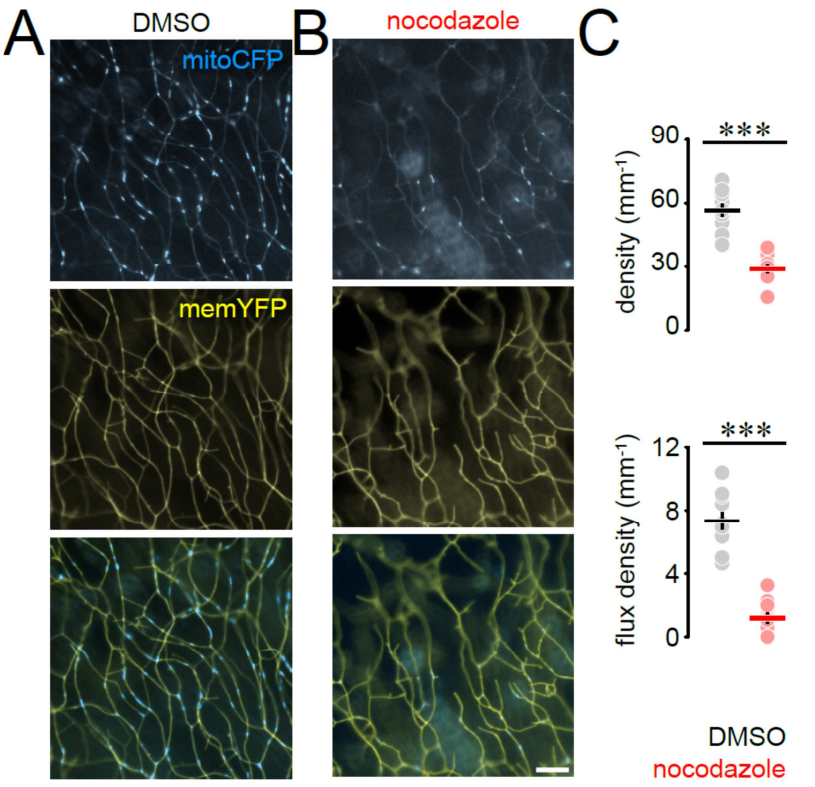

Figure 4.10. Nocodazole treatment impairs mitochondrial distribution and transport.

(**A, B**) Peripheral RB arbors in *MitoFish* treated with DMSO (**A**) and nocodazole (**B**). (**C**) Mitochondrial density (**top**), flux density (**bottom**) in DMSO- and nocodazole-treated *MitoFish*. Scale bar: 10µm. Data points: fish; lines, mean ± SEM.

4.3.2. Genetic transport modulation in the bulk assay - Tau

In the next step together with Dominik Paquet, I assessed the possibility of using *MitoFish* for testing the effects of genetic manipulation on mitochondrial transport. We decided to use a previously described model of tauopathy – *TauFish* (Paquet et al., 2009). These fish carry a birectional UAS construct encoding a mutated version of Tau (P301L) and DsRed as a fluorescent indicator. A responder line that expressed DsRed, but no Tau (*RedFish*) served as control. We imaged mitochondrial movement in the Rohon-Beard neurons of *TauFish* crossed to *MitoFish*. These neurons can be classified into two categories: the DsRed positives are considered expressing Tau and DsRed negative served us as an internal control (**Fig. 4.11A, B**). We compared the results we obtained in *TauFish* × *MitoFish* with the *RedFish* × *MitoFish*. We observed a profound reduction in the density of total and moving mitochondria in *TauFish* (density – control *RedFish*: 59.9 ± 3.3 mitochondria/mm axon, n = 10 fish; *TauFish*, non-red axons, i.e. "internal control": 48.1 ± 2.3, n = 14 fish; *TauFish*, red axons: 14.1 ± 2.3, n = 14 fish; $p < 0.0001$; flux density – *RedFish*: 6.82 ± 0.4 moving mitochondria/mm axon; *TauFish*, internal control: 6.4 ± 0.7; *TauFish*, red axons: 1.1 ± 0.4; $p < 0.0001$; **Fig. 4.11C, D**). Since DsRed-negative RB neurites in the *MitoFish* × *TauFish* had normal transport (**Fig. 4.11D**), we could exclude non-specific transgene integration effects as reason for the observed transport disruption. Transport was also found to be normal in the *MitoFish* × *RedFish*, which express DsRed levels comparable to *MitoFish* × *TauFish* (Paquet et al., 2009), excluding a major effect of DsRed over-expression on axonal transport. Lastly when we compared the movement behavior of individual mitochondria in *MitoFish* with or without Tau overexpression (**Fig. 4.12**), we found that the average speed was reduced (*RedFish*: 0.68 ± 0.03, *TauFish*: 0.48 ± 0.06 µm/sec, n > 20 mitochondria per group; $p = 0.002$). The detailed analysis of mitochondrial movement behavior revealed that in *TauFish* × *MitoFish* the moving speed of mitochondria is overall higher (*RedFish*: 1.27 ± 0.02, *TauFish*: 1.6 ± 0.01 mito/sec; n > 20 mitochondria per group; $p = 0.01$), but the pause duration and frequency are increased (pause duration: *RedFish*: 5.7 ± 0.7, *TauFish*: 13.6 ± 4.7 sec; stop frequency: *RedFish*: 6.6 ± 0.3, *TauFish*: 7.0 ± 0.7 sec-1; n > 20; $p > 0.05$; **Fig. 4.12**). Alterations in the last two parameters overcompensate for the increased moving speed.

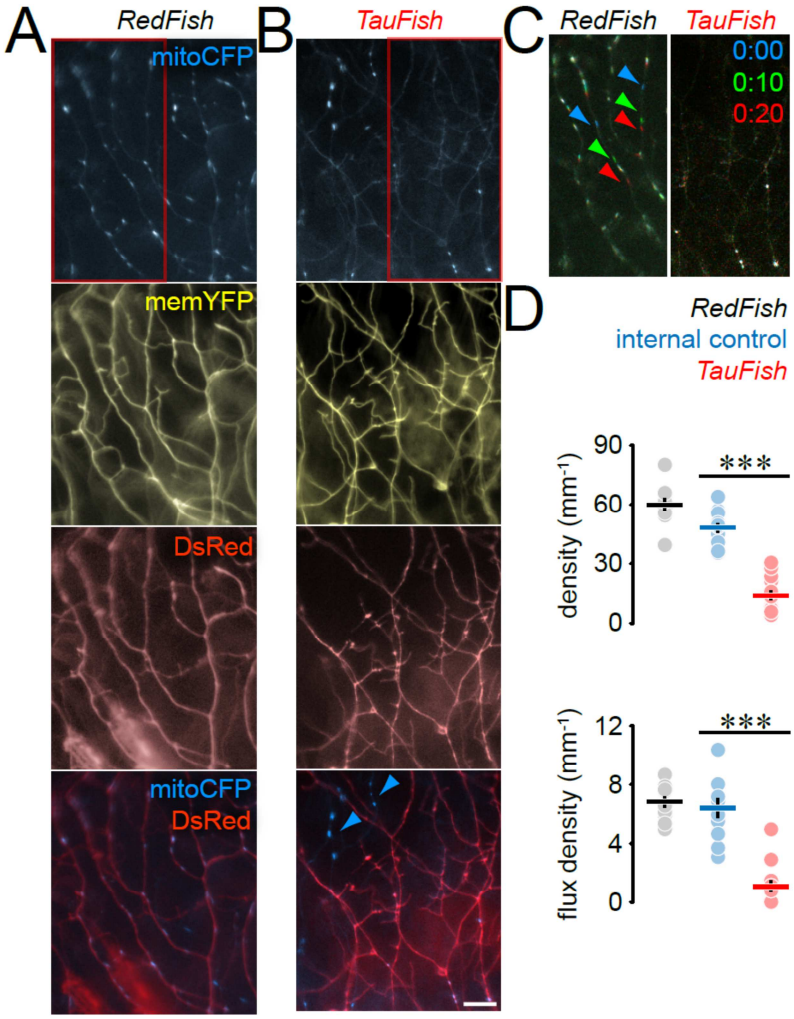

Figure 4.11. Overexpression of Tau^{P301L} reduces mitochondrial density and motility.

(**A, B**) Peripheral RB arbors in DsRed-expressing control (**A**; *RedFish*) and Tau^{P301L}-expressing (**B**; *TauFish*) transgenic lines crossed into the *MitoFish*. Arrow-heads, DsRed- (and hence, Tau^{P301L}-) negative neurites ("internal control"). (**C**) Transport of mitochondria in red boxes in **A** and **B** represented as in **Figure 9D**. (**D**) Mitochondrial density (**top**) and flux density (**bottom**) in *RedFish vs. TauFish* (also indicated, "internal control" neurites). Scale bar: 10µm. Data points: fish; lines, mean ± SEM.

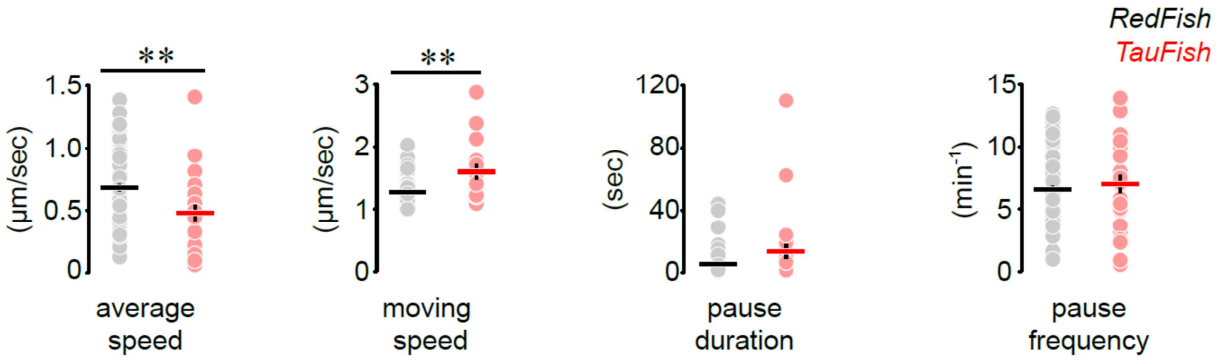

Figure 4.12. Effects of Tau^{P301L} overexpression on single mitochondrion movement

Left: Average speed of mitochondria, **left-middle**: moving speed of mitochondria, **right-middle**: pause frequency of mitochondria, **right**: time spend stopping. Data points: mitochondria; lines: mean ± SEM.

4.3.3. Modulation of transport – mechanistic insights into Tau overexpression effects

In vitro studies of Tau-induced transport deficits point towards microtubule affinity-regulating kinase 2 (MARK2) as a potential modulator of Tau removal from microtubules (Drewes et al., 1997). MARK2 phosphorylates Tau at the microtubule-binding domain, which leads to detachment of Tau from microtubules (Mandelkow et al., 2003). To test this hypothesis in collaboration with Dominik Paquet and Alexander Hruscha from Prof. Haass laboratory, we overexpressed MARK in the *MitoFish* × *TauFish* by mRNA injection. To correct for potential unspecific effects, we used GFP mRNA as a control. Indeed, MARK2 partially rescued mitochondrial density and transport deficits of *TauFish*, while our mGFP control had no effect on mitochondria. (density – MARK2 in *TauFish*: 34.3 ± 3.8 mitochondria/mm; GFP in *TauFish*: 16.8 ± 4.4, $n \geq 7$ fish; $p = 0.02$; flux density – MARK2 6.34 ± 1.4 mitochondria/mm; GFP 0.1 ± 0.1; $p = 0.001$; **Fig. 4.13**). MARK2 overexpression in *MitoFish* without Tau or in "internal control" Tau-negative axons (in *TauFish*) had little effect on mitochondrial density or flux (density – MARK2 in *MitoFish*: 50.2 ± 2.6 mitochondria/mm; GFP 50.8 ± 2.6; $n \geq 8$ fish; $p > 0.05$; flux density – MARK2: 3.4 ± 0.3 mitochondria/mm; GFP 5.5 ± 0.4; $p > 0.05$; data for internal control axons not shown).

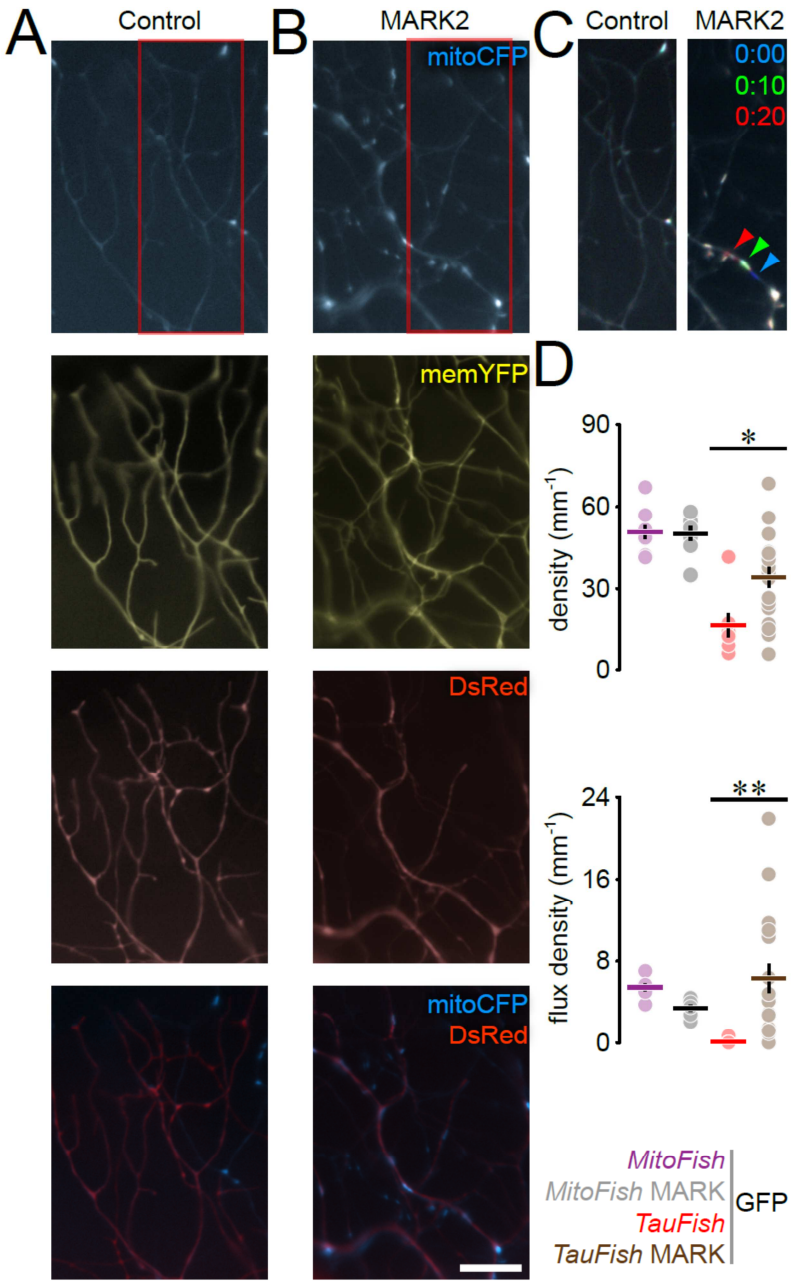

Figure 4.13. MARK overexpression rescues *TauFish* phenotype.

(**A, B**) Peripheral RB arbors in control (**A**) and MARK (**B**) -expressing *TauFish x MitoFish*. Arrow-heads, DsRed- (i.e., Tau^{P301L}-) negative neurites. (**C**) Transport of mitochondria in red boxes in **B** and **C** represented as in **Figure 9D**. (**D**) Mitochondrial density (**top**), flux density (**bottom**) in *MitoFish vs.* MARK-expressing *MitoFish* and *TauFish vs.* MARK-expressing *TauFish*; dashed lines show mean values for *RedFish* and *TauFish* from **Figure 11D**. Scale bar: 10µm. Data points: fish; lines, mean ± SEM.

4.4. Developing tools to study mitochondrial dynamics

My initial experiments of transport measurements together with calculations of mitochondrial mass translocation identified a population of mitochondria which were neither used for the growth of the arbor, nor were they returned to the soma by retrograde transport (**Fig. 4.14**). One of the possibilities for what is happening to this "missing" population of mitochondria is that it undergoes mitophagy in the peripheral arbor. Alternatively these mitochondria could fuse with other mitochondria, which I would not be able to distinguish due to the resolution limit of my imaging techniques. Therefore I set out to develop tools to study the degradation and dynamics of mitochondria in the peripheral arbor.

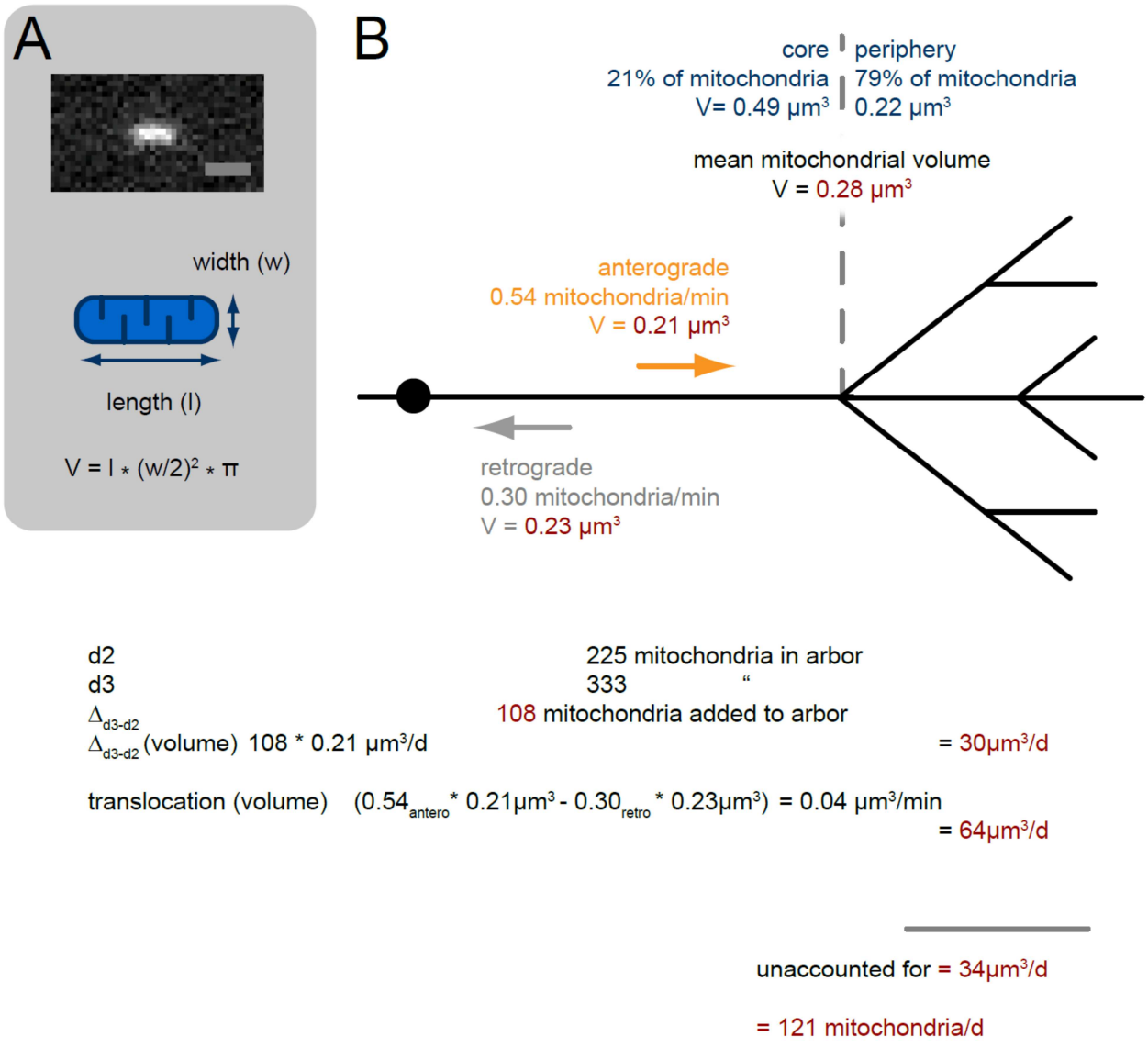

Figure 4.14. Schematic of mitochondrial mass translocation and turn-over

(**A**) Wide field image of a single mitochondrion and schematic calculation of mitochondrial volume. Scale bar: 1µm. (**B**) Schematic representation of different mitochondrial populations' volumes and calculation of mitochondrial mass translocation.

4.4.1. Mitophagy

To explore the possibility of peripheral mitophagy, I first decided to image peripheral arbors of RBNs at different developmental stages to identify sites of mitochondrial disappearance. While this analysis clearly showed that with age neuronal arbors become less dynamic, I did not observe any disappearing mitochondria (**Fig. 4.15**). This, however, does not rule out the peripheral mitophagy, as it may occur inside clusters of mitochondria that we cannot resolve, such as those sometimes found at branching points.

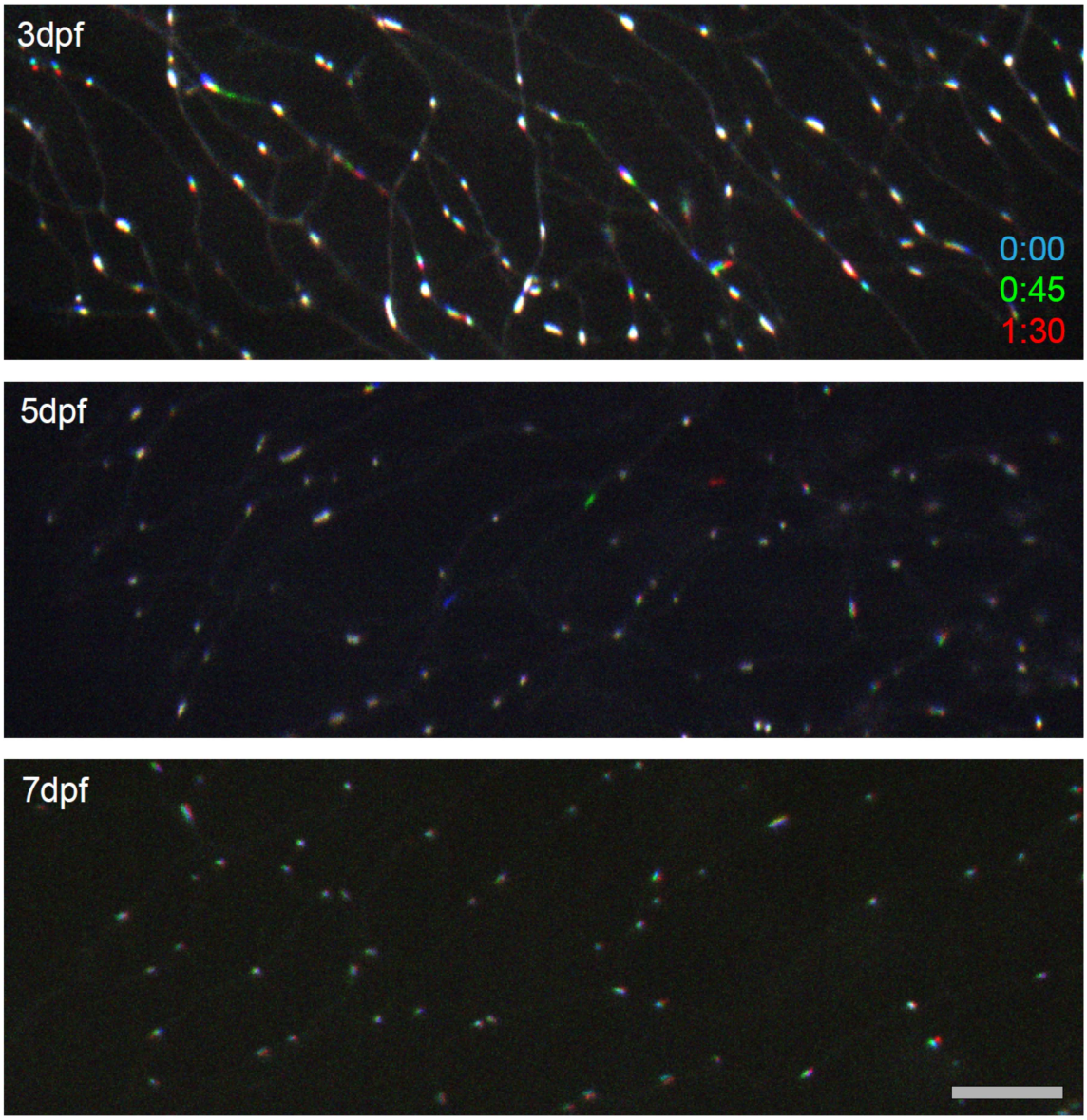

Figure 4.15. Transport of mitochondria in the peripheral RB neurons over time

Wide-field images of mitochondrial transport at different developmental stages. Representation as in figure **9D**. **Top**: 3dpf, **middle**: 5dpf, **bottom**: 7dpf. Scale bar: 10µm.

4.4.1.1. Parkin

Hence, in order to overcome this limitation, I tried to use specific "positive" markers for autophagic events. To do so, I obtained a construct encoding parkin (Fett et al., 2010), which is a specific marker of mitophagy fused to YFP (parkin-YFP) and subcloned it into a UAS-driven vector (**Fig. 4.16A**). Injections of UAS:parkin-YFP resulted in the cytoplasmic labeling with easily identifiable parkin accumulations (**Fig. 4.16B**). However, when co-expressed with a spectrally-distinct mitochondrial marker, these parkin-YFP accumulations co-localized with most mitochondria, which is implausible for a specific mitophagy marker (**Fig. 4.16B**). This effect was most probably due to overexpression with the Gal4-UAS system. Ongoing experiments therefore include titrating UAS:parkin.YFP, as well as using other expression systems to lower expression levels.

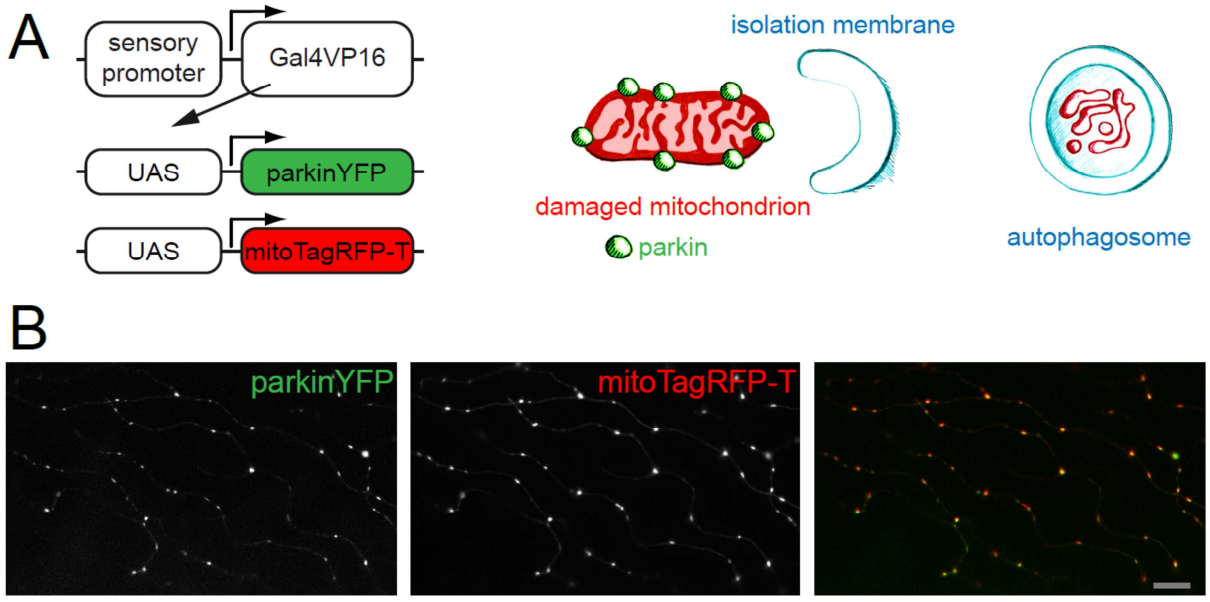

Figure 4.16. Localization of mitophagy sites through parkin labeling

(**A**) Schematic of constructs used to label mitochondria (mitoTagRFP-T) and mitophagic sites (parkinYFP) in RB neurons and representation of Parkin.YFP accumulations at damaged mitochondria (**B**) Wide-field image of co-localization of mitochondria and parkinYFP punctae. Scale: 10µm.

4.4.1.2. LC3

In parallel to parkin-YFP, I also tested a general marker of autophagy – LC3. This short protein was fused to GFP to allow visualizing early autophagosomes (Kabeya et al., 2000; **Fig. 4.17A**). I co-injected UAS:LC3.GFP with UAS:mitoTagRFP-T into the Isl2b:Gal4 transgenic line. Like UAS:parkin.YFP, UAS:LC3.GFP was highly overexpressed in Rohon-Beard neurons. However closer analysis of the confocal images of expressing fish allowed identification of neurites with lower expression levels of LC3.GFP and more specific-appearing labeling of autophagosomes (**Fig. 4.17B**, blue arrows). These accumulations co-localized with mitochondria and were mostly localized at branching points. This is in line with our initial hypothesis of mitophagy occurring in mitochondrial clusters. Future experiments will include precise titration of the construct and time-lapse of the LC3.GFP positive mitochondria, to see, whether they are fated for disappearance.

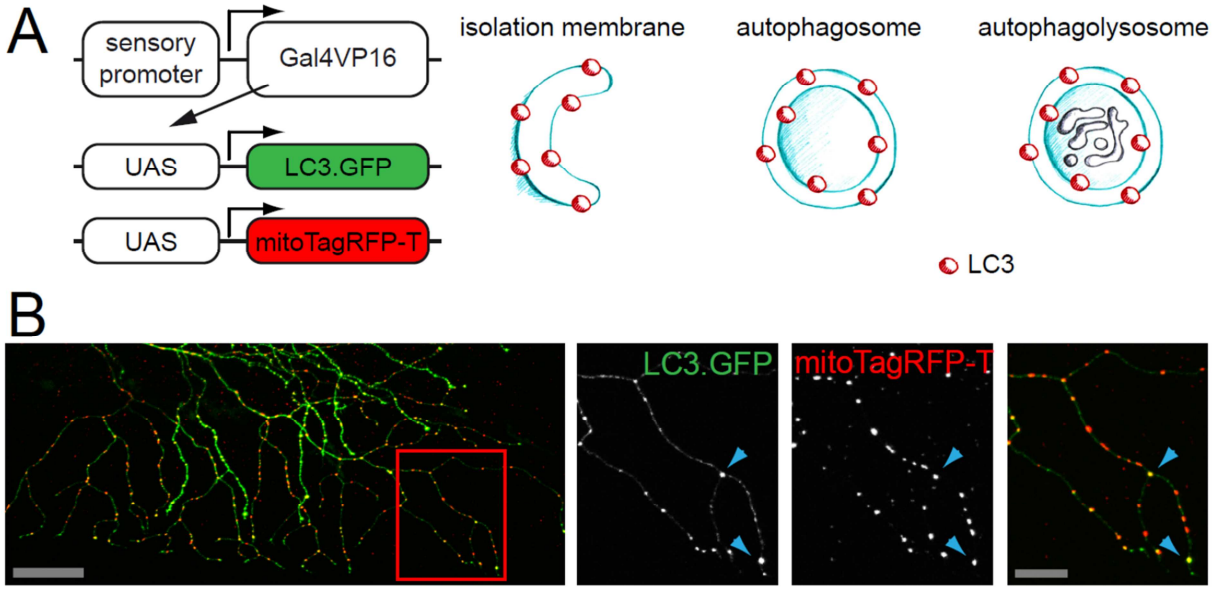

Figure 4.17 - Localization of mitophagy sites through LC3 labeling

(**A**) **Left**: schematic of constructs used to label mitochondria (mitoTagRFP-T) and mitophagic sites (LC3.GFP) in RB neurons. **Right**: schematic representation of LC3.GFP accumulations at damaged material (**B**) Confocal image of co-localization of mitochondria and LC3.GFP punctae. **Red box**: Area magnified to right, showing LC3.GFP (left), mitochondria (middle) and merged (right). Scale: 50µm, magnifications: 20µm.

4.4.2. Fusion

Another phenomenon I observed while acquiring time-lapse movies of peripheral arbors were two mitochondria that established contact. Often this lead to apparent formation of a single mitochondrion, suggestive of fusion - but with the single-color labeling, it proved impossible to show the actual exchange of the mitochondrial material. Therefore I started to developed tools to distinguish between fusion and mere co-localization (non-fusion) events, where two mitochondria get too close to be resolved, but do not actually fuse.

4.4.2.1. Photo-conversion

In previous *in vitro* studies, distinct labeling of individual organelles has been achieved through use of photo-convertible and photo-activatable proteins (Patterson and Lippincott-Schwartz, 2002; Twig et al., 2006). With this approach a subset of mitochondria is distinctly labeled and can be tracked over time. Based on the previous experience in the lab with measuring transport flux with Kaede, I started by using this photo-convertible protein. Kaede is a fluorescent protein, which in its ground state emits green fluorescence (Kaede-green, excitation 508nm, emission 518nm). Upon exposure to UV light, Kaede is cleaved, which causes formation of a new red-emitting chromophore (Kaede-red, excitation 572nm, emission 582nm; Ando et al., 2002; **Fig. 4.18A**). I co-injected a UAS:mitoKaede construct together with UAS:memYFP (**Fig. 4.18A**). This combination of FPs is not optimal due to overlapping spectra of YFP and Kaede-green, but as the tracking signal comes from Kaede-red, this spectral overlap does not obscure the experiment readout. Double positive cells were selected and reconstructed on the confocal microscope. I used a 405 nm laser to convert cell's soma (**Fig. 4.18B, C**). The conversion was very effective and almost all of the green fluorescence was gone after UV exposure and red fluorescence increased 21-fold (**Fig. 4.18C**). Following conversion, images were taken after 1 and 2 hours. An easily discernible subpopulation of red mitochondria was observed in the distal parts of the cells at the 1 hour time point (**Fig. 4.18D**). As expected after 2 hours, the number of red mitochondria further increased (1 hour: 11 mitochondria, 2 hours: 30 mitochondria). The number of red mitochondria observed in the peripheral arbor corresponded well with the number of anterogradely moving mitochondria measured in the stem axon (**Fig. 4.2B**). During the experiment addionally to green-only and red-only mitochondria I was able to observe third populations of mitochondria (**Fig. 4.18D**). These were red positive mitochondria which were also positive for Kaede-green. A simple explanation would be that these are two mitochondria which reside so closely together that they are non-resolvable. Alternatively, this could be a mitochondrion which arose as a fusion

of the stationary (green, unconverted) mitochondrion and newly delivered (red, converted) mitochondrion. To distinguish between these two possibilities, imaging at higher temporal resolution would be required.

Despite my initial enthusiasm, it turned out that Kaede has a few caveats. First of all, it is very sensitive to the blue spectrum of light. Therefore experiments have to be performed in the darkness, using only red light illumination. The low conversion threshold is also a problem when using a 488 nm laser to image Kaede-green, as this wavelength has a low ability to photo-convert. Additionally, Kaede is a pH sensitive protein and in high concentration of H^+ the protein can spontaneously undergo cleavage and conversion (Mizuno et al., 2003).

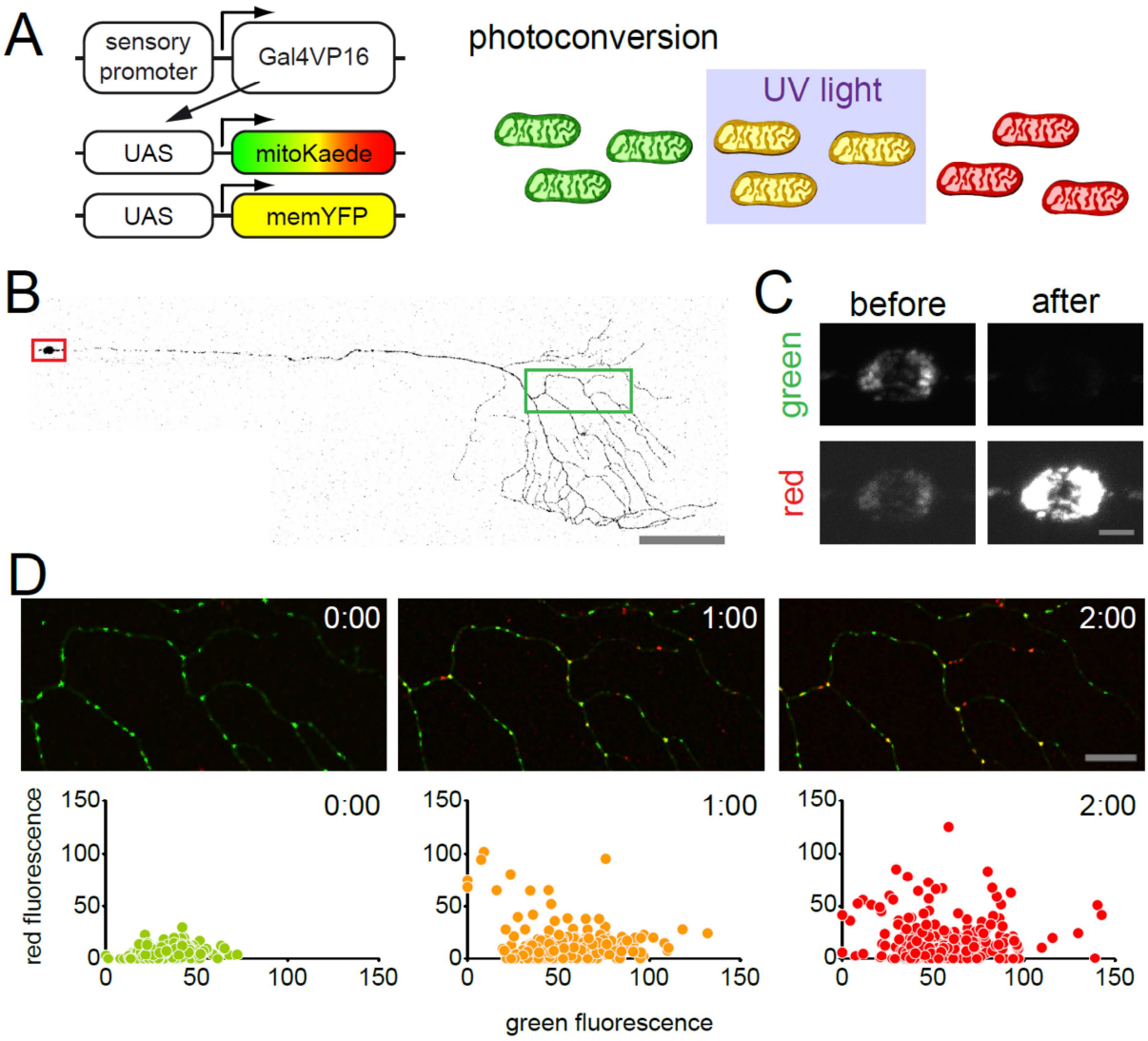

Figure 4.18. Newly exported mitochondria locate in the peripheral branches

(**A**) **Left**: schematic of constructs used to label mitochondria (mitoKaede) and membranes (memYFP) in RB neurons. **Right**: schematic of conversion paradigm with UV light. (**B**) 2dpf RB neuron labeled with memYFP **Red box**; Area of photo-conversion in **D**. **Green box:** Area magnified in **E**. (**C**) RB soma before (left) and after (right) UV exposure (**D**) Peripheral arbor immediately, 1 hour and 2 hours after photo-conversion of the soma. Below: quantification of single mitochondria green and red fluorescence brightness relative to the time point above. Scales: **B** 100µm, **C** 5µm, **D** 20µm, data points: mitochondria.

4.4.2.2. Photo-activation

As an alternative to Kaede, I explored the possibility of using the photo-activatable form of green fluorescent protein (PA-GFP). Unlike Kaede, PA-GFP is not visible in its basic state. Upon UV irradiation PA-GFP undergoes photo-conversion and shifts predominantly to the anionic form giving rise to an increase in peak absorbance (excitation 488nm, emission 504nm; Patterson and Lippincott-Schwartz, 2002; **Fig. 4.19A**). As in the non-activated state mitochondria are not visible, this approach requires an additional mitochondrial label to be able to visualize the entire mitochondrial population (and screen for expressing cells). Therefore one cell stage embryos of Isl2b:Gal4 driver line were injected with two mitochondrially targeted UAS constructs (UAS:mitoPA-GFP and UAS:mitoTagRFP-T; **Fig. 4.19A**). At 3 dpf I selected larvae positive for mitoTagRFP-T. Activation with UV light resulted in 20-fold increase in fluorescence of GFP and a slight decrease (0.8-fold) in the red fluorescence due to bleaching (**Fig. 4.19B**). Doubly labeled mitochondria were visible only in the field of view and mitochondria outside of the activated region remained red only (**Fig. 4.19C**). Both proteins were very stable and allowed imaging for long time periods in the peripheral arbor of RBNs (up to 2 hours at 0.3Hz imaging frequency). Time-lapse imaging of the converted area allowed distinguishing between fusion events and non-fusion crossings (**Fig. 4.19D**).

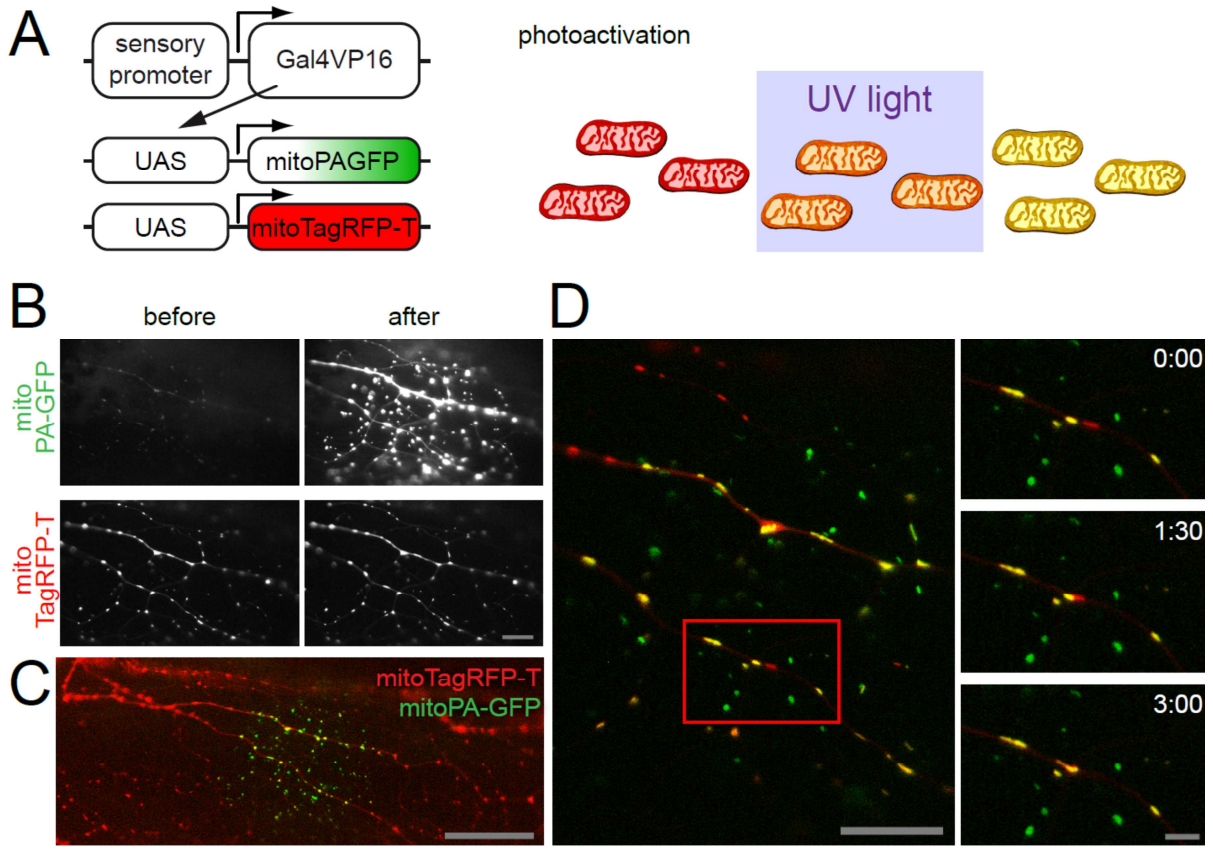

Figure 4.19. Activation of PA-GFP allows distinguishing between fusing and non-fusing mitochondrial crossings

(**A**) Left: schematic of constructs used to double label mitochondria (mitoPAGFP and mitoTagRFP-T) in RB neurons. **Right**: Schematic of activation of mitochondria upon UV light exposure. (**B**) Wide-field of the 3dpf RB arbor labeled with mitoTagRFP-T and mitoPAGFP before (left) and after (right) photo-activation (**C**) Low magnification overview of the photo-activated region of the cell. (**D**) Photo-acivated region 17 minutes after photo-activation. **Red box**: area magnified to the right. **Magnified area**: single time-lapse frames of mitochondrial crossing. Scales: **B** 20µm, **C** 50µm, **D** 20µm, magnified area: 5µm.

5. Discussion

Increasingly the study of neuronal mitochondria and their transport is recognized as central to a pathomechanistic understanding of numerous neurological diseases. By now, it is accepted that neurons show a particular vulnerability to disturbed mitochondrial transport and distribution. Proper organelle transport depends on homeostatic support both from within the neuron, as well as by surrounding glia. Based on these premises, studying organelle dynamics in neurons that exist in their 'natural habitat' *in vivo* is desirable – but remains limited by the lack of animal models and matching imaging techniques that would allow to quantitatively assay the transport and turnover of a neuronal organelle population *in vivo*. In this work I established a set of tools for simple measurement of the transport and turn-over of neuronal mitochondria in a living vertebrate, zebrafish. I demonstrate that co-injecting DNA-constructs that encode distinct mitochondrially and membrane-targeted fluorescent proteins permits non-invasive and repetitive *in vivo* co-visualization of axonal arbors in their entire geometry, as well as their near complete mitochondrial population. This allows for quantitative assessment of transport and turn-over. Starting from such base-line characteristics, my colleagues in the Haass lab and I additionally present a transgenic reporter fish that enables rapid and sensitive characterization of genetically induced disease-related changes in transport. Using these *MitoFish*, screening for modulators or transport alterations becomes possible.

5.1. Zebrafish as a model to study mitochondrial dynamics

In my view, the work presented here demonstrates the unique versatility of zebrafish for organelle transport and turn-over studies. However, attempts to visualize axonal transport *in vivo* or at least in semi-intact preparations are not without precedent. Beyond the classical studies using video-enhanced differential interference contrast microscopy on unusually large invertebrate axons (such as the giant axon of squid), recent efforts to visualize specific organelles (such as mitochondria) span the phylogenetic spectrum from nematodes to mammals. For example, the transport of genetically tagged organelles has been studied in *Drosophila* larvae, offering the distinctive advantage of easy genetic manipulation to explore the molecular mechanisms of the transport machinery and regulation (Pilling et al., 2006; Wang et al., 2011). On the other end of the spectrum, a number of transgenic mice have been generated with mitochondria tagged with spectral variants of GFP (up to now including CFP, GFP, YFP, DsRed, Tag-RFP-t and Dendra2 driven by regulatory elements of the thy1, the

nse, the hb9 and the ROSA26 locus, as well as under conditional control using tetracycline-response elements; Misgeld et al., 2007; Pham et al., 2012). However, neither of these models allows visualizing transport non-invasively, and to my knowledge up to this date, no repetitive *in vivo* measurement of transport in the same axon has been achieved in any species. Central questions in the field of axonal transport studies are the relationship between transport and nerve cell remodeling, and the mechanisms of mitochondrial turn-over – mostly motivated by genetic and cell biological evidence that insufficient transport and disrupted clearance might be key pathogenic events in a number of common neurological diseases, including Charcot-Marie-Tooth and Parkinson's disease (Baloh et al., 2007; Chu et al., 2012).

The zebrafish-based *in vivo* assay that I present here can overcome many limitations that affected previous models, and hence constitutes a valuable addition to the available armamentarium of models. The central advantages of the zebrafish-based assays are:

(1) Zebrafish larvae at the initial stages of development are transparent, which allows for non-invasive imaging with subcellular resolution;

(2) Simple access to large numbers of eggs and external development, which makes generation of transient or stable transgenic fish easy;

(3) Comprehensive mutant collections, straight-forward morphant generation and recently, zinc-finger- or TALEN-based targeted gene disruptions allow probing molecular mechanism of transport and turn-over;

(4) Presence of myelinated axon tracks in zebrafish, which invertebrates lack, allows studying the role of extrinsic axon-glia interactions in transport;

(5) Handling and imaging of zebrafish larvae can be automated to a degree that makes small high-content drug screens possible – together with an increasing number of zebrafish models of human disease processes, this might allow for direct identification or at least verification of drug candidates that affect subcellular transport and homeostasis (Pardo-Martin et al., 2010).

In this work, I decided to focus on Rohon-Beard sensory neurons and their peripheral branches. This choice was motivated by the fact that it is easy and cheap to use wide-field microscopy to image in these superficial neurites. Moreover, the simple quasi two-dimensional geometry, as well as the relative sparseness of skin innervation, makes these cells a popular choice in attempts to understand neurite development and regeneration in zebrafish. These neurons, however, are non-myelinated cells of the PNS, and also appear to degenerate

in some species during development, this choice could be seen as disadvantageous. However, in my hands (and other groups have reported similar observations), RBNs persist well into the second week after fertilization, so that at the time of my imaging (2-3 dpf), interference of later degeneration with my measurements is not likely. Additional disadvantage of RBNs is that they do not form synapses. RB neurites end below the first layer of skin and act as mechanical or chemical sensors (O'Brien et al. 2009). This is an important point in studies of mitochondrial destination, as this organelle is considered to be targeted to the pre- and post-synaptic sites of the neuron. Alternatively, studies of synaptogenesis and relevance of mitochondria in this process can be performed on retinal ganglion cells (Niell et al., 2004). While this neuronal cell type form regular synapses their location in the tectum and 3-dimensionality requires using a slower and more expensive 2-photon or confocal microscope.

5.2. Commonalities and diversities between systems

As imaging mitochondria in RBNs is a novel system the important question arises whether results obtained in this assay are comparable with other models or if the certain differences exist. One of the most commonly measured parameters in mitochondrial studies is the number of moving *vs*. resting mitochondria. Usually the moving mitochondria are 15 – 30 % of entire mitochondria population. Indeed app. 20% of mitochondria were motile when the measurement was performed in the most proximal part of the axon. However this number drops to 1% the distal branches, due to reduction of number of motile mitochondria by the factor of 2 at every branching point.

Flux rates are another parameter often used to quantify the transport. However exact values of the rates need to be considered in relation to where they were measured. They vary between the species, axons and dendrites (Chang and Reynolds, 2006), cell compartments, but also between different imaging protocols (Louie et al., 2008). Despite all of the differences there always seems to be a discrepancy between number of anterograde and retrograde moving mitochondria with prevailing number of mitochondria traveling towards peripheral parts of the neuron. This positive net flux stays constant among the entire life-span of the mouse (Marinkovic et al., 2012) and is independent of the neuron size (**Fig. 4.4**). Additional calculations of motile mitochondrial size show that mitochondria moving in antero- and retrograde direction have the same volume. Together these two numbers (net flux and volume) provide insightful data for overall increase of the peripheral mitochondrial mass or peripheral mitochondrial digestion.

As I discussed in the Introduction transport of mitochondria happens along microtubule tracks using kinesins (anterograde transport) and dyneins (retrograde transport). These motor proteins have been described in detail. Isolated kinesins move at a maximal speed of 0.6 µm/sec and dynein 0.7 µm/sec (King and Schroer, 2000; Gross et al., 2007). Due to cytoplasm viscosity, but also because of the interaction between kinesins and dyneins speed of moving mitochondrion differs from speed of isolated motors. Especially, the interaction of motors has an effect on the speed of the organelle as shown in peroxisome study (Kural et al., 2005). The additive effect of interaction between motors results in increased speed of the organelle in comparison to isolated motor studies. In the assay I developed as well as in other studies of mitochondrial transport average speed does not differ between directions. However more detail analysis of running speeds, number of pauses and pausing frequency reveals some differences. Mitochondria moving in the retrograde direction tend to stop more frequently and for longer times. This is most probably due to a lower processivity of this motor, which results in more frequent detachments of the dynein from the microtubules (Gross et al., 2007).

5.3. Modulation of mitochondrial transport

One of the intriguing hallmarks of mitochondrial dynamics in neurons is that the majority of mitochondria present in the neuron are actually stationary - and that the moving and resting populations of mitochondria seem to be rather distinct, with little interchange between the populations, which suggests that a mitochondrion remains in one state for relatively long periods of time. This observation is consistent with *in vitro* studies (Morris and Hollenbeck, 1993) as well as with measurements in Drosophila and mouse models (Louie et al., 2008). This raises the question of what regulates the transition from one state to another and what cellular consequences result from disruptions of such regulatory mechanisms. A number of chemical compounds and proteins are known to interfere with mitochondrial transport and docking, allowing exploration of the relationship between transport and cellular fate. The fact that in zebrafish, axonal arbor size and mitochondrial localization can be determined in conjunction now allows directly addressing this question *in vivo*. I showed here that treatment with nocodazole, which depolymerizes microtubules and hence blocks transport, results in a reduced mitochondrial density specifically in the axon's periphery. I made similar observations when different compartments of mitochondrial transport machinery were disturbed by genetic means (dominant-negative kinesins, syntaphilin and Tau). This suggests that zebrafish can be used to better characterize modulators of transport and the resulting consequences for the affected organelle population - or even screen for modulators of such

effects. However what regulates the physiological transition from one state to another and whether subpopulations with different residence times of mitochondria exist (e.g. permanently "resident" *vs*. "cycling"; Wong et al., 2012) remains unknown. Some studies of this question suggest Ca^{2+} as a regulator of mitochondrial movement, others rather point to the energetic state as a decisive factor (Sheng and Cai, 2012). Despite many efforts to understand the transition between the moving and resting state of neuronal mitochondria a comprehensive *in vivo* test of the available hypotheses is outstanding. I believe that the zebrafish system offers the opportunity to verify some of these postulates. Combination of *in vivo* imaging with assessing mitochondrial function through one of the many available sensors of mitochondrial function (ATP production, Ca^{2+} or ROS levels) would be a step forward in understanding the dynamics of mitochondria in relation to their functional status. Additionally available methods of gene manipulation would be helpful in understanding the molecular basis of the transition from the moving to the resting state. For these reasons analysis of transport disturbances in single cell assay can be insightful in regards to mechanism behind observed alterations. The results of such approach are presented in the Result section 3.2. Based on the data I collected however the meaningful conclusions cannot be drawn as obtained results vary significantly between each experiment. This is most probably due to different levels of transgene expression which cannot be accurately controlled for. Moreover obtaining sufficient number of repeats for statistical testing is very laborious and time consuming, therefore making this method not suitable for large drug and gene screens. To overcome the time budget requirements we teamed up with the Haass lab to developed transgenic *MitoFish* with labeled neuronal mitochondria, which allow for a much faster "first-pass" analysis. These fish were used to characterize the effects of mutant forms of Tau on axonal transport of mitochondria. This work is discussed in the next paragraph, but I want to stress the fact that the experimental work to address this question was performed in close collaboration with my colleagues Dominik Paquet and Alexander Hruscha (both Schmid/Haass lab at LMU).

5.4. Tau-induced changes in transport

Alterations in axonal transport are emerging as a central pathomechanism in several neurological diseases. As it have been demonstrated, pathologic aspects of neurodegenerative diseases can be modeled in zebrafish by overexpressing disease-related human genes (Bandmann and Burton, 2010; Kabashi et al., 2011). A particularly promising variant of such models is based on the Gal4-UAS expression system, which allows concomitant expression of disease-related genes and fluorescent markers and therefore simple identification of

transgenic fish (or even transgene-expressing cells) by fluorescence microscopy (Paquet et al., 2009). In addition, the Gal4-UAS expression system also facilitates characterizing pathologic mechanisms in disease-modeling fish by crossing them with reporter lines, such as the *MitoFish* presented in this study. As a proof-of-principle experiment, we crossed *TauFish* with *MitoFish* to analyze whether the overexpression of Tau alters axonal transport *in vivo*. Alterations of mitochondrial transport caused by Tau overexpression have been described in cultured neurons (Ebneth et al., 1998; Stamer et al., 2002; Mandelkow et al., 2003) and flies (Mudher et al., 2004), but there are conflicting reports about transport changes in higher vertebrate Tauopathy models, such as transgenic mice (Stokin et al., 2005; Yuan et al., 2008). Importantly, transport alterations in these mouse models have only been analyzed in an indirect way, e.g. by looking at putative consequences of transport deficits, such as axonal swellings, or by quantifying the levels of axonal proteins by biochemical methods. The *MitoFish* presented in this study enabled us to study axonal transport in a Tauopathy model for the first time directly *in vivo*. Intriguingly, we were able to detect profound changes in transport of mitochondria, validating the *MitoFish* as a promising new tool to study this pathology in living animals. It is important to note that the effect we observed might be underestimated due to the silencing of one of the sites of bidirectional construct. That means that some of the Tau-expressing neurites will not express DsRed and some of the DsRed-positive neurites are not expressing Tau. Such misclassification of the neurites biases the measurement towards the smaller differences. Nevertheless, we were still able to detect significant differences between the Tau and DsRed groups. Interestingly, while the number of motile mitochondria was greatly reduced in the *TauFish*, and their average speed was decreased due to increased pauses. Indeed, a detailed analysis of the behavior of single mitochondria revealed that once moving, mitochondria faced with excessive Tau levels actually appear to move faster than in controls (probably because some short pauses in movement flow are now extended, and can thus be resolved and excluded from a “run”) – but once mitochondria disengage, they often do so for longer periods of time and might even leave the moving pool. This points to an explanation where supernumerary Tau molecules occupy the microtubule surface and interfere with motor protein binding to microtubules (Mandelkow et al., 2003; Dixit et al., 2008), rather than unbound Tau affecting the motors directly. This model is supported by the observation that we could rescue the Tau phenotype by overexpressing MARK2, which regulates Tau's affinity to microtubules by phosphorylating the repeat domain of Tau (Drewes et al., 1997) and thus directly demonstrate the influence of MARK2 on axonal transport *in vivo*. However, proving the mechanism of

such a rescue directly *in vivo* is challenging, and requires detailed biochemical and biophysical experiments. Still, the ability to swiftly test hypotheses generated from such *in vitro* work in a living vertebrate will be an important addition to the attempts to unravel the mechanisms of mitochondrial transport disturbances. Taken together, these findings underscore the utility of *MitoFish* for rapid and sensitive *in vivo* transport assays and open up the possibility of their use in high-content screening efforts (Zon and Peterson, 2005) for drugs that ameliorate axonal transport deficits common to numerous neurological diseases.

5.5. Mitochondrial turn-over

One important advantages of the zebrafish system is the ability of monitoring arbor size and dynamics as well as mitochondrial number and flux in the *same* neuron over time. This allows deducing important parameters such as potential sites of mitochondrial digestion, estimated residence time of mitochondria in axons and the relationship between transport and axon remodeling. For example, the data set represented in **Fig. 4.2** shows that there is a consistent excess in the number of anterogradely transported mitochondria over the number of retrogradely transported ones. While plausibly interpreted as representing an excess of supply needed for growth, observations that this bias persists throughout the life of mice suggests the alternative of a consistent distal digestion of mitochondria. As disturbed removal of mitochondria seems to be a central pathomechanisms in Parkinson's disease (Burman et al., 2012), and given the persisting uncertainty of the site of mitochondrial digestion in neurons, distinguishing between these two models - growth-related use *vs.* peripheral digestion - is interesting. Quantitative analysis of my data shows that the net translocation of individual mitochondria between 2 and 3 dpf exceeds what is needed to maintain a stable mitochondrial density in the growing arbors roughly by a factor of 2 (~60% of the imported mitochondrial volume returns via retrograde transport, ~20% remains and compensates for growth, another ~20% are lost; **Fig. 4.14**). This imbalance points to the parallel existence of peripheral removal (Wang et al., 2011) and mitochondrial return (Miller and Sheetz, 2004). However, there are a number of caveats regarding these calculations. First, my volume estimate of mitochondria rests on geometrical assumptions (cylindrical approximation) that are plausible, but not precise. Second, while the length of mitochondria can be determined quite reliably using conventional light microscopy, the thickness of mitochondria is in the range of the wavelength of visible light, and hence impacted significantly by diffraction. If anterogradely and retrogradely moving mitochondria differed subtly in shape, I would probably miss this difference. Third, peripheral digestion could be matched by peripheral biogenesis which

would underestimate my measurements of “lost” mitochondria. Fourth, as mitochondria might reside in densely packed clusters in axonal branch points (see next paragraph), the estimates of mitochondrial numbers might be impacted by the resulting uncertainty of counting clustered organelles. Finally, one has to consider that few if any of the mitochondria in the axons I studied are older than 3 days (the age of the organisms). This is within the estimated life-time of single mitochondria; hence the need to remove mitochondria may vary between different developmental stages. Imaging RBN arbor at later time points however also did not allow answering the question about sites of mitophagy. In order to ensure that mitophagy indeed can occur peripherally, I used the mitophagic and autophagic markers. Expressing LC3.GFP revealed that the potential sites of mitophagy might be branching points. This observation of mitophagic event requires further conformation through time-lapse recordings that confirm actual disappearance of mitochondria, but it raises an interesting possibility that branching points are decision points of mitochondrial fate.

5.6. Branching points and mitochondria

Mitochondria are directed to sites of high energy demand - for example synapses or, in myelinating axons, nodes of Ranvier (MacAskill and Kittler, 2010; Ohno et al., 2011) suggesting that the accumulation of mitochondria at branch points is a primary feature and might actually precede the development of nodes or synapses. Interstingly, axonal branch points are typically found at nodes of Ranvier. Remarkably, in non-myelinated axons, which lack nodes, mitochondria also locate to neuronal bifurcations (Toth et al., 2012). Similar patterns of mitochondria co-localizing with branching points have been observed is the developing axons which have not been myelinated yet (Ruthel and Hollenbeck, 2003). This suggests that mitochondrial distribution might influence neuronal arborization. Along this line, several recent studies point to mitochondria as set decision points for growth or retraction of axonal branches. However, as previous models based on time-lapse studies of synaptic markers and branching in retinotectal neurons ascribed a similar role to synapses (Niell et al., 2004; Meyer and Smith, 2006), a clear decision as to whether mitochondrial localization determines branching, or rather just secondarily follows a synaptogenic pattern is currently unresolved. Recent studies certainly suggest (but do not yet prove) that mitochondria might play a primary role in neuritogenesis. For example, in cortical neurons of the mouse, the group of Franck Polleux has shown that the level of mitochondrial motility correlates with the development of neuronal branches with the ability of mitochondria to dock being a decisive branching determinant (Courchet et al., 2013). Interestingly, the assay that I

have developed in this work offers the possibility to study the role of mitochondria in establishing new branches as peripheral sensory axons, such as the RB neurons, lack synapses. This means that role of mitochondria in this process can be studied independently of synapse formation. Indeed, during the imaging of neuronal arbors I observed that mitochondria are often accumulating at the branching points and occasionally form there clusters of several mitochondria (**Fig. 4.19D**). Additionally, anecdotal observation suggests that moving mitochondria tend to pause more frequently at these specific sites. These observations, together with the LC3 accumulations at neurite bifurcation points that I found, suggest that mitochondrial localization at neuronal branch points might allow for bidirectional signaling processes where branch and organelle fate intersect. In this (hypothetical) view mitochondria which pass such a point would undergo quality control and - according to their functional state - could be directed to a retrograde journey, to fusion within the cluster in order to be "rejuvenated" (see Introduction, Fusion) or to the degradation pathway. Such decisions again - for example though apoptotic signals that have been implicated in neurite fate - could also impact the subsequent formation and/or maintenance of the downstream branches. While this is an interesting hypothesis that is supported by my preliminary observations, it requires sound experimental conformation. Zebrafish offers a set of tools which would allow testing this and related hypotheses *in vivo*. The ability to distinguish fusion events through photo-activateable and photo-convertible FPs (**Fig. 4.18, 4.19**) and the possibility to use specific markers for mitochondrial function opens an interesting field of study. Furthermore, the use of new "ultra-resolution" optical techniques, which have proven their power in visualizing mitochondria with a precision below a tenth of a mitochondrion's diameter, will probably be soon transferred to zebrafish *in vivo*, given the unique optical accessibility of this organism, and can help resolve the ambiguity of identifying single mitochondria at branching points and determining their volume and structure, allowing to link mitochondrial state with neurite fate.

5.7. General conclusions

Mitochondrial dynamics are currently considered crucial for maintaining neuronal cells and their proper functioning. Multiple different models both *in vitro* and *in vivo* have been developed in order to understand the mechanisms of individual steps of the life of a mitochondrion. Each of these models has greatly contributed to our current knowledge about mitochondrial dynamics. However, so far none of them was able to fully answer the question of spatial compartmentalization of the mitochondrial life-cycle. This is in part due to the fact that it was difficult to visualize mitochondria in their natural habitat *in vivo*.

The aim of my study was to establish the zebrafish as an *in vivo* model organism for studying mitochondrial dynamics. The optical accessibility of the fish is of great benefit for answering questions about the spatial organization of mitochondrial dynamics. Therefore, I performed a set of *in vivo* time-lapse experiments in the RBNs. The observations based on these measurements allowed comparing basic transport characteristics between different *in vitro* and animal models. It turns out that zebrafish flux rates correspond to the numbers observed in unmyelinated cultured neurons (Morris and Hollenbeck, 1993). Like all measurements in other model organisms also in RBNs I observed a bias of mitochondrial translocation towards the peripheral parts of the neuron. Moreover, in this paradigm I was able to relate flux with cell dynamics over days. While the single cell assay presented in the first section of this work sets the stage for understanding the specific effects of transport defects on neuronal development and maintenance it is not suitable for higher through-put screens of transport modulators based on genetic and pharmacological interventions. This, however, can be overcome by using a *MitoFish* assay, which is a fast and effective method of assessing gene and compound effects on transport. Development of these two assays creates a powerful set of tools for testing modulators of transport.

In the second part of my work I set out to develop tools to study other steps of the mitochondrial life-cycle. Firstly, I focused on mitophagy. Degradation of mitochondria is an important part of maintaining cellular health as impaired mitochondria can be sources of ROS or apoptotic factors. Also defects in mitophagy are implicated in the Parkinson's disease. Mitophagy is mainly considered to be restricted to the cell body and proximal parts of a neuron. However, *in vivo* evidence to definitively support this notion is still missing. Here I used specific markers of autophagy in order to identify sites of mitochondrial degradation. In the first attempts I was able to identify such potential mitophagy sites in the distal parts of the neuron. These preliminary results require further confirmation. The second process I was

interested in is studying where mitochondrial fusion takes place. In order to be able to unambiguously identify such events I tested photo-convertible (Kaede) and photo-activatable (PA-GFP) fluorescent proteins. Both of them were useful in labeling subpopulations of mitochondria. By following such “photo-tagged” organelles I was able to observe fusions of mitochondria *in vivo*, during which some of the fluorescent material was exchanged between two mitochondria. Currently this technique works reliably and can be used for future *in vivo* studies of fusion in neurons.

Overall this work shows that zebrafish is a very useful addition to the currently available animal models to study mitochondrial dynamics. However, the fact that for harnessing the full potential of the zebrafish system, (transparent) larvae have to be used means that this is mostly a system to study mitochondria in a developing environment. This limitation means that zebrafish, rather than substituting will co-exist with other models, such as transgenic mice together allowing a comprehensive characterization of how mitochondria, an important and fascinating organelle, behave in neurons *in vivo*.

6. Publications

Plucińska G, Marinković P, Breckwoldt T, Misgeld T Studying the 'life-cycle' of neuronal mitochondria in vivo, *in preparation*

Plucińska G, Paquet D, Hruscha A, Godinho L, Haass C, Schmid B, Misgeld T (2012) In vivo imaging of disease-related mitochondrial dynamics in a vertebrate model system The Journal of Neuroscience 32:16203 - 16212

7. References

Abe T, Kiyonari H, Shioi G, Inoue K, Nakao K, Aizawa S, Fujimori T (2011) Establishment of conditional reporter mouse lines at ROSA26 locus for live cell imaging. Genesis 49:579 - 590.

Amiri M, Hollenbeck PJ (2008) Mitochondrial Biogenesis in the Axons of Vertebrate Peripheral Neurons. Developmental Neurobiology 68:1348 - 1361.

Ando R, Hama H, Yamamoto-Hino M, Mizuno H, Miyawaki A (2002) An optical marker based on the UV-induced green-to-red photoconversion of a fluorescent protein. Proc Natl Acad Sci U S A 99:12651 - 12656.

Attwel D, Lauglin SB (2001) An Energy Budget for Signaling in the Grey Matter of the Brain. Journal of Cerebral Blood Flow and Metabolism 21:1133- 1145.

Bai X, Yan Y, Canfield S, Muravyeva MY, Kikuchi C, Zaja I, Corbett JA, Bosnjak ZJ (2013) Ketamine enhances human neural stem cell proliferation and induces neuronal apoptosis via reactive oxygen species-mediated mitochondrial pathway. Anesthesia & Analgesia 116:869 - 880.

Bakota L, Brandt R (2009) Live-cell imaging in the study of neurodegeneration. International Review of Cell and Molecular Biology 276:49 - 103.

Baloh RH, Schmidt RE, Pestronk A, Milbrandt J (2007) Altered axonal mitochondrial transport in the pathogenesis of Charcot-Marie-Tooth disease from mitofusin 2 mutations. The Journal of Neuroscience 27:422 - 430.

Bandmann O, Burton EA (2010) Genetic zebrafish models of neurodegenerative diseases. Neurobiology of Disease 40:58 - 65.

Bauer MP, Goetz FW (2001) Isolation of gonadal mutations in adult zebrafish from a chemical mutagenesis screen. Biology of reproduction 64:548 - 554.

Bedell VM, Wang Y, Campbell JM, Poshusta TL, Starker CG, Krug RG 2nd, Tan W, Penheiter SG, Ma AC, Leung AY, Fahrenkrug SC, Carlson DF, Voytas DF, Clark KJ, Essner JJ, Ekker SC (2012) In vivo genome editing using a high-efficiency TALEN system. Nature 491:114 - 118.

Ben Fredj N, Hammond S, Otsuna H, Chien CB, Burrone J, Meyer MP (2010) Synaptic activity and activity-dependent competition regulates axon arbor maturation, growth arrest, and territory in the retinotectal projection. The Journal of Neuroscience 30:10939 - 10951.

Berg J, Hung YP, Yellen G (2009) A genetically encoded fluorescent reporter of ATP:ADP ratio. Nature Methods 6:161 - 166

Blesa JR, Prieto-Ruiz JA, Hernández JM, Hernández-Yago J (2007) NRF-2 transcription factor is required for human TOMM20 gene expression. Gene 391:198 - 208.

Boesch P, Weber-Lotfi F, Ibrahim N, Tarasenko V, Cosset A Paulus F, Lightowlers RN, Dietrich A (2011) DNA repair in organelles: Pathways, organization, regulation, relevance in disease and aging. Biochimica et Biophysica Acta 1813:186 - 200.

Breckwoldt MO, Pfister F, Bradley PM, Marinković P, Williams PR, Brill MS, Plomer B, Schmalz A, St. Clair DK, Naumann R, Griesbeck O, Schwarzländer M, Godinho L, Bareyre FM, Dick TP, Kerschensteiner, Misgeld T (2013) Multi-parametric optical analysis of mitochondrial redox signals during neuronal physiology and pathology in vivo. Nature Medicine, in press.

Brockerhoff SE, Dowling JE, Hurley JB (1998) Zebrafish retinal mutants. Vision research 38:1335 - 1339.

Brösamle C, Halpern ME (2002) Characterization of myelination in the developing zebrafish. Glia 39:47 - 57.

Burman JL, Yu S, Poole AC, Decal RB, Pallanck L (2012) Analysis of neural subtypes reveals selective mitochondrial dysfunction in dopaminergic neurons from parkin mutants. Proc Natl Acad Sci U S A 109:10438 - 10443.

Cai Q, Gerwin C, Sheng ZH (2005) Syntabulin-Mediated Anterograde Transport of Mitochondria along Neuronal Processes. The Journal of Cell Biology 170:959 - 969.

Cai Q, Mostafa Zakaria H, Simone A Sheng ZH (2012) Spatial Parkin Translocation and Degradation of Damaged Mitochondria via Mitophagy in Live Cortical Neurons. Current Biology 22:1 - 8.

Chacinska A, Koehler CM, Milenkovic D, Lithgow T, Pfanner N (2009) Importing Mitochondrial Proteins: Machineries and Mechanisms. Cell 138:628 - 644.

Chang DT, Reynolds IJ (2006) Mitochondrial trafficking and morphology in healthy and injured neurons. Progress in Neurobiology 80:241 - 268.

Chapman AL, Bennett EJ, Ramesh TM, De Vos KJ, Grierson AJ (2013) Axonal Transport Defects in a Mitofusin 2 Loss of Function Model of Charcot-Marie-Tooth Disease in Zebrafish. PLoS One 8:e67276.

Chazotte B (2011) Labeling mitochondria with MitoTracker dyes. Cold Spring Harbor Protocols 2011:990 - 992.

Chen Y, Sheng ZH (2013) Kinesin-1-syntaphilin coupling mediates activity-dependent regulation of axonal mitochondrial transport. The Journal of Cell Biology 202:351 - 364.

Cheng A, Hou Y, Mattson MP (2010) Mitochondria and neuroplasticity. ASN NEURO 2:243.

Cho KI, Cai Y, Yi H, Yeh A, Aslanukov A, Ferreira PA (2007) Association of the kinesin-binding domain of RanBP2 to KIF5B and KIF5C determines mitochondria localization and function. Traffic 8:1722 - 1735.

Chu Y, Morfini GA, Langhamer LB, He Y, Brady ST, Kordower JH (2012) Alterations in axonal transport motor proteins in sporadic and experimental Parkinson's disease. Brain 135:2058 - 2073.

Clark KJ, Urban MD, Skuster KJ, Ekker SC (2011) Transgenic zebrafish using transposable elements. Methods in Cell Biology 104:137 - 149.

Clayton DA (2003) Mitochondrial DNA Replication: What We Know. IUBMB Life 55:213 - 217.

Clemente D, Porteros A, Weruaga E, Alonso JR, Arenzana FJ, Aijón J, Arévalo R (2004) Cholinergic elements in the zebrafish central nervous system: Histochemical and immunohistochemical analysis. The Journal of Comparative Neurology 474:75 - 107.

Cookson MR (2003) Parkin’s Substrates and the Pathways Leading to Neuronal Damage. NeuroMolecular Medicine 3:1 - 13.

Cooper MS, Szeto DP, Sommers-Herivel G, Topczewski J, Solnica-Krezel L, Kang HC, Johnson I, Kimelman D (2005) Visualizing morphogenesis in transgenic zebrafish embryos using BODIPY TR methyl ester dye as a vital counterstain for GFP. Developmental Dynamics 232:359 - 368.

Courchet J, Lewis TL Jr, Lee S, Courchet V, Liou DY, Aizawa S, Polleux F (2013) Terminal axon branching is regulated by the LKB1-NUAK1 kinase pathway via presynaptic mitochondrial capture. Cell 153:1510 - 1525.

Cowan CM, Mudher A (2013) Are tau aggregates toxic or protective in tauopathies? Frontiers of neurology 4.

Davis AF, Clayton DA (1996) In Situ Localization of Mitochondrial DNA Replication in Intact Mammalian Cells. The Journal of Cell Biology 135:883 - 893.

de Brito OM, Scorrano L (2008) Mitofusin 2 tethers endoplasmic reticulum to mitochondria. Nature 456:605 - 610.

Dixit R, Ross JL, Goldman YE, Holzbaur EL (2008) Differential regulation of dynein and kinesin motor proteins by tau. Science 319:1086 - 1089

Dong Z, Yang N, Yeo SY, Chitnis A, Guo S (2012) Intralineage directional Notch signaling regulates self-renewal and differentiation of asymmetrically dividing radial glia. Neuron 74:65 - 78.

Doyon Y, McCammon JM, Miller JC, Faraji F, Ngo C, Katibah GE, Amora R, Hocking TD, Zhang L, Rebar EJ, Gregory PD, Urnov FD, Amacher SL (2008) Heritable targeted gene disruption in zebrafish using designed zinc-finger nucleases. Nature Biotechnology 26:702 - 708.

Drewes G, Ebneth A, Preuss U, Mandelkow EM, Mandelkow E (1997) MARK, a novel family of protein kinases that phosphorylate microtubule-associated proteins and trigger microtubule disruption. Cell 89:297 - 308.

Duffy P, Wang X, Siegel CS, Tu N, Henkemeyer M, Cafferty WB S, trittmatter SM (2012) Myelin-derived ephrinB3 restricts axonal regeneration and recovery after adult CNS injury. Proc Natl Acad Sci U S A 109:5063 - 5068.

Ebneth A, Godemann R, Stamer K, Illenberger S, Trinczek B, Mandelkow E (1998) Overexpression of tau protein inhibits kinesin-dependent trafficking of vesicles, mitochondria, and endoplasmic reticulum: implications for Alzheimer's disease. The Journal of Cell Biology 143:777 - 794.

Eisen JS, Smith JC (2008) Controlling morpholino experiments: don't stop making antisense. Development 135:1735 - 1743.

England SJ, Adams RJ (2011) Blastomere injection of cleavage-stage zebrafish embryos and imaging of labeled cells. Cold Spring Harbor Protocols 2011:958 - 966.

Fett ME, Pilsl A, Paquet D, van Bebber F, Haass C, Tatzelt J, Schmid B, Winklhofer KF (2010) Parkin is protective against proteotoxic stress in a transgenic zebrafish model. PLoS One 5:e11783

Flinn L, Mortiboys H, Volkmann K, Köster RW, Ingham PW, Bandmann O (2009) Complex I deficiency and dopaminergic neuronal cell loss in parkin-deficient zebrafish (Danio rerio). Brain 132:1613 - 1323.

Fricker FR, Antunes-Martins A, Galino J, Paramsothy R, La Russa F, Perkins J, Goldberg R, Brelstaff J, Zhu N, McMahon SB, Orengo C, Garratt AN, Birchmeier C, Bennett DL (2013) Axonal neuregulin 1 is a rate limiting but not essential factor for nerve remyelination. Brain 136:2279 - 2297.

Friedman JR, Lackner LL, West M, DiBenedetto JR, Nunnari J, Voeltz GK (2011) ER Tubules Mark Sites of Mitochondrial Division. Science 334:358 - 362.

Fujita T, Maturana AD, Ikuta J, Hamada J, Walchli S, Suzuki T, Sawa H, Wooten MW, Okajima T, Tatematsu K, Tanizawa K, Kuroda S (2007) Axonal guidance protein FEZ1 associates with tubulin and kinesin motor protein to transport mitochondria in neurites of NGF-stimulated PC12 cells. Biochemical and Biophysical Research Communications 361:605 - 610.

Gaiano N, Amsterdam A, Kawakami K, Allende M, Becker T, Hopkins N (1996) Insertional mutagenesis and rapid cloning of essential genes in zebrafish. Nature 383:829 - 832.

Gioio AE, Eyman M, Zhang H, Scotto Lavina Z, Giuditta A, Kaplan BB (2001) Local Synthesis of Nuclear-Encoded Mitochondrial Proteins in the Presynaptic Nerve Terminal. Journal of Neuroscience Research 64:447 - 453.

Godinho L (2011) Live imaging of zebrafish development. Cold Spring Harbor Protocols 2011:770 - 777.

Godinho L, Williams PR, Claassen Y, Provost E, Leach SD, Kamermans M, Wong RO (2007) Nonapical symmetric divisions underlie horizontal cell layer formation in the developing retina in vivo. Neuron 56:597 - 603.

Gomes LC, Di Benedetto G, Scorrano L (2011) During autophagy mitochondria elongate, are spared from degradation and sustain cell viability. Nature Cell Biology 13:589 - 598.

Gross SP, Vershinin M, Shubeita GT (2007) Cargo transport: two motors are sometimes better than one. Current Biology 17:478 - 486.

Grunwald DJ, Streisinger G (1992) Induction of recessive lethal and specific locus mutations in the zebrafish with ethyl nitrosourea. Genetical Research 59:103 - 116.

Guo X, Macleod GT, Wellington A, Hu F, Panchumarthi S, Schoenfield M, Marin L, Charlton MP, Atwood HL, Zinsmaier KE (2005) The GTPase dMiro is required for axonal transport of mitochondria to Drosophila synapses. Neuron 47:379 - 393.

Haffter P, Granato M, Brand M, Mullins MC, Hammerschmidt M, Kane DA, Odenthal J, van Eeden FJ, Jiang YJ, Heisenberg CP, Kelsh RN, Furutani-Seiki M, Vogelsang E, Beuchle D, Schach U, Fabian C, Nüsslein-Volhard C (1996) The identification of genes with unique and essential functions in the development of the zebrafish, Danio rerio. Development 123:1 - 36.

Hayashi S, McMahon AP (2002) Efficient recombination in diverse tissues by a tamoxifen-inducible form of Cre: a tool for temporally regulated gene activation/inactivation in the mouse. Developmental Biology 244:305 - 318.

Hendricks AG, Lazarus JE, Holzbaur EL (2010) Dynein at odd angles? Nature Cell Biology 12:1126 - 1128.

Hirokawa N, Niwa S, Tanaka Y (2010) Molecular Motors in Neurons: Transport Mechanisms and Roles in Brain Function, Development, and Disease. Neuron 68:610 - 638.

Howe K et al. (2013) The zebrafish reference genome sequence and its relationship to the human genome. Nature 496:498 - 503.

Hunter PR, Lowe AS, Thompson ID, Meyer MP (2013) Emergent properties of the optic tectum revealed by population analysis of direction and orientation selectivity. The Journal of Neuroscience 33:13940 - 13945

Hwang WY, Fu Y, Reyon D, Maeder ML, Tsai SQ, Sander JD, Peterson RT, Yeh JR, Joung JK (2013) Efficient genome editing in zebrafish using a CRISPR-Cas system. Nature 31:227 - 229.

Ingerman E, Perkins EM, Marino M, Mears JA, McCaffery JM, Hinshaw JE, Nunnari J (2005) Dnm1 forms spirals that are structurally tailored to fit mitochondria. The Journal of Cell Biology 170:1021 - 1027.

Ishihara N, Nomura M, Jofuku A, Kato H, Suzuki SO, Masuda K, Otera H, Nakanishi Y, Nonaka I, Goto Y, Taguchi N, Morinaga H, Maeda M, Takayanagi R, Yokota S, Mihara K (2009) Mitochondrial fission factor Drp1 is essential for embryonic development and synapse formation in mice. Nature Cell Biology 11:958 - 966.

Kabashi E, Brustein E, Champagne N, Drapeau P (2011) Zebrafish models for the functional genomics of neurogenetic disorders. Biochimica et Biophysica Acta 1812:335 - 345.

Kabeya Y, Mizushima N, Ueno T, Yamamoto A, Kirisako T, Noda T, Kominami E, Ohsumi Y, Yoshimori T (2000) LC3, a mammalian homologue of yeast Apg8p, is localized in autophagosome membranes after processing. The EMBO Journal 19:5720 - 5728.

Kane DA, Hammerschmidt M, Mullins MC, Maischein HM, Brand M, van Eeden FJ, Furutani-Seiki M, Granato M, Haffter P, Heisenberg CP, Jiang YJ, Kelsh RN, Odenthal J, Warga RM, Nüsslein-Volhard C (1996) The zebrafish epiboly mutants. Development 123:47 - 55.

Kang JS, Tian JH, Pan PY, Zald P, Li C, Deng C, Sheng ZH (2008) Docking of axonal mitochondria by syntaphilin controls their mobility and affects short-term facilitation. Cell 132:137 - 148.

Karlovich CA, John RM, Ramirez L, Stainier DY, Myers RM (1998) Characterization of the Huntington's disease (HD) gene homologue in the zebrafish Danio rerio. Gene 217:117 - 125.

Kim MJ, Kang KH, Kim CH, Choi SY (2008) Real-time imaging of mitochondria in transgenic zebrafish expressing mitochondrially targeted GFP. Biotechniques 45:331 - 334.

Kimmel CB, Ballard WW, Kimmel SR, Ullmann B, Schilling TF (1995) Stages of embryonic development of the zebrafish. Developmental Dynamics 203:253 - 310.

King SJ, Schroer TA (2000) Dynactin increases the processivity of the cytoplasmic dynein motor. Nature Cell Biology 2:20 - 24.

Kizil C, Kaslin J, Kroehne V, Brand M (2012) Adult neurogenesis and brain regeneration in zebrafish. Developmental Neurobiology 72:429 - 461.

Ko SK, Chen X, Yoon J, Shin I (2011) Zebrafish as a good vertebrate model for molecular imaging using fluorescent probes. Chemical Society Reviews 40:2120 - 2130.

Korzh V, Edlund T, Thor S (1993) Zebrafish primary neurons initiate expression of the LIM homeodomain protein Isl-1 at the end of gastrulation. Development 118:417 - 425.

Köster RW, Fraser SE (2001) Tracing transgene expression in living zebrafish embryos. Developmental Biology 233:329 - 346.

Kural C, Kim H, Syed S, Goshima G, Gelfand VI, Selvin PR (2005) Kinesin and dynein move a peroxisome in vivo: a tug-of-war or coordinated movement? Science 308:1469 - 1472.

Li J, Mack JA, Souren M, Yaksi E, Higashijima S, Mione M, Fetcho JR, Friedrich RW (2005) Early development of functional spatial maps in the zebrafish olfactory bulb. The Journal of Neuroscience 25:5784 - 5795.

Liu X, Weaver D, Shirihai O, Hajnoczky G (2009) Mitochondrial 'kiss-and-run': interplay between mitochondrial motility and fusion–fission dynamics. The EMBO Journal 28:3074 - 3089.

Louie K, Russo GJ, Salkoff DB, Wellington A, Zinsmaier KE (2008) Effects of imaging conditions on mitochondrial transport and length in larval motor axons of Drosophila. Comparative Biochemistry and Physiology 151:159 - 172.

MacAskill AF, Kittler JT (2010) Control of mitochondrial transport and localization in neurons. Trends in cell biology 20:102 - 112.

Macaskill AF, Rinholm JE, Twelvetrees AE, Arancibia-Carcamo IL, Muir J, Fransson A, Aspenstrom P, Attwell D, Kittler JT (2009) Miro1 is a calcium sensor for glutamate receptor-dependent localization of mitochondria at synapses. Neuron 61:541 - 555.

Maday S, Wallace KE, Holzbaur EL (2012) Autophagosomes initiate distally and mature during transport toward the cell soma in primary neurons. The Journal of Cell Biology 196:407 - 417.

Mandelkow EM, Stamer K, Vogel R, Thies E, Mandelkow E (2003) Clogging of axons by tau, inhibition of axonal traffic and starvation of synapses. Neurobiology of Aging 24:1079 - 1085.

Marinkovic P, Reutera MS, Brill MS, Godinho L, Kerschensteiner M, Misgeld T (2012) Axonal transport deficits and degeneration can evolve independently in mouse models of amyotrophic lateral sclerosis. Proc Natl Acad Sci U S A 109:4296 - 4301.

Martin SM, O'Brien GS, Portera-Cailliau C, Sagasti A (2010) Wallerian degeneration of zebrafish trigeminal axons in the skin is required for regeneration and developmental pruning. Development 137:3985 - 3994.

Mateus R, Pereira T, Sousa S, de Lima JE, Pascoal S, Saúde L, Jacinto A (2012) In vivo cell and tissue dynamics underlying zebrafish fin fold regeneration. PLoS One 7:e51766.

Matsuda N, Sato S, Shiba K, Okatsu K, Saisho K, Gautier CA, Sou Y, Saiki S, Kawajiri S, Sato F, Kimura M, Komatsu M, Hattori N, Tanaka K (2010) PINK1 stabilized by mitochondrial depolarization recruits Parkin to damaged mitochondria and activates latent Parkin for mitophagy. The Journal of Cell Biology 189:211 - 221.

Metcalfe WK, Myers PZ, Trevarrow B, Bass MB, Kimmel CB (1990) Primary neurons that express the L2/HNK-1 carbohydrate during early development in the zebrafish. Development 110:491 - 504.

Meyer MP, Smith SJ (2006) Evidence from in vivo imaging that synaptogenesis guides the growth and branching of axonal arbors by two distinct mechanisms. The Journal of Neuroscience 26:3604 - 3614.

Miller KE, Sheetz MP (2004) Axonal mitochondrial transport and potential are correlated. Journal of Cell Science 117:2791 - 2804.

Miller VM, Nelson RF, Gouvion CM, Williams A, Rodriguez-Lebron E, Harper SQ, Davidson BL, Rebagliati MR, Paulson HL (2005) CHIP suppresses polyglutamine aggregation and toxicity in vitro and in vivo. The Journal of Neuroscience 25:9152 - 9161.

Misgeld T, Kerschensteiner M, Bareyre FM, Burgess RW, Lichtman JW (2007) Imaging axonal transport of mitochondria in vivo. Nature Methods 4:559 - 561.

Mizuno H, Mal TK, Tong KI, Ando R, Furuta T, Ikura M, Miyawaki A (2003) Photo-induced peptide cleavage in the green-to-red conversion of a fluorescent protein. Molecular Cell 12:1051 - 1058

Morfini G, Szebenyi G, Elluru R, Ratner N, Brady ST (2002) Glycogen synthase kinase 3 phosphorylates kinesin light chains and negatively regulates kinesin-based motility. The EMBO Journal 21:281 - 293.

Morris RL, Hollenbeck PJ (1993) The regulation of bidirectional mitochondrial transport is coordinated with axonal outgrowth. Journal of Cell Science 104:917 - 927.

Morris RL, Hollenbeck PJ (1995) Axonal transport of mitochondria along microtubules and F-actin in living vertebrate neurons. The Journal of Cell Biology 131:1315 - 1326

Mudher A, Shepherd D, Newman TA, Mildren P, Jukes JP, Squire A, Mears A, Drummond JA, Berg S, MacKay D, Asuni AA, Bhat R, Lovestone S (2004) GSK-3beta inhibition reverses axonal transport defects and behavioural phenotypes in Drosophila. Molecular Psychiatry 9:522 - 530.

Mueller T, Vernier P, Wullimann MF (2004) The adult central nervous cholinergic system of a neurogenetic model animal, the zebrafish Danio rerio. Brain Research 1011:156 - 169.

Mueller T, Wullimann MF (2005) Atlas of early zebrafish brain development. A tool for molecular neurogenetics. First Edition, Elsevier.

Mullins MC, Hammerschmidt M, Haffter P, Nüsslein-Volhard C (1994) Large-scale mutagenesis in the zebrafish: in search of genes controlling development in a vertebrate. Current Biology 4:189 - 202.

Narendra D, Tanaka A, Suen D-F, Youle RJ (2008) Parkin is recruited selectively to impaired mitochondria and promotes their autophagy. The Journal of Cell Biology 183:795 - 803.

Nasevicius A, Ekker SC (2000) Effective targeted gene 'knockdown' in zebrafish. Nature Genetics 26:216 - 220.

Neuspiel M, Schauss AC, Braschi E, Zunino R, Rippstein P, Rachubinski RA, Andrade-Navarro MA, McBride HM (2008) Cargo-Selected Transport from the Mitochondria to Peroxisomes Is Mediated by Vesicular Carriers. Current Biology 18:102 - 108.

Niell CM, Meyer MP, Smith SJ (2004) In vivo imaging of synapse formation on a growing dendritic arbor. Nature Neuroscience 7:254 - 260

O'Brien GS, Martin SM, Söllner C, Wright GJ, Becker CG, Portera-Cailliau C, Sagasti A (2009) Developmentally regulated impediments to skin reinnervation by injured peripheral sensory axon terminals. Current Biology 19:2086 - 2090.

O'Toole M, Latham R, Baqri RM, Miller KE (2008) Modeling mitochondrial dynamics during in vivo axonal elongation. Journal of Theoretical Biology 255:369 - 377.

Obashi K, Okabe S (2013) Regulation of mitochondrial dynamics and distribution by synapse position and neuronal activity in the axon. The European Journal of Neuroscience 38:2350 - 2363.

Odenthal J, Haffter P, Vogelsang E, Brand M, van Eeden FJ, Furutani-Seiki M, Granato M, Hammerschmidt M, Heisenberg CP, Jiang YJ, Kane DA, Kelsh RN, Mullins MC, Warga RM, Allende ML, Weinberg ES, Nüsslein-Volhard C (1996) Mutations affecting the formation of the notochord in the zebrafish, Danio rerio. Development 123:103 - 115.

Ohno N, Kidd GJ, Mahad D, Kiryu-Seo S, Avishai A, Komuro H, Trapp BD (2011) Myelination and axonal electrical activity modulate the distribution and motility of mitochondria at CNS nodes of Ranvier. The Journal of Neuroscience 31:7249 - 7258.

Overly CC, Rieff HI, Hollenbeck PJ (1996) Organelle motility and metabolism in axons vs dendrites of cultured hippocampal neurons. Journal of Cell Science 109:971 - 980.

Paquet D, Bhat R, Sydow A, Mandelkow EM, Berg S, Hellberg S, Fälting J, Distel M, Köster RW, Schmid B, Haass C (2009) A zebrafish model of tauopathy allows in vivo imaging of neuronal cell death and drug evaluation. The Journal of Clinical Investigation 119:1382 - 1395.

Pardo-Martin C, Chang TY, Koo BK, Gilleland CL, Wasserman SC, Yanik MF (2010) High-throughput in vivo vertebrate screening. Nature Methods 7:634 - 636.

Park J, Lee SB, Lee S, Kim Y, Song S, Kim S, Bae E, Kim J, Shong M, Kim JM, Chung J (2006) Mitochondrial dysfunction in Drosophila PINK1 mutants is complemented by parkin. Nature 441:1157 - 1161.

Patterson GH, Lippincott-Schwartz J (2002) A photoactivatable GFP for selective photolabeling of proteins and cells. Science 297:1873 - 1877.

Peri F, Nüsslein-Volhard C (2008) Live imaging of neuronal degradation by microglia reveals a role for v0-ATPase a1 in phagosomal fusion in vivo. Cell 133:916 - 927.

Pham AH, Meng S, Chu QN, Chan DC (2012) Loss of Mfn2 results in progressive, retrograde degeneration of dopaminergic neurons in the nigrostriatal circuit. Human molecular genetics 21:4817 - 4826.

Pilling AD, Horiuchi D, Lively CM, Saxton WM (2006) Kinesin-1 and Dynein Are the Primary Motors for Fast Transport of Mitochondria in Drosophila Motor Axons. Molecular Biology of the Cell 17:2057 - 2068.

Pittman AJ, Law MY, Chien CB (2008) Pathfinding in a large vertebrate axon tract: isotypic interactions guide retinotectal axons at multiple choice points. Development 135:2865 - 2871.

Plucińska G, Paquet D, Hruscha A, Godinho L, Haass C, Schmid B, Misgeld T (2012) In vivo imaging of disease-related mitochondrial dynamics in a vertebrate model system. The Journal of Neuroscience 32:16203 - 16212

Quigley IK, Parichy DM (2002) Pigment pattern formation in zebrafish: a model for developmental genetics and the evolution of form. Microscopy Research and Technique 58:442 - 455.

Rajewsky K, Gu H, Kühn R, Betz UA, Müller W, Roes J, Schwenk F (1996) Conditional gene targeting. The Journal of Clinical Investigation 98:600 - 603.

Rambold AS, Kostelecky B, Elia N, Lippincott-Schwartz J (2011) Tubular network formation protects mitochondria from autophagosomal degradation during nutrient starvation. Proc Natl Acad Sci U S A 108:10190 - 10195.

Ranieri M, Brajkovic S, Riboldi G, Ronchi D, Rizzo F, Bresolin N, Corti S, Comi GP (2013) Mitochondrial Fusion Proteins and Human Diseases. Neurology Research International 2013:1 - 11.

Reyes R, Haendel M, Grant D, Melancon E, Eisen JS (2004) Slow degeneration of zebrafish Rohon-Beard neurons during programmed cell death. Developmental Dynamics 229:30 - 41.

Ribera AB, Nüsslein-Volhard C (1998) Zebrafish touch-insensitive mutants reveal an essential role for the developmental regulation of sodium current. The Journal of Neuroscience 18:9181 - 9191.

Rieger S, Sagasti A (2011) Hydrogen peroxide promotes injury-induced peripheral sensory axon regeneration in the zebrafish skin. PLoS One 9:e1000621.

Rival T, Macchi M, Arnaune´-Pelloquin L, Poidevin M, Maillet F, Richard F, Fatmi A, Belenguer P, Royet J (2011) Inner-membrane proteins PMI/TMEM11 regulate mitochondrial morphogenesis independently of the DRP1/MFN fission/fusion pathways. EMBO reports 12:223 - 230.

Ro H, Soun K, Kim EJ, Rhee M (2004) Novel vector systems optimized for injecting in vitro-synthesized mRNA into zebrafish embryos. Molecules and Cells 17:373 - 376.

Ruthel G, Hollenbeck PJ (2003) Response of mitochondrial traffic to axon determination and differential branch growth. The Journal of Neuroscience 23:8618 - 8624

Sadowski I, Ma J, Triezenberg S, Ptashne M (1988) GAL4-VP16 is an unusually potent transcriptional activator. Nature 335:563 - 564.

Sagasti A, Guido MR, Raible DW, Schier AF (2005) Repulsive interactions shape the morphologies and functional arrangement of zebrafish peripheral sensory arbors. Current Biology 15:804 - 814.

Sager JJ, Bai Q, Burton EA (2010) Transgenic zebrafish models of neurodegenerative diseases. Brain Structure & Function 214:285 - 302.

Saint-Amant L, Drapeau P (1998) Time course of the development of motor behaviors in the zebrafish embryo. Journal of Neurobiology 37:622 - 632.

Saotome M, Safiulina D, Szabadkai G, Das S, Fransson A, Aspenstrom P, Rizzuto R, Hajnóczky G (2008) Bidirectional Ca2+-dependent control of mitochondrial dynamics by the Miro GTPase. Proc Natl Acad Sci U S A 105:20728 - 20733.

Schmid B, Hruscha A, Hogl S, Banzhaf-Strathmann J, Strecker K, van der Zee J, Teucke M, Eimer S, Hegermann J, Kittelmann M, Kremmer E, Cruts M, Solchenberger B, Hasenkamp L, van Bebber F, Van Broeckhoven C, Edbauer D, Lichtenthaler SF, Haass C (2013) Loss of ALS-associated TDP-43 in zebrafish causes muscle degeneration, vascular dysfunction, and reduced motor neuron axon outgrowth. Proc Natl Acad Sci U S A 110:4986 - 4991.

Schroeter EH, Wong RO, Gregg RG (2006) In vivo development of retinal ON-bipolar cell axonal terminals visualized in nyx::MYFP transgenic zebrafish. visual neuroscience 23:833 - 843.

Sheng ZH, Cai Q (2012) Mitochondrial transport in neurons: impact on synaptic homeostasis and neurodegeneration. Nature Reviews Neuroscience 13:77 - 93.

Shimizu S, Mori N, Kishi M, Sugata H, Tsuda A, Kubota N (2003) A novel mutation in the OPA1 gene in a Japanese patient with optic atrophy. AMERICAN JOURNAL OF OPHTHALMOLOGY 135:256 - 257.

Shutt TE, McBride HM (2012) Staying cool in difficult times: Mitochondrial dynamics, quality control and the stress response. Biochimica et Biophysica Acta 1833:417 - 424.

Sieger D, Peri F (2013) Animal models for studying microglia: the first, the popular, and the new. Glia 61:3 - 9.

Sorbara C, Misgeld T, Kerschensteiner M (2012) In vivo imaging of the diseased nervous system: an update. Current Pharmaceutical Design 18:4465 - 4470.

Soubannier V, Rippstein P, Kaufman BA, Shoubridge EA, McBride HM (2012) Reconstitution of Mitochondria Derived Vesicle Formation Demonstrates Selective Enrichment of Oxidized Cargo. PLoS One 7:1 - 9.

Stamer K, Vogel R, Thies E, Mandelkow E, Mandelkow EM (2002) Tau blocks traffic of organelles, neurofilaments, and APP vesicles in neurons and enhances oxidative stress. The Journal of Cell Biology 156:1051 - 1063.

Stokin GB, Lillo C, Falzone TL, Brusch RG, Rockenstein E, Mount SL, Raman R, Davies P, Masliah E, Williams DS, Goldstein LS (2005) Axonopathy and transport deficits early in the pathogenesis of Alzheimer's disease. Science 307:1282 - 1288.

Stowers RS, Megeath LJ, Go´rska-Andrzejak J, Meinertzhagen IA, Schwarz TL (2002) Axonal Transport of Mitochondria to Synapses Depends on Milton, a Novel Drosophila Protein. Neuron 36:1063 - 1077.

Streisinger G, Walker C, Dower N, Knauber D, Singer F (1981) Production of clones of homozygous diploid zebra fish (Brachydanio rerio). Nature 291:293 - 296.

Streisinger G, Coale F, Taggart C, Walker C, Grunwald DJ (1989) Clonal origins of cells in the pigmented retina of the zebrafish eye. Developmental Biology 131:60 - 69.

Sun T, Qiao H, Pan PY, Chen Y, Sheng ZH (2013) Motile axonal mitochondria contribute to the variability of presynaptic strength. Cell Reports 4:413 - 419.

Svoboda KR, Linares AE, Ribera AB (2001) Activity regulates programmed cell death of zebrafish Rohon-Beard neurons. Development 128:3511 - 3520.

Tanaka A, Cleland MM, Xu S, Narendra DP, Suen D-F, Karbowski M, Youle RJ (2010) Proteasome and p97 mediate mitophagy and degradation of mitofusins induced by Parkin. The Journal of Cell Biology 191:1367 - 1380.

Tao J, Rolls MM (2011) Dendrites have a rapid program of injury-induced degeneration that is molecularly distinct from developmental pruning. The Journal of Neuroscience 31:5398 - 5405.

Tomasiewicz HG, Flaherty DB, Soria JP, Wood JG (2002) Transgenic zebrafish model of neurodegeneration. Journal of Neuroscience research 70:734 - 745.

Tomizawa K, Inoue Y, Doi S, Nakayasu H (2000) Monoclonal antibody stains oligodendrocytes and Schwann cells in zebrafish (Danio rerio). Anatomy and Embryology 201:399 - 406.

Tondera D, Grandemange S, Jourdain A, Karbowski M, Mattenberger Y, Herzig S, Da Cruz S, Clerc P, Raschke I, Merkwirth C, Ehses S, Krause F, Chan DC, Alexander C, Bauer C, Youle R, Langer T, Martinou J-C (2009) SLP-2 is required for stress-induced mitochondrial hyperfusion. The EMBO Journal 28:1589 - 1600.

Toth ML, Melentijevic I, Shah L, Bhatia A, Lu K, Talwar A, Naji H, Ibanez-Ventoso C, Ghose P, Jevince A Xue J, Herndon LA, Bhanot G, Rongo C, Hall DH, Driscoll M (2012) Neurite sprouting and synapse deterioration in the aging Caenorhabditis elegans nervous system. The Journal of Neuroscience 32:8778 - 8790.

Twig G, Graf SA, Wikstrom JD, Mohamed H, Haigh SE, Elorza A, Deutsch M, Zurgil N, Reynolds N, Shirihai OS (2006) Tagging and tracking individual networks within a complex mitochondrial web with photoactivatable GFP. Am J Physiol Cell Physiol 291:176 - 184.

Vale RD, Reese TS, Sheetz MP (1985) Identification of a Novel Force-Generating Protein, Kinesin, Involved in Microtubule-Based Motility. Cell 42:39 - 50.

van Spronsen M, Mikhaylova M, Lipka J, Schlager MA, van den Heuvel DJ, Kuijpers M, Wulf PS, Keijzer N, Demmers J, Kapitein LC, Jaarsma D, Gerritsen HC, Akhmanova A, Hoogenraad CC (2013) TRAK/Milton motor-adaptor proteins steer mitochondrial trafficking to axons and dendrites. Neuron 77:485 - 502.

Vasquez RJ, Howell B, Yvon AM, Wadsworth P, Cassimeris L (1997) Nanomolar concentrations of nocodazole alter microtubule dynamic instability in vivo and in vitro. Mol Biol Cell 8:973 - 985.

Verstreken P, Ly CV, Venken KJT, Koh T-W, Zhou Y, Bellen HJ (2005) Synaptic Mitochondria Are Critical for Mobilization of Reserve Pool Vesicles at Drosophila Neuromuscular Junctions. Neuron 47:365-378.

Virbasius JV, Scarpulla RC (1994) Activation of the human mitochondrial transcription factor A gene by nuclear respiratory factors: a potential regulatory link between nuclear and mitochondrial gene expression in organelle biogenesis. Proc Natl Acad Sci U S A 91:1309 - 1313.

Vitorino M, Jusuf PR, Maurus D, Kimura Y, Higashijima S, Harris WA (2009) Vsx2 in the zebrafish retina: restricted lineages through derepression. Neural Development 4.

Vives-Bauza C, Zhou C, Huang Y, Cui M, de Vries RLA, Kim J, May J, Tocilescu MA, Liud W, Seok Ko H, Magrané J, Moore DJ, Dawson VL, Grailhe R, Dawson TM, Li C, Tieu K, Przedborski S (2010) PINK1-dependent recruitment of Parkin to mitochondria in mitophagy. Proc Natl Acad Sci U S A 107:378 - 383.

Wang DB, Garden GA, Kinoshita C, Wyles C, Babazadeh N, Sopher B, Kinoshita Y, Morrison RS (2013) Declines in Drp1 and Parkin Expression Underlie DNA Damage-Induced Changes in Mitochondrial Length and Neuronal Death. The Journal of Neuroscience 33:1357 - 1365.

Wang X, Winter D, Ashrafi G, Schlehe J, Wong YL, Selkoe D, Rice S, Steen J, LaVoie MJ, Schwarz TL (2011) PINK1 and Parkin Target Miro for Phosphorylation and Degradation to Arrest Mitochondrial Motility. Cell 147:893 - 906.

Wareski P, Vaarmann A, Choubey V, Safiulina D, Liiv J, Kuum M, Kaasik A (2009) PGC-1 and PGC-1Regulate Mitochondrial Density in Neurons. THE JOURNAL OF BIOLOGICAL CHEMISTRY 284:21379 - 21385.

Waterman-Storer CM, Karki SB, Kuznetsov SA, Tabb JS, Weiss DG, Langford GM, Holzbaur EL (1997) The interaction between cytoplasmic dynein and dynactin is required for fast axonal transport. Proc Natl Acad Sci U S A 94:12180 - 12185.

Webber E, Li L, Chin L-S (2008) Hypertonia-associated Protein Trak1 is a Novel Regulator of Endosome-to-Lysosome Trafficking. Journal of Molecular Biology 382:638 - 651.

Westerfield M (2000) The Zebrafish Book. A Guide for the Laboratory Use of Zebrafish (Danio rerio), 4th Edition. Eugene, Oregon: University of Oregon Press.

Westermann B (2010) Mitochondrial fusion and fission in cell life and death. Nature Reviews Molecular Cell Biology 11:872 - 884.

Wienholds E, Schulte-Merker S, Walderich B, Plasterk RH (2002) Target-selected inactivation of the zebrafish rag1 gene. Science 297:99 - 102.

Wong MY, Zhou C, Shakiryanova D, Lloyd TE, Deitcher DL, Levitan ES (2012) Neuropeptide delivery to synapses by long-range vesicle circulation and sporadic capture. Cell 148:1029 - 1038.

Wu Z, Puigserver P, Andersson U, Zhang C, Adelmant G, Mootha V, Troy A, Cinti S, Lowell B, Scarpulla RC, Spiegelman BM (1999) Mechanisms Controlling Mitochondrial Biogenesis and Respiration through the Thermogenic Coactivator PGC-1. Cell 98:115 - 124.

Xiao T, Baier H (2007) Lamina-specific axonal projections in the zebrafish tectum require the type IV collagen Dragnet. Nature Neuroscience 10:1529 - 1537.

Xiong J, Verkhratsky A, Toescu EC (2002) Changes in mitochondrial status associated with altered Ca2+ homeostasis in aged cerebellar granule neurons in brain slices. The Journal of Neuroscience 22:10761 - 10771.

Yan M, Rayapuram N, Subramani S (2005) The control of peroxisome number and size during division and proliferation. Current Opinion in Cell Biology 17:376 - 383.

Yuan A, Kumar A, Peterhoff C, Duff K, Nixon RA (2008) Axonal transport rates in vivo are unaffected by tau deletion or overexpression in mice. The Journal of Neuroscience 28:1682 - 1687.

Ziviani E, Tao RN, Whitworth AJ (2009) Drosophila Parkin requires PINK1 for mitochondrial translocation and ubiquitinates Mitofusin. Proc Natl Acad Sci U S A 107:5018 - 5023.

Zon LI, Peterson RT (2005) In vivo drug discovery in the zebrafish. NATURE REVIEWS DRUG DISCOVERY 4:35 - 44.

Züchner S et al. (2004) Mutations in the mitochondrial GTPase mitofusin 2 cause Charcot-Marie-Tooth neuropathy type 2A. Nature Genetics 36:449 - 451.